THE UNIVERSITY OF CALGARY

Heat and Momentum Transfer to Drag Reducing Fluids

by

Arun Sood

A THESIS

SUBMITTED TO THE FACULTY OF GRADUATE STUDIES

IN PARTIAL FULFILLMENT OF THE REQUIREMENTS FOR THE

DEGREE OF MASTER OF SCIENCE

DEPARTMENT OF CHEMICAL AND PETROLEUM ENGINEERING

CALGARY, ALBERTA

SEPTEMBER, 1993

Canada

Name _____ _ARUN_____SOOD_____

Dissertation Abstracts International is arranged by broad, general subject categories. Please select the one subject which most nearly describes the content of your dissertation. Enter the corresponding four-digit code in the spaces provided.

ENGINEERING — CHEMICAL

SUBJECT TERM

| 0 | 5 | 4 | 2 | U·M·I

SUBJECT CODE

Subject Categories

THE HUMANITIES AND SOCIAL SCIENCES

COMMUNICATIONS AND THE ARTS
Architecture 0729
Art History 0377
Cinema 0900
Dance 0378
Fine Arts 0357
Information Science 0723
Journalism 0391
Library Science 0399
Mass Communications 0708
Music 0413
Speech Communication 0459
Theater 0465

EDUCATION
General 0515
Administration 0514
Adult and Continuing 0516
Agricultural 0517
Art 0273
Bilingual and Multicultural 0282
Business 0688
Community College 0275
Curriculum and Instruction 0727
Early Childhood 0518
Elementary 0524
Finance 0277
Guidance and Counseling 0519
Health 0680
Higher 0745
History of 0520
Home Economics 0278
Industrial 0521
Language and Literature 0279
Mathematics 0280
Music 0522
Philosophy of 0998
Physical 0523

Psychology 0525
Reading 0535
Religious 0527
Sciences 0714
Secondary 0533
Social Sciences 0534
Sociology of 0340
Special 0529
Teacher Training 0530
Technology 0710
Tests and Measurements 0288
Vocational 0747

LANGUAGE, LITERATURE AND LINGUISTICS
Language
    General 0679
    Ancient 0289
    Linguistics 0290
    Modern 0291
Literature
    General 0401
    Classical 0294
    Comparative 0295
    Medieval 0297
    Modern 0298
    African 0316
    American 0591
    Asian 0305
    Canadian (English) 0352
    Canadian (French) 0355
    English 0593
    Germanic 0311
    Latin American 0312
    Middle Eastern 0315
    Romance 0313
    Slavic and East European 0314

PHILOSOPHY, RELIGION AND THEOLOGY
Philosophy 0422
Religion
    General 0318
    Biblical Studies 0321
    Clergy 0319
    History of 0320
    Philosophy of 0322
Theology 0469

SOCIAL SCIENCES
American Studies 0323
Anthropology
    Archaeology 0324
    Cultural 0326
    Physical 0327
Business Administration
    General 0310
    Accounting 0272
    Banking 0770
    Management 0454
    Marketing 0338
Canadian Studies 0385
Economics
    General 0501
    Agricultural 0503
    Commerce-Business 0505
    Finance 0508
    History 0509
    Labor 0510
    Theory 0511
Folklore 0358
Geography 0366
Gerontology 0351
History
    General 0578

Ancient 0579
Medieval 0581
Modern 0582
Black 0328
African 0331
Asia, Australia and Oceania 0332
Canadian 0334
European 0335
Latin American 0336
Middle Eastern 0333
United States 0337
History of Science 0585
Law 0398
Political Science
    General 0615
    International Law and
        Relations 0616
    Public Administration 0617
Recreation 0814
Social Work 0452
Sociology
    General 0626
    Criminology and Penology ... 0627
    Demography 0938
    Ethnic and Racial Studies 0631
    Individual and Family
        Studies 0628
    Industrial and Labor
        Relations 0629
    Public and Social Welfare 0630
    Social Structure and
        Development 0700
    Theory and Methods 0344
Transportation 0709
Urban and Regional Planning 0999
Women's Studies 0453

THE SCIENCES AND ENGINEERING

BIOLOGICAL SCIENCES
Agriculture
    General 0473
    Agronomy 0285
    Animal Culture and
        Nutrition 0475
    Animal Pathology 0476
    Food Science and
        Technology 0359
    Forestry and Wildlife 0478
    Plant Culture 0479
    Plant Pathology 0480
    Plant Physiology 0817
    Range Management 0777
    Wood Technology 0746
Biology
    General 0306
    Anatomy 0287
    Biostatistics 0308
    Botany 0309
    Cell 0379
    Ecology 0329
    Entomology 0353
    Genetics 0369
    Limnology 0793
    Microbiology 0410
    Molecular 0307
    Neuroscience 0317
    Oceanography 0416
    Physiology 0433
    Radiation 0821
    Veterinary Science 0778
    Zoology 0472
Biophysics
    General 0786
    Medical 0760

EARTH SCIENCES
Biogeochemistry 0425
Geochemistry 0996

Geodesy 0370
Geology 0372
Geophysics 0373
Hydrology 0388
Mineralogy 0411
Paleobotany 0345
Paleoecology 0426
Paleontology 0418
Paleozoology 0985
Palynology 0427
Physical Geography 0368
Physical Oceanography 0415

HEALTH AND ENVIRONMENTAL SCIENCES
Environmental Sciences 0768
Health Sciences
    General 0566
    Audiology 0300
    Chemotherapy 0992
    Dentistry 0567
    Education 0350
    Hospital Management 0769
    Human Development 0758
    Immunology 0982
    Medicine and Surgery 0564
    Mental Health 0347
    Nursing 0569
    Nutrition 0570
    Obstetrics and Gynecology .. 0380
    Occupational Health and
        Therapy 0354
    Ophthalmology 0381
    Pathology 0571
    Pharmacology 0419
    Pharmacy 0572
    Physical Therapy 0382
    Public Health 0573
    Radiology 0574
    Recreation 0575

Speech Pathology 0460
Toxicology 0383
Home Economics 0386

PHYSICAL SCIENCES
Pure Sciences
Chemistry
    General 0485
    Agricultural 0749
    Analytical 0486
    Biochemistry 0487
    Inorganic 0488
    Nuclear 0738
    Organic 0490
    Pharmaceutical 0491
    Physical 0494
    Polymer 0495
    Radiation 0754
Mathematics 0405
Physics
    General 0605
    Acoustics 0986
    Astronomy and
        Astrophysics 0606
    Atmospheric Science 0608
    Atomic 0748
    Electronics and Electricity 0607
    Elementary Particles and
        High Energy 0798
    Fluid and Plasma 0759
    Molecular 0609
    Nuclear 0610
    Optics 0752
    Radiation 0756
    Solid State 0611
Statistics 0463

Applied Sciences
Applied Mechanics 0346
Computer Science 0984

Engineering
    General 0537
    Aerospace 0538
    Agricultural 0539
    Automotive 0540
    Biomedical 0541
    Chemical 0542
    Civil 0543
    Electronics and Electrical 0544
    Heat and Thermodynamics ... 0348
    Hydraulic 0545
    Industrial 0546
    Marine 0547
    Materials Science 0794
    Mechanical 0548
    Metallurgy 0743
    Mining 0551
    Nuclear 0552
    Packaging 0549
    Petroleum 0765
    Sanitary and Municipal 0554
    System Science 0790
Geotechnology 0428
Operations Research 0796
Plastics Technology 0795
Textile Technology 0994

PSYCHOLOGY
General 0621
Behavioral 0384
Clinical 0622
Developmental 0620
Experimental 0623
Industrial 0624
Personality 0625
Physiological 0989
Psychobiology 0349
Psychometrics 0632
Social 0451

♲

Nom _____

Dissertation Abstracts International est organisé en catégories de sujets. Veuillez s.v.p. choisir le sujet qui décrit le mieux votre thèse et inscrivez le code numérique approprié dans l'espace réservé ci-dessous.

SUJET   CODE DE SUJET
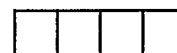
Catégories par sujets

HUMANITÉS ET SCIENCES SOCIALES

COMMUNICATIONS ET LES ARTS
Architecture 0729
Beaux-arts 0357
Bibliothéconomie 0399
Cinéma 0900
Communication verbale 0459
Communications 0708
Danse 0378
Histoire de l'art 0377
Journalisme 0391
Musique 0413
Sciences de l'information 0723
Théâtre 0465

ÉDUCATION
Généralités 515
Administration 0514
Art 0273
Collèges communautaires 0275
Commerce 0688
Économie domestique 0278
Éducation permanente 0516
Éducation préscolaire 0518
Éducation sanitaire 0680
Enseignement agricole 0517
Enseignement bilingue et
  multiculturel 0282
Enseignement industriel 0521
Enseignement primaire. 0524
Enseignement professionnel 0747
Enseignement religieux 0527
Enseignement secondaire 0533
Enseignement spécial 0529
Enseignement supérieur 0745
Évaluation 0288
Finances 0277
Formation des enseignants 0530
Histoire de l'éducation 0520
Langues et littérature 0279

Lecture 0535
Mathématiques 0280
Musique 0522
Orientation et consultation 0519
Philosophie de l'éducation 0998
Physique 0523
Programmes d'études et
  enseignement 0727
Psychologie 0525
Sciences 0714
Sciences sociales 0534
Sociologie de l'éducation 0340
Technologie 0710

LANGUE, LITTÉRATURE ET LINGUISTIQUE
Langues
  Généralités 0679
  Anciennes 0289
  Linguistique 0290
  Modernes 0291
Littérature
  Généralités 0401
  Anciennes 0294
  Comparée 0295
  Médiévale 0297
  Moderne 0298
  Africaine 0316
  Américaine 0591
  Anglaise 0593
  Asiatique 0305
  Canadienne (Anglaise) 0352
  Canadienne (Française) 0355
  Germanique 0311
  Latino-américaine 0312
  Moyen-orientale 0315
  Romane 0313
  Slave et est-européenne 0314

PHILOSOPHIE, RELIGION ET THÉOLOGIE
Philosophie 0422
Religion
  Généralités 0318
  Clergé 0319
  Études bibliques 0321
  Histoire des religions 0320
  Philosophie de la religion 0322
Théologie 0469

SCIENCES SOCIALES
Anthropologie
  Archéologie 0324
  Culturelle 0326
  Physique 0327
Droit 0398
Économie
  Généralités 0501
  Commerce-Affaires 0505
  Économie agricole 0503
  Économie du travail 0510
  Finances 0508
  Histoire 0509
  Théorie 0511
Études américaines 0323
Études canadiennes 0385
Études féministes 0453
Folklore 0358
Géographie 0366
Gérontologie 0351
Gestion des affaires
  Généralités 0310
  Administration 0454
  Banques 0770
  Comptabilité 0272
  Marketing 0338
Histoire
  Histoire générale 0578

Ancienne 0579
Médiévale 0581
Moderne 0582
Histoire des noirs 0328
Africaine 0331
Canadienne 0334
États-Unis 0337
Européenne 0335
Moyen-orientale 0333
Latino-américaine 0336
Asie, Australie et Océanie 0332
Histoire des sciences 0585
Loisirs 0814
Planification urbaine et
  régionale 0999
Science politique
  Généralités 0615
  Administration publique 0617
  Droit et relations
    internationales 0616
Sociologie
  Généralités 0626
  Aide et bien-être social 0630
  Criminologie et
    établissements
    pénitentiaires 0627
  Démographie 0938
  Études de l' individu et
    de la famille 0628
  Études des relations
    interethniques et
    des relations raciales 0631
  Structure et développement
    social 0700
  Théorie et méthodes. 0344
  Travail et relations
    industrielles 0629
Transports 0709
Travail social 0452

SCIENCES ET INGÉNIERIE

SCIENCES BIOLOGIQUES
Agriculture
  Généralités 0473
  Agronomie. 0285
  Alimentation et technologie
    alimentaire 0359
  Culture 0479
  Élevage et alimentation 0475
  Exploitation des péturages 0777
  Pathologie animale 0476
  Pathologie végétale 0480
  Physiologie végétale 0817
  Sylviculture et faune 0478
  Technologie du bois 0746
Biologie
  Généralités 0306
  Anatomie 0287
  Biologie (Statistiques) 0308
  Biologie moléculaire 0307
  Botanique 0309
  Cellule 0379
  Écologie 0329
  Entomologie 0353
  Génétique 0369
  Limnologie 0793
  Microbiologie 0410
  Neurologie 0317
  Océanographie 0416
  Physiologie 0433
  Radiation 0821
  Science vétérinaire 0778
  Zoologie 0472
Biophysique
  Généralités 0786
  Medicale 0760

SCIENCES DE LA TERRE
Biogéochimie 0425
Géochimie 0996
Géodésie 0370
Géographie physique 0368

Géologie 0372
Géophysique 0373
Hydrologie 0388
Minéralogie 0411
Océanographie physique 0415
Paléobotanique 0345
Paléoécologie 0426
Paléontologie 0418
Paléozoologie 0985
Palynologie 0427

SCIENCES DE LA SANTÉ ET DE L'ENVIRONNEMENT
Économie domestique 0386
Sciences de l'environnement 0768
Sciences de la santé
  Généralités 0566
  Administration des hipitaux .. 0769
  Alimentation et nutrition 0570
  Audiologie 0300
  Chimiothérapie 0992
  Dentisterie 0567
  Développement humain 0758
  Enseignement 0350
  Immunologie 0982
  Loisirs 0575
  Médecine du travail et
    thérapie 0354
  Médecine et chirurgie 0564
  Obstétrique et gynécologie .. 0380
  Ophtalmologie 0381
  Orthophonie 0460
  Pathologie 0571
  Pharmacie 0572
  Pharmacologie 0419
  Physiothérapie 0382
  Radiologie 0574
  Santé mentale 0347
  Santé publique 0573
  Soins infirmiers 0569
  Toxicologie 0383

SCIENCES PHYSIQUES
Sciences Pures
Chimie
  Généralités 0485
  Biochimie 487
  Chimie agricole 0749
  Chimie analytique 0486
  Chimie minérale 0488
  Chimie nucléaire 0738
  Chimie organique 0490
  Chimie pharmaceutique 0491
  Physique 0494
  PolymCres 0495
  Radiation 0754
Mathématiques 0405
Physique
  Généralités 0605
  Acoustique 0986
  Astronomie et
    astrophysique 0606
  Electronique et électricité 0607
  Fluides et plasma 0759
  Météorologie 0608
  Optique 0752
  Particules (Physique
    nucléaire) 0798
  Physique atomique 0748
  Physique de l'état solide 0611
  Physique moléculaire 0609
  Physique nucléaire 0610
  Radiation 0756
Statistiques 0463

Sciences Appliqués Et Technologie
Informatique 0984
Ingénierie
  Généralités 0537
  Agricole 0539
  Automobile 0540

Biomédicale 0541
Chaleur et ther
  modynamique 0348
Conditionnement
  (Emballage) 0549
Génie aérospatial 0538
Génie chimique 0542
Génie civil 0543
Génie électronique et
  électrique 0544
Génie industriel 0546
Génie mécanique 0548
Génie nucléaire 0552
Ingénierie des systämes 0790
Mécanique navale 0547
Métallurgie 0743
Science des matériaux 0794
Technique du pétrole 0765
Technique minière 0551
Techniques sanitaires et
  municipales 0554
Technologie hydraulique 0545
Mécanique appliquée 0346
Géotechnologie 0428
Matières plastiques
  (Technologie) 0795
Recherche opérationnelle 0796
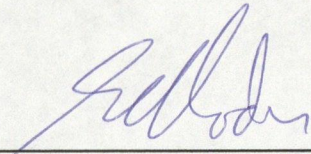Textiles et tissus (Technologie) 0794

PSYCHOLOGIE
Généralités 0621
Personnalité 0625
Psychobiologie 0349
Psychologie clinique 0622
Psychologie du comportement 0384
Psychologie du développement 0620
Psychologie expérimentale 0623
Psychologie industrielle 0624
Psychologie physiologique 0989
Psychologie sociale 0451
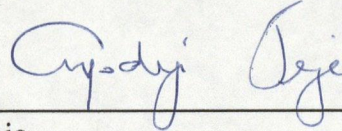Psychométrie 0632

♲

THE UNIVERSITY OF CALGARY
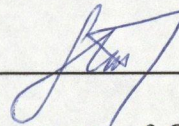
FACULTY OF GRADUATE STUDIES

The undersigned certify that they have read, and recommend to the Faculty of Graduate Studies for acceptance, a thesis entitled, "Heat and Momentum Transfer to Drag Reducing Fluids", submitted by Arun Sood in partial fulfilment of the requirements for the degree of Master of Science.
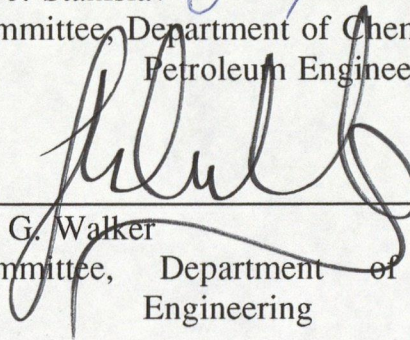
Dr. E. Rhodes
Supervisor, Department of Chemical and
               Petroleum Engineering

Dr. A. Jeje
Committee, Department of Chemical and
               Petroleum Engineering

Dr. J. Stanislav
Committee, Department of Chemical and
               Petroleum Engineering

Dr. G. Walker
Committee, Department of Mechanical
               Engineering

Date   Sept 20, 1993

ABSTRACT

Addition of low concentrations of Poly(ethylene oxide) to water causes reductions in the frictional drag and convective heat transfer in turbulent flow. The reductions are influenced by the quantity of the additive, pipe diameter, solution viscosity and the average velocity.

Apparent shear viscosities of the solutions were measured for different amounts of additive and at different temperatures. Steel tubings of two different diameters were used as the test section. Joule heating was applied at the walls of the tubes which were externally insulated. This system provided a constant heat flux condition for the fluid in motion within the tubes.

A threshold value of shear stress at the wall was observed for the reduction in friction and heat transfer to become apparent which was found to be independent of the diameter of the tubing. Same shear stress at the wall produced similar drag reduction and heat transfer reduction effects.

ACKNOWLEDGEMENTS

TABLE OF CONTENTS

LIST OF TABLES

LIST OF FIGURES

NOMENCLATURE

C_p Specific heat of the fluid, J/kg °K

D diameter, m

DR Drag reduction, %

f friction factor

F Force, N

h_{fs} Energy loss due to friction (equation 6.6), M-m/kg

h_i Average heat transfer coefficient, W/m² °C

HTR Heat transfer reduction, %

k_s Thermal conductivity of the tube wall, W/m °C

L length of the tube, m

m mass flow rate, kg/s

Nu Nusselt number, dimensionless

Pr Prandtl number, dimensionless

Q Heat generated per unit volume, W/m³

r tube radius, m

Re Reynolds number, dimensionless

T Temperature, °C

u fluid velocity, m/s

x Distance in the axial direction of the tube, m

y plane perpendicular to the direction of the flow

ΔP Pressure drop, N/m^2

μ fluid viscosity, kg/m-s

ρ fluid density, kg/m^3

τ shear stress, N/m^2

∇ differential operator

Subscripts

a polymer solution

b bulk flow

i inner

iw inner wall

m mean

o outer

ow outer wall

s pure solvent

w wall

x axial position x

1. INTRODUCTION

1.1. Drag Reduction

Addition of small amounts of a suitable polymer additive, to the extent of only a few parts per million by weight, can reduce the frictional drag in turbulent flow through pipes. This phenomenon, known as drag reduction, is not caused by an improvement in the wall properties but by changes in the flow field near the wall with the bulk flow still remaining turbulent (Merrill and Shaver, 1959). Polymeric materials which are suitable for producing this effect have a linear, unbranched, long chain structure. Macromolecular additives such as synthetics, biopolymers, surfactants, suspended fibres and solid particles have proved to be effective drag reducers (Kulicke et. al, 1989). In this study, Poly(ethylene oxide) Water Soluble Resin 301 which is manufactured by Union Carbide, has been used as the drag reducing additive in water.

In practical use, drag reduction can create significant economic advantage. Typical applications are listed in Table 1.1. By using a drag reducing additive, it is possible to reduce the actual pressure loss in a pipeline, or by using the same pumping head more fluid can be transported or, in pumping at the same flow rate, less energy can be expended. Alternatively, the fluid can be pumped to a greater

TABLE 1.1

Applications of Drag Reduction and Heat Transfer Reduction

Engineering Application	Reference
Oil well operations	Hoyt, 1972
Crude oil movement by pipelines	Burger et. al, 1980
Fire fighting	Fabula, 1971
Agriculture	Singh et. al, 1989
Sewage and storm water disposal	Sellin, 1982
Long distance heat transport	Sellin, 1982
Transport of solid particle suspensions	Golda, 1984
Increasing speed of boats & submarines	Hoyt, 1972
Biomedical applications	Greene, 1980

distance using the same amount of power. Figure 1.1 shows some typical results obtained during our fluid dynamics experiments and provides a better understanding of the phenomenon.

Drag reduction for a pipe is given by the following equation ;

$$DR = \frac{(\Delta P_s - \Delta P_a)}{\Delta P_s} \times 100\% \quad (at \; constant \; flow \; rate) \qquad (1.1)$$

Drag reduction can also be calculated by using one of the following relationships ;

$$DR = \left(1 - \frac{f_a}{f_s}\right) \times 100\% \quad (at \; constant \; flow \; rate) \qquad (1.2)$$

where,

$$f = Darcy \; friction \; factor = \frac{8\tau_w}{\rho u_m^2} \qquad (1.3)$$

1.2. Heat Transfer Reduction

Reduction in drag for turbulent pipe flows of polymer solutions is
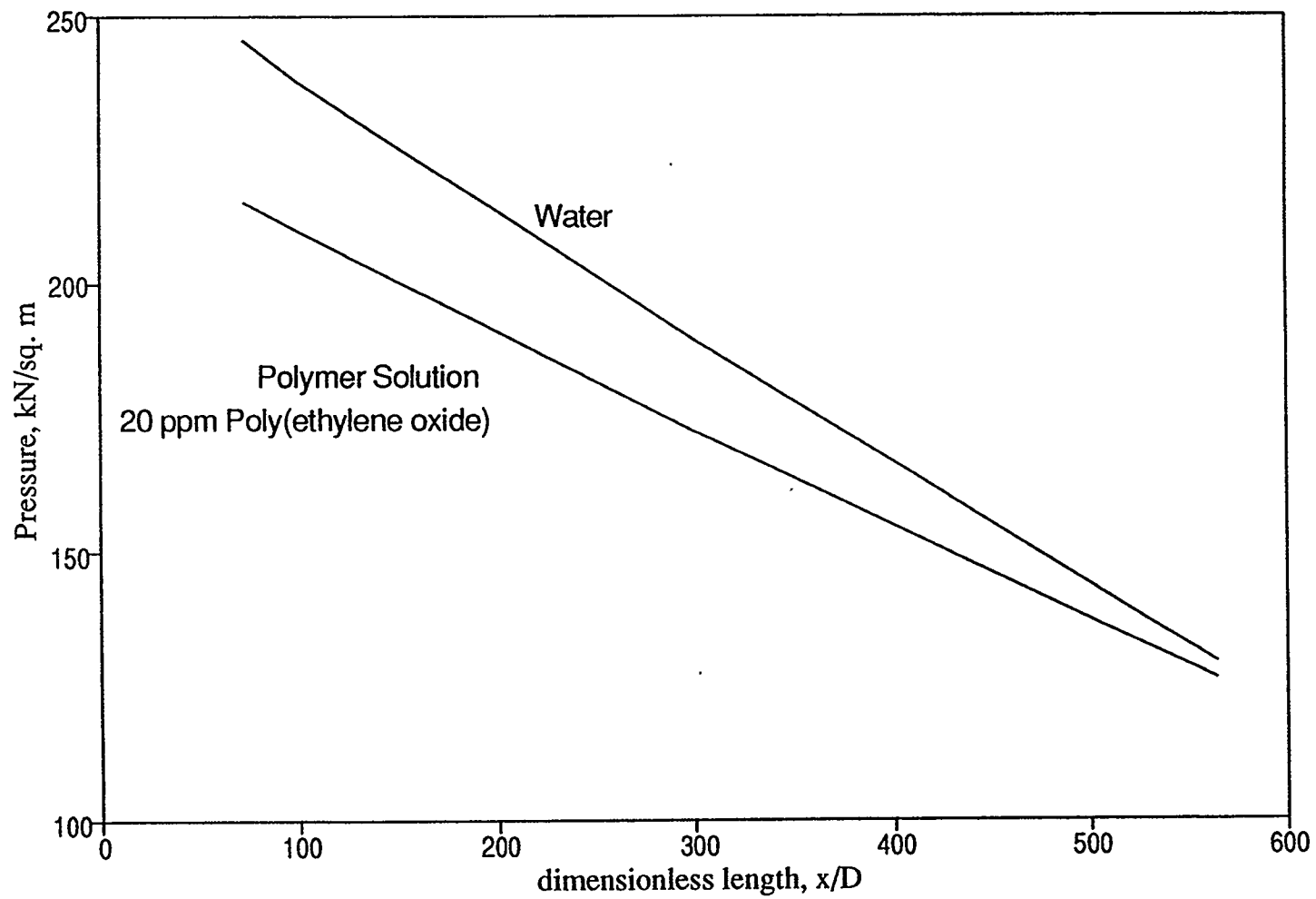
Figure 1.1. Comparison of Pressure Drop (m = 0.2 kg/s)

4

accompanied by a corresponding reduction in convective heat transfer (Dimant and Poreh,1976). During heat transfer measurements using constant flux heating for drag reducing solutions flowing in a circular pipe, obtained by passing direct current through the walls with or without a heated hydrodynamic entrance length, reduced heat transfer coefficients result in increased temperature differences between bulk of the fluid and the inner wall. This can be understood better from figure 1.2, where a comparison between fluid bulk temperature and wall temperature for a 20 ppm Poly(ethylene oxide) solution and water is made at the same flow rate and given constant flux heating.

This reduction in heat transfer can be used beneficially for transport of cooling or heating fluids over long distances where a combination of reduced pumping power and lowered heat losses may be useful. Although the reduction in friction is generally beneficial, reduction in heat transfer may have some counterproductive effects. For example, use of drag reducing additives in heat exchangers will result in enhanced flow characteristics but, at the same time a higher heat flux or increased surface area will be required to produce the same heat transfer effect (Matthys, 1991).

Reduction in heat losses can also be particularly welcome in applications which involve transport of fluids which need to be kept hot in order to decrease

$T_{i,wall}$

= 2.9 deg. C

T_{bulk}

$q = 28.9 \text{ kW/m}^2$

$m = 0.14 \text{ kg/s}$

Temperature, deg. C

Dimensionless length, x/D
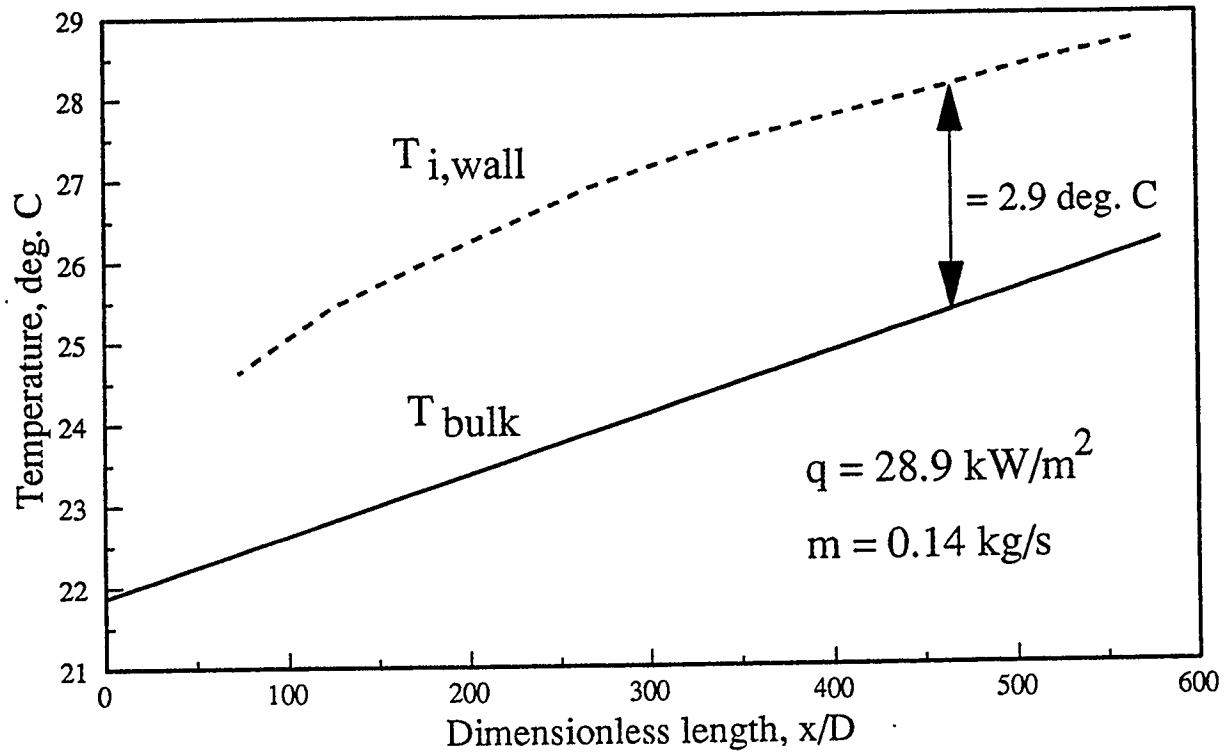
TEMPERATURE PROFILE FOR WATER

$T_{i,wall}$

= 2.3 deg. C

T_{bulk}

$q = 28.9 \text{ kW/m}^2$

$m = 0.14 \text{ kg/s}$

Temperature, deg. C

Dimensionless length, x/D
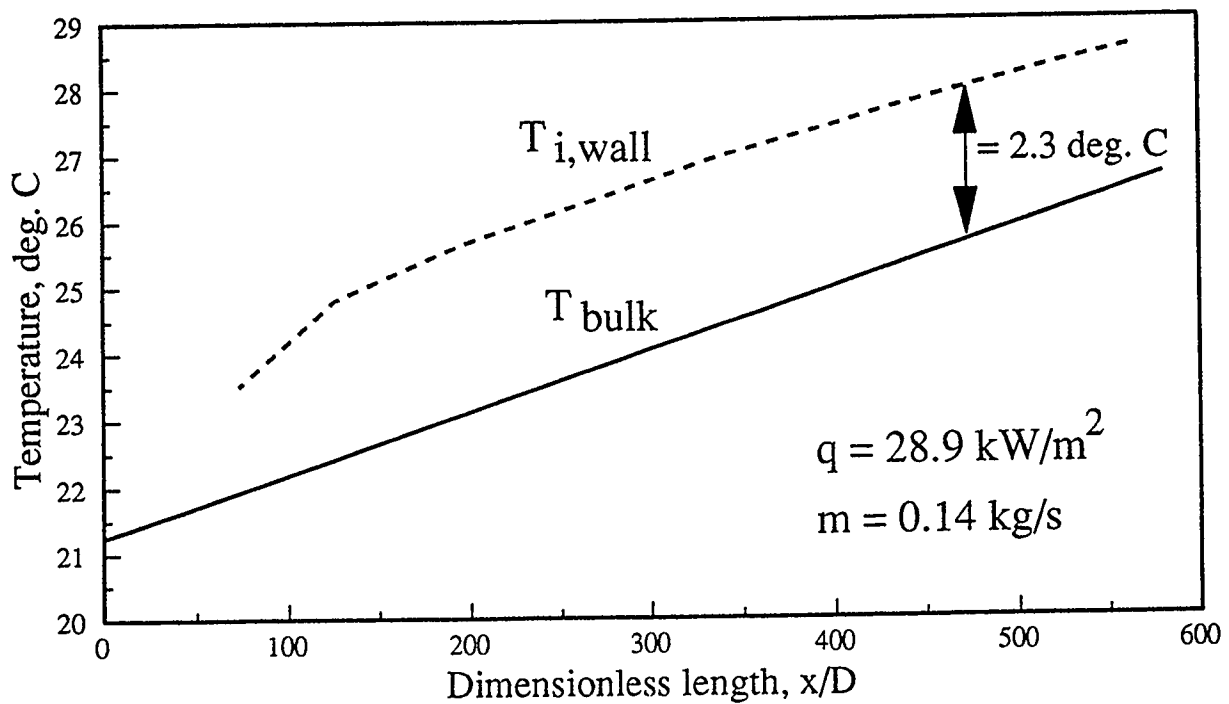
Fig. 1.2 : Comparison of temperature profiles

their viscosity. A reduction in heat transfer can also cut down the cost of thermal insulation for the pipeline wall.

1.3. Present State of Knowledge

Even though almost five decades of research have gone into studying the drag reduction produced by macromolecular additives in turbulent flow, the exact mechanism of drag reduction is not yet known. Many theories have been put forward which attempt to explain the effect. A brief review of these theories is given in the next chapter. All of them agree that the drag reduction effect is produced by the interaction of the polymer molecules with the flow in the region near the wall of the pipe. This has been proven by numerous experimental observations over the years. Investigators however are not unanimous on how exactly the molecules alter the flow field and dampen turbulence in the boundary layer region leading to a reduction in friction at the wall.

The problem of comparing experimental data with theoretical models is compounded by the difficulties involved in measuring the viscosity as a function of shear rates for very dilute solutions. In the viscometers available commercially, it is difficult to go up to very high shear rates and still keep the flow laminar thus making it impossible to measure shear viscosity in those ranges. A number of

constitutive equations are available for calculating the molecular parameters, e.g., relaxation time (see section 2.1.4.3) and low shear and high shear limiting Newtonian viscosities, for these polymer solutions but are redundant in the absence of experimental techniques to measure these parameters.

A molecule in turbulent flow is subjected to both extensional and shear deformation. The solution property named extensional viscosity (Neilsen, 1977) is likely to play a significant role, even in dilute concentrations, as it would be several hundred times larger than the shear viscosity for some drag reducing solutions (Bird, 1977). Methods have been devised to measure the extensional viscosity of concentrated polymer solutions or polymer melts (Neilsen, 1977), but very dilute solutions do not exhibit elasticity which could be measured by the current instruments that use the concept of elongational flow. Hence the constitutive equations developed based on experiments done on concentrated solutions are extrapolated with a large degree of uncertainty to describe the dilute solutions.

Most of the earlier work in the field of drag and heat transfer reduction was generally expressed in terms of a Reynolds Number based on the solution viscosity at the average bulk temperature. However, dilute polymer solutions exhibit non-Newtonian behaviour at low shear rates, while in the high shear rate

regime, the viscosity is approximately independent of shear rate (see chapter 5). In addition to being a function of shear rate, the viscosity of these solutions is also effected by change in temperature since these polymer solutions are highly susceptible to thermal degradation. Temperature correction factors need to be incorporated in all viscosity correlations to account for this effect. Recent authors (Matthys, 1987) have used the apparent viscosity at the wall, calculated at the wall temperatures, for correlating their results. This is calculated at the apparent turbulent wall shear rate based on laminar viscometric data. Measurement of shear viscosity has been done by many investigators (Hartnett,1982; Darby et.al,1991) but since the polymer solutions undergo mechanical degradation, accurate and reproducible measurements have been very difficult to obtain.

Friction and heat transfer results published in the literature on drag reducing fluids are shown against the Reynolds number of the flow, which is calculated using shear viscosity data. But, as mentioned earlier in Chapter 1, accurate measurement of shear viscosity of dilute drag reducing polymer solutions is a difficult proposition. For example, Matthys (1991) and Yoon et. al (1988) have reported heat transfer measurements for 200 ppm Poly(acryl amide) solutions wherein similar flow and heating conditions were maintained. The Prandtl numbers for these solutions differed by almost 40%, indicating that the viscosity used in the calculations were very different as the specific heat and thermal

conductivity of the fluids do not vary much with temperature. One explanation for these inconsistent results is that commercially available viscometers are unable to maintain laminar flow at extremely high shear rates that are encountered in the highly turbulent region. Hence the choice of viscosity and Reynolds number, which are essential for meaningful representation of data in fluid dynamics still remains a subject of controversy for drag reducing polymer solutions.

1.4. Focus of Current Study

For Newtonian fluids, a Reynolds number is sufficient to characterize the flow through different diameter pipes. Such is not the case with drag reducing solutions where for the same Reynolds number flow in different diameter pipes, the drag reduction and heat transfer effects are not similar. This is known as the 'Diameter Effect'. The aim of the current study was to generate a data base for future work in correlating the diameter effect for drag reducing solutions.

Friction and heat transfer measurements were obtained for flow of different concentrations of Poly(ethylene oxide) in water through two different diameter steel tubings. In addition, runs with water were also done for comparison purposes. Constant heat flux electrical heating of the wall was used to study the heat transfer reduction effect.

Viscosity measurements of four different concentrations of Poly(ethylene oxide) in water, at three different temperatures and as a function of shear rate were done to study the temperature and concentration effects on viscosity. Various constitutive equations available in the literature were tested on this viscosity data and their ability to predict the solution viscosity at very high shear rates was studied.

2. LITERATURE REVIEW

Extensive literature has been published over the last 25 years to deal with the various aspects of drag reduction and it is difficult to list all the work done in this area. This review is limited to a general account of the major lines of research developed over the years.

B.A Toms, in 1948, was the first one to notice the drag reduction phenomenon, which is also known as the 'Toms Phenomenon' after him. He observed that the friction factors exhibited during pipe flow by solutions of Poly(methyl methacrylate) in monochlorobenzene were lower than those obtained for the pure solvent. Over the next two decades, a number of drag reducing additives were identified by researchers (as listed in Table 2.1).

2.1. Drag Reduction

The complexities involved in the study of the drag reduction effect are compounded by a number of other peculiar effects that are associated with it. Each of these effects is an area for extensive investigation in itself.

TABLE 2.1 (P.S. Virk, 1975)

Drag Reducing Additives

Drag reducing Additive	Solvent
Poly(ethylene oxide)	Water
Poly(acryl amide)	Water
Poly(iso butylene)	Cyclohexane
Poly(dimethyl siloxane)	Toluene
Poly(methyl methacrylate)	Toluene
Poly cisisoprene	Toluene
Guar gum	Water
Guaran Triacetate	Acetonitrile
Hydroxyethyl cellulose	Water

2.1.1. The Diameter Effect on Drag Reduction

The degree of drag reduction is dependent on the diameter of the pipe even for the same Reynolds number and fluid. This could be interpreted as being due to the influence of the polymer molecules on the boundary layer next to the wall of the pipe and thus the effect would be seen in small pipes before large ones since the boundary layer would form a large portion of the flow in a small pipe (Savins, 1964). For Newtonian fluids a Reynolds number is sufficient to characterize flow through different diameter pipes. This 'Diameter Effect', which is typical of non-Newtonian drag reducing fluids, implies that another parameter, incorporating the fluid characteristics, is necessary to describe the flow besides the Reynolds number. Since measurement of intrinsic molecular properties (refer to section 1.4.4) of the dilute polymer solutions is an extremely difficult proposition, most of the efforts on predicting the diameter effect have been limited to methods involving scale up of results to bigger diameters for a single fluid, assuming its characteristics are constant in different diameter pipes. A set of experiments covering a large range of diameters were conducted by De Loof et. al (1977) and by Sellin et. al in 1983. Interthal et. al (1985) conducted experiments in industrial scale pipelines. Survey of literature published in the field of drag reduction till early part of 1993 reveals that scaling up methods have been proposed by T.T. Huang (3.85, 19.18, 31.81 and 50.8 mm internal diameter tubes

in 1974), Savins et. al (6.98 and 25.4 mm internal diameter tubes in 1977), Matthys et. al (1982) and Darby et. al (1.78, 2.16, 4.06, 4.67, 6.16, 7.04 and 10.21 mm internal diameter tubes in 1984). All these models have proved unsuccessful for reasonably predicting drag reduction in different diameter pipes.

2.1.2. Maximum Drag Reduction Effect (figure 2.1)

The macromolecular additives in solution will decrease the wall friction below that corresponding to its Newtonian solvent, but only down to a certain point. The solution is then said to have reached the asymptotic drag reducing conditions (Virk, 1971). Under these conditions, a further increase in polymer concentration does not lead to an additional further decrease in friction coefficient at the same Reynolds number. Virk, in 1971, proposed a correlation for calculating the maximum drag reduction asymptote in the friction factor diagram. He constructed a three layer model for the velocity profile having the usual viscous sub-layer, an elastic intermediate layer and an outer core region. The turbulent Newtonian core region diminishes if the reduction in friction increases. The maximum drag reduction effect is achieved when the elastic intermediate layer extends over the whole pipe cross section, with the exception of the viscous sub-layer. This limiting feature is also known as the 'Virk's asymptote'.
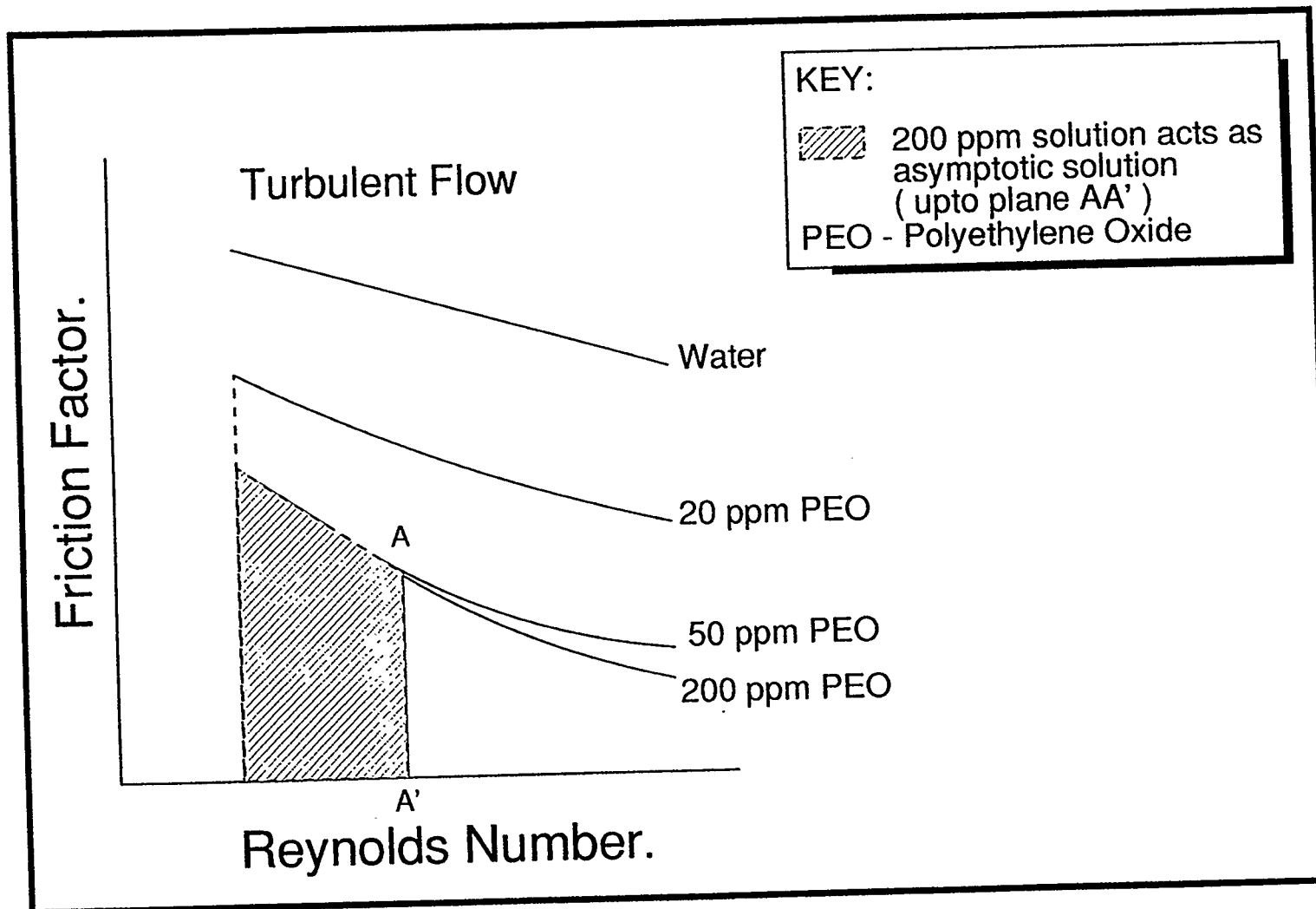
Figure 2.1 Asymptotic Drag Reduction.

2.1.3. Onset of Drag Reduction (figure 2.2)

For the drag reduction effect to become apparent, there appears to be a critical value of shear stress at the wall that should be exceeded (Gadd, 1968). In flow of the same drag reducing fluid through pipes of increasing diameter, a larger Reynolds number is required to achieve the same shear stress. For several years, a controversy has existed as to whether the onset phenomenon could be identified by a length scale or a time scale (Lumley, 1973). In turbulent flow near a wall, it is possible to identify a smallest length and a least amount of time based on kinematic viscosity and the shear velocity. Either of these could be related to a length (root mean square radius of gyration) or time (relaxation time) characterizing the molecule. Results of experiments done by Virk in 1967, demonstrated that onset occurs at a critical value of wall shear stress and that this is related to the dimensions of the polymer molecules normally defined by the root mean square radius of gyration. This suggested that the onset of drag reduction depends only on a length scale parameter. Later experiments by Berman in 1974 and Gampert in 1982 have tried to prove that the time scale hypothesis is relevant to the onset of drag reduction with polymers.

Turbulent Flow

Water

Large Diameter

Small Diameter

Polymer Solutions

Threshold
Reynolds
Numbers

Friction Coefficient
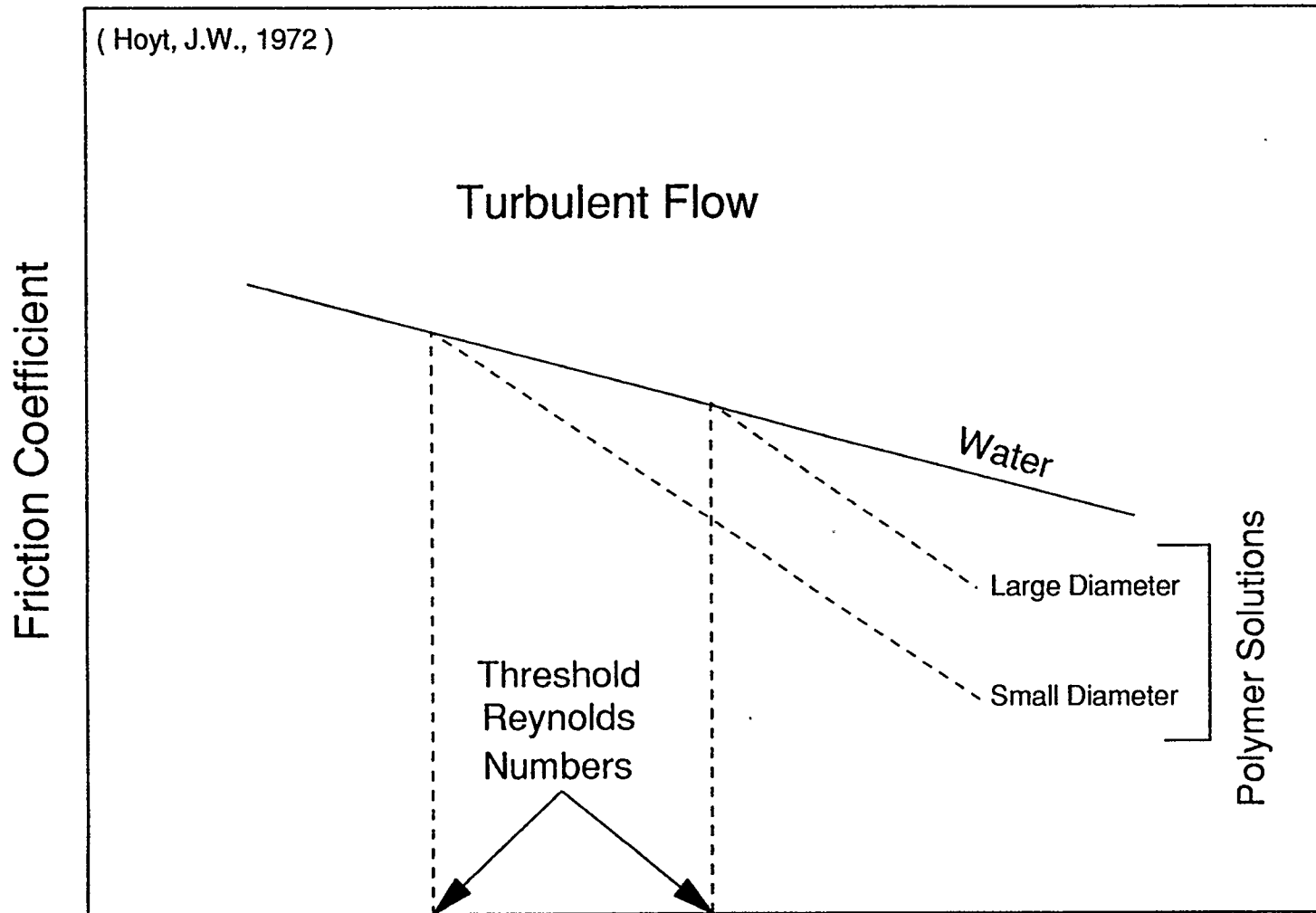
Figure 2.2 Onset of Drag Reduction

2.1.4. Theories of Drag Reduction

Many theoretical explanations have been offered over the last few decades for the drag reducing effect, although the mechanism producing drag reduction is still not known.

2.1.4.1. The Wall Effect

Experiments done by Merrill and Shaver (1959) suggested that the region near the wall plays the main role in drag reduction occurring in turbulent pipe flow of very dilute solutions of macromolecules. They injected a coloured polymer solution at the centre line of the experimental tube in which a pure solvent was flowing and observed that the drag reduction effect manifested itself only when the polymer solution diffused to the wall of the tube. B.A Toms (1948) suggested the possibility of the flow containing a shear thinning wall layer due to additional lowering of viscosity at the wall, having an extremely low viscosity which resulted in lower friction coefficients for drag reducing solutions. The possibility of the presence of a shear thinning (decrease in viscosity with an increase in shear rate) wall layer was discounted by the rheograms of drag reducing polymers (Hoyt, 1972), Poly(ethylene oxide) and Guar gum, which are not shear thinning and are in fact Newtonian by conventional viscometric methods

in the concentrations needed for optimum drag reduction. It was shown by Walsh (1967) that Polymethacrylic acid, which is essentially a shear thickening (increase in viscosity with an increase in shear rate) substance, gave considerable drag reduction. Lumley (1964) showed that turbulence should not be appreciably sensitive to shear induced changes in viscosity. The inertial forces dominate the changing viscosity effects.

El'Perin (1967) proposed the existence of an adsorbed layer of polymer molecules at the pipe wall during flow which could lower viscosity, dampen turbulence and prevent any initiation of vortices at the wall. Later work by Little (1969), with rotating disks of various materials, has shown that the surface composition of the disk does not change the observed drag reduction in polymer solutions.

2.1.4.2. Decreased Production of Turbulence

Gadd (1965, 1966) proposed that the cause of drag reduction was the decreased production of turbulence. Johnson and Barchi (1968) were the first to show experimentally the decreased production of small eddies in a developing boundary layer containing polymer. According to Walsh (1967), the polymer molecules slightly alter the energy balance of the turbulent fluctuations close to

the wall. Turbulent shear stresses (Reynolds stresses) stretch out and tend to store energy in the polymer molecules, which have a very high extensional viscosity. This process leads to viscous dissipation to destroy disturbances which would have had sufficient kinetic energy to grow into large scale disturbances downstream, resulting in lower Reynolds stresses and hence lower friction. Walsh's theory was given further support by experiments done by Wells (1971) where polymer was injected into a pipe in which the pure solvent was flowing. He found that during the injection of polymer solution into the turbulent core, no reduction in local pressure gradient occurred until the polymer has diffused into the wall region. Walsh's theory does not predict turbulence damping in a free flow and is based on the assumption that the phenomenon is essentially due to the existence of a wall boundary layer flow.

2.1.4.3. Extensional Viscosity

Another possible explanation for drag reduction involves the idea of elongational flow. It is quite likely that the addition of small quantities of polymer to a solvent leads to a substantial increase in resistance to elongational flow (i.e., resistance to deformation by tensile stresses) which is also known as extensional viscosity, thereby resulting in less turbulent fluctuations and thus lowering the turbulent drag. Maxwell's model of visco-elastic materials states that with a

purely viscous fluid, energy imparted to the system as work during shear becomes dissipated as heat, and in contrast, energy imparted to an ideally elastic material during strain becomes stored as potential energy, and may be recovered on removal of the stress. Drag reducing fluids which are visco-elastic in nature impart energy by both mechanisms (Dodge, 1959). If steady state laminar motion of a visco-elastic fluid is suddenly stopped, the Maxwell model predicts that the shear stress will decay exponentially. A parameter called 'Relaxation Time' represents a characteristic time constant for the stress decay and as such is indicative of the degree of elasticity of the system. Measurement of Relaxation time for dilute polymer solutions is extremely difficult as these solutions do not exhibit readily measurable elasticity.

Peterlin (1965) expanded this idea in such a manner that the statistical coiled polymer molecules were stretched strongly in areas with elongational flow character, which probably exists between adjacent eddies.

Tulin (1966) proposed that the polymer molecules become greatly extended in the shear direction, thus providing a stiffening effect, which absorbs energy from the turbulent eddies and radiates it away as elastic shear waves, which later decay due to viscosity. Lumley (1969) concurred with Tulin's theory that the growth of the laminar sub-layer could be explained by molecular extension, but

he found by calculation that the elongation itself is very slight. Cottrell (1970) came to the same conclusions on the basis of his experiments. In Bird's (1977) theory, the elongational viscosity can increase by up to hundred times if the polymer molecules could be stretched to their full extent.

2.2. Heat Transfer Reduction

Though the problem of drag reduction has been under investigation for over three decades now, the phenomenon of convective heat transfer reduction that accompanies it has not received as much attention. Drag reducing visco-elastic solutions have heat transfer characteristics which are totally different from the Newtonian fluids, a fact that was ignored by early investigators and led to experimental measurements and modelling efforts based on wrong assumptions as mentioned below.

Turbulent heat transfer performance of drag reducing fluids flowing through circular pipes is characterized by thermal entrance lengths as long as 400-500 pipe diameters (Ng et. al, 1977). This is in sharp contrast to Newtonian fluids in turbulent flow, which have thermal entrance lengths of the order of 10-15 pipe diameters (Deissler, 1955). Most of the early researchers were unaware of this critical fact and hence carried out runs in relatively short tubes, leading to

collection of data in the thermal entrance region rather than in the region of fully developed flow (e.g. Astarita, 1967; Gupta et. al, 1967; Smith et. al, 1969). Hence steady state heat transfer characteristics in the fully developed temperature and velocity profile region, which have practical implications, could not be studied.

Reynolds analogy assumes that eddy diffusivities for momentum and heat transfer are approximately equal. It is based on the concept that the physical mechanisms leading to the transport of momentum and energy by mixing are very similar. This analogy does not hold true for drag reducing solutions ($Pr \cong 10$), which typically have rather long thermal entrance lengths as compared to the hydrodynamic entrance lengths. Khabakhpasheva and Perepelitsa (1973) measured velocity and temperature profiles for aqueous solutions of Poly(acryl amide) and used them to calculate the eddy diffusivities of momentum and heat. They observed that eddy diffusivity of heat was smaller than the eddy diffusivity of momentum. This was the first visco-elastic heat transfer study not based on the Reynolds analogy.

Drag reducing fluids are highly susceptible to mechanical degradation. Yoo (1974) and Matthys (1985) measured the friction factor and heat transfer coefficient for a degrading aqueous solution of 100 ppm Separan AP-30 in a recirculating flow loop. They showed that both the friction factor and heat transfer

coefficients increased substantially, approaching the values of Newtonian fluids for the severely degraded case.

Ever since Virk et. al (1970) reported the existence of the maximum drag reducing asymptote for drag reducing fluids, there have been attempts to identify the corresponding maximum heat transfer reduction, or the minimum heat transfer asymptote. Correlations for predicting the minimum heat transfer asymptote were postulated by Cho and Hartnett (1982) and Matthys (1991). As in the case of friction, the non dimensional numbers used in the case of Newtonian fluids are not sufficient to correlate non-asymptotic heat transfer results in different diameter pipes.

2.2.1. Diameter Effect on Heat Transfer Reduction

Very little work has been done in the field of predicting the 'Diameter Effect' on heat transfer reduction. Cho and Hartnett (1982) carried out heat transfer measurements in three different diameter pipes for different concentrations of Poly(acryl amide) solutions in water.

A prediction technique for drag reduction and heat transfer reduction was developed by Matthys et. al (1982). A simplified three layered model for velocity

profile (Virk, 1975) was assumed which included a shift of the logarithmic layer. A relationship was derived between this shift and the friction velocity and assumed to be valid regardless of the diameter of the pipe. Analogous assumptions were made for deriving the correlation for prediction of heat transfer reduction in different diameter pipes. This technique was not tested at the time for lack of experimental data.

Yoon and Ghajar (1988) developed another prediction technique. They used the characteristic frequency of the smallest energy dissipating eddies (Astarita et. al, 1969) to correlate heat transfer reduction in different diameter pipes. This technique reportedly fits their experimental data obtained in two different diameter pipes.

3. EXPERIMENTAL SET-UP AND TECHNIQUES

The main objectives of the research project were to make friction and heat

transfer measurements for a polymer solution flowing through different diameter

steel tubings. The design of the experimental set-up was done keeping in view the

constraints imposed by the characteristic of the polymer solution to undergo shear

induced degradation.

To inhibit degradation of the polymer solution in the system, the following

features were incorporated while building the experimental set-up:

- A single pass system was used.

- To avoid contact of the polymer solution with any moving parts (i.e., in

    a pump which leads to high shear zones), air pressure was used to make

    the solution flow through the system.

- Flexible Polypropylene tubing was used everywhere, except for the test

    section which was made of SS 304 tubing, to avoid bends and fittings

    which cause additional friction due to discontinuous surfaces and lead to

    unnecessary degradation of the polymer solution.

- Agitation in the solution preparation tank was done by passing air bubbles

    from a compressed air cylinder. The air entered the tank at the bottom

    and a gentle flow over a period of one hour was observed to provide

sufficient circulation to mix the solution and break up any small gels formed in the tank. This proved to be an effective substitute to mechanical agitation, which would have degraded the polymer solution to a certain extent even before the actual run. This method was relied upon since no chemical or visual method is available to test the homogeneity of the solution.

- The holes drilled on the tubing for pressure tappings were carefully cleaned on the inside to remove any pieces of metal sticking to the inside of the holes.

- Instead of using an online flowmeter, which might have moving parts in contact with the solution, the mass flow rates were measured by collecting samples over a period of time and weighing them. This is probably the most accurate way of measuring the flow rates.

The data acquisition system selected for making measurements was directly connected up to a PC386 which made it possible to simultaneously collect data at a large number of points. It could make measurements as a function of time and perform averaging of the data as the run progressed. The software also enabled graphical monitoring of measured data during the course of a run.

A constant heat flux mode was employed to study the heat transfer

characteristics of the polymer solution, which was obtained by direct heating of the stainless steel tubing. A DC power supply was connected to the two ends of the test section and the electrical resistance of the tube generated the heat flux. Care was taken to isolate the test section from the rest of the flow loop.

As the fluid flows through the tube, the temperature of the wall and the bulk fluid rises in the axial direction. Also, due to the insulated boundary condition at the outer wall surface, a temperature profile exists in the wall in the radial direction. Effect of these temperature variations on the heat flux is discussed in Chapter 5.

The entire test section was supported in such a way that it allowed for free thermal expansion of the tube at both ends. No clamps were used all along the test length and the supports were designed so that the tube rested freely on them. The supports could slide on a square metal tube which was used as the base support.

A detailed flow diagram of the experimental set-up is shown in figure 3.1.
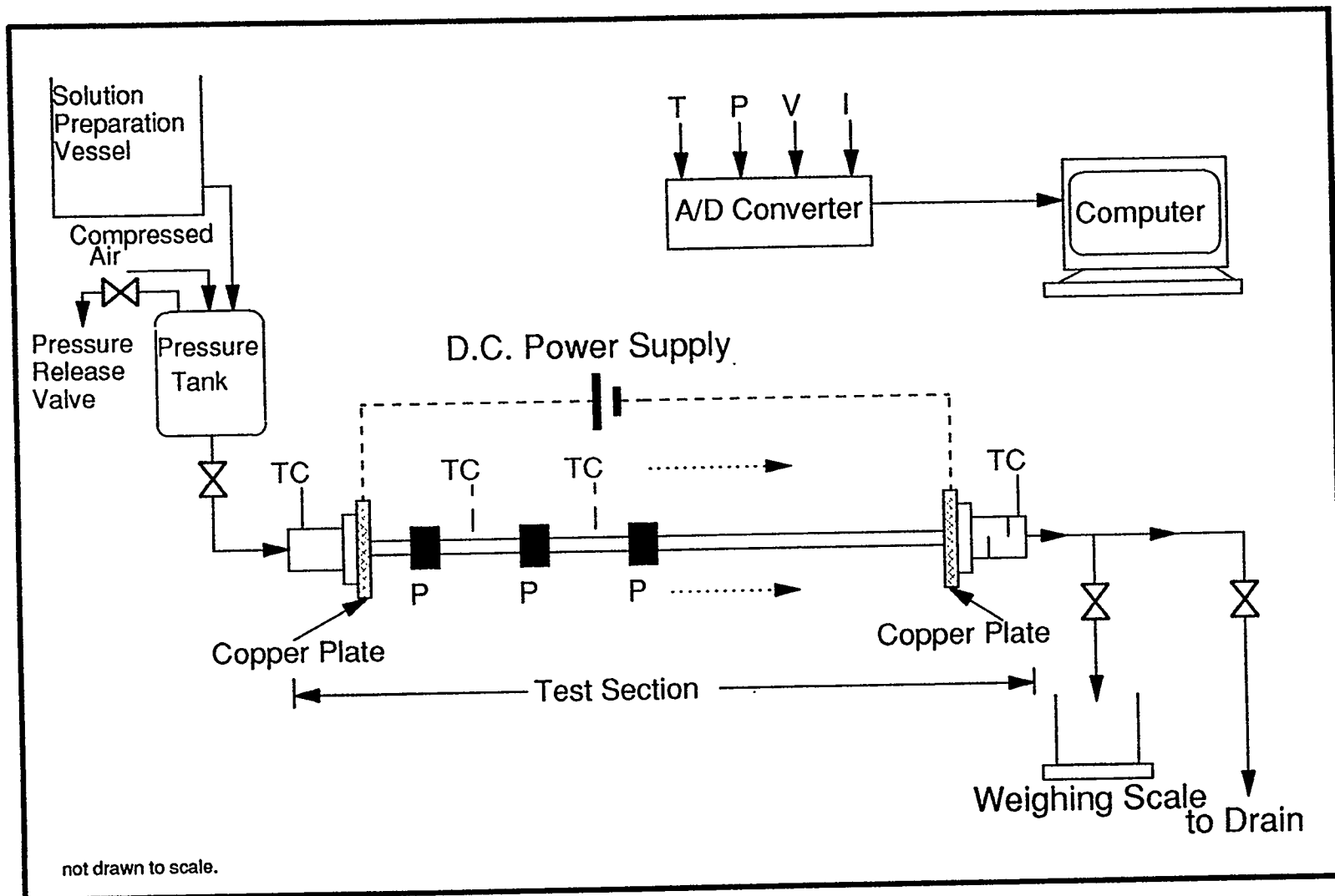
Figure 3.1 Experimental Setup

3.1. Experimental Set-up

3.1.1. Solution Preparation Tank (figure 3.2)

The polymer solution was prepared in a 1.15 m^3 high density polyethylene tank. The dimensions of the tank are shown in figure 3.2. The tank was elevated on a steel platform to facilitate transfer of the solution to the pressure tank by gravity drainage. The tank was provided with a draining line at the bottom to allow cleaning of the tank before solution preparation.

3.1.2. Pressure Tank (figure 3.2)

The prepared polymer solution was gravity drained into an SS 304 cylindrical pressure tank of 0.45 m^3 capacity with dished ends. As shown in figure 3.2, the pressure tank was fitted with a plastic sight tube for monitoring the level of liquid inside the tank. Air at 311-346 kN/m^2 from a compressed air cylinder was used to push the solution from the bottom of the tank and through the flow loop. The tank has a pressure release valve which was set to go off at 484 kN/m^2 and a pressure gauge to monitor the pressure inside the tank. According to the design specifications supplied by the manufacturer, the tank has a maximum operating pressure limit of 830 kN/m^2 and a burst pressure of 1245
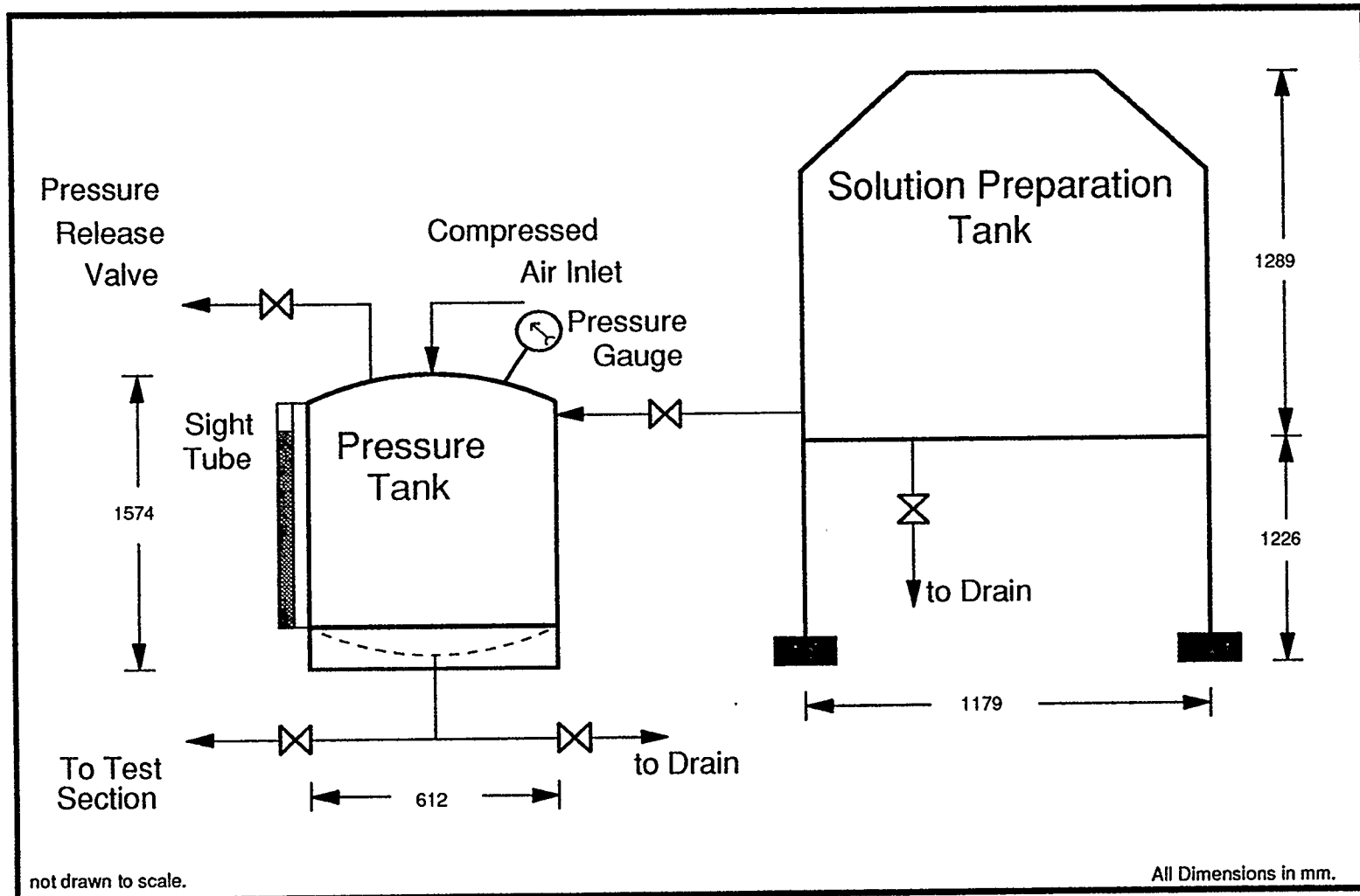
Figure 3.2 Layout of Pressure Tank & Solution Preparation Tank.

kN/m^2. The bottom of the tank was connected to the test tube using 12.7 mm OD flexible high pressure polypropylene tubing. An SS 316 needle valve with a regulating stem was fitted to the line coming out of the pressure tank to control the flow rate through the test section.

3.1.3. Flow Calming / Flow Mixing Chamber (figure 3.3)

Just before the solution entered the test section, it passed through a flow calming section which was a plexiglass chamber of 75 mm inside diameter. Turbulent fluid flow in a circular pipe is characterized by a boundary layer flow and an inner core of bulk flow. In the bulk flow region, the velocity profile is flat and coherent eddy structures are present. Turbulent fluctuations are confined to the boundary later flow. The flow calming chamber, which is approximately 10 times in diameter than the test section, ensured that uniform flow with a flat velocity profile entered the test section. Also, an increase in diameter from the vinyl tubing (2.00 cm) to flow calming chamber (8.9 cm) reduced the shear stress at the wall and hence less turbulent fluctuations resulted in the flow calming chamber. The inlet temperature of the liquid going to the test section was measured here by means of a thermocouple probe sitting in a glass capillary tube which projected into the chamber.
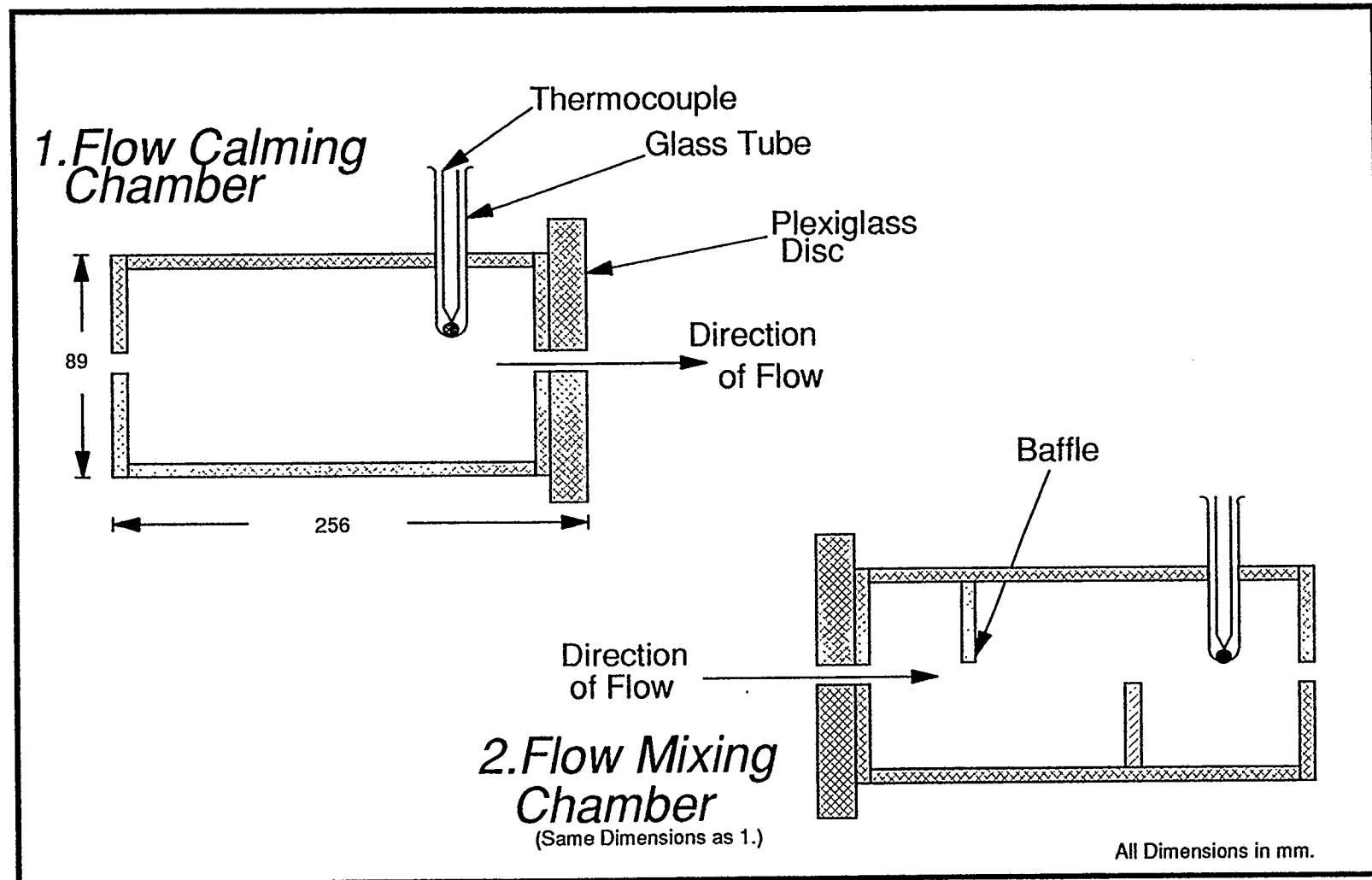
Figure 3.3 Flow Calming & Flow Mixing Chambers.

At the end of the test section a flow mixing chamber ensured that a well mixed outlet temperature was measured. The flow mixing chamber was a plexiglass chamber of same dimensions as the flow calming section with two half discs fitted inside to act as baffles. When the fluid flows past an obstruction, such as a flat plate, a high vorticity region is generated at the back of the plate due to flow separation and leads to the formation of wakes which increase the intensity of turbulence and provide effective mixing. Such an arrangement was necessary because the constant flux heating at the walls results in non-uniform fluid temperatures across a given cross section as the fluid next to the wall has a higher temperature than the fluid near the centre of the tube.

3.1.4. Test Tube (figure 3.4)

Two different diameter SS 304 tubings (9.53 mm OD and 12.7 mm OD) were used in the current study for making pressure drop and heat transfer measurements. Both the tubes had a wall thickness of 1.2 mm. Drag reducing polymer solutions in the 500 ppm concentration range reportedly (Cho and Hartnett, 1982) have a thermal entrance length of about 500 diameter for high Reynolds number flow, which led to the use of approximately 600 diameter long tubes in both the cases.

+
to A/D Converter Card
-
Pressure Transducer

Pressure Tap Collar

Steel Tube

Screw Head(Adjustable Height)

Plexiglass Support

Square Tube Base

not drawn to scale.
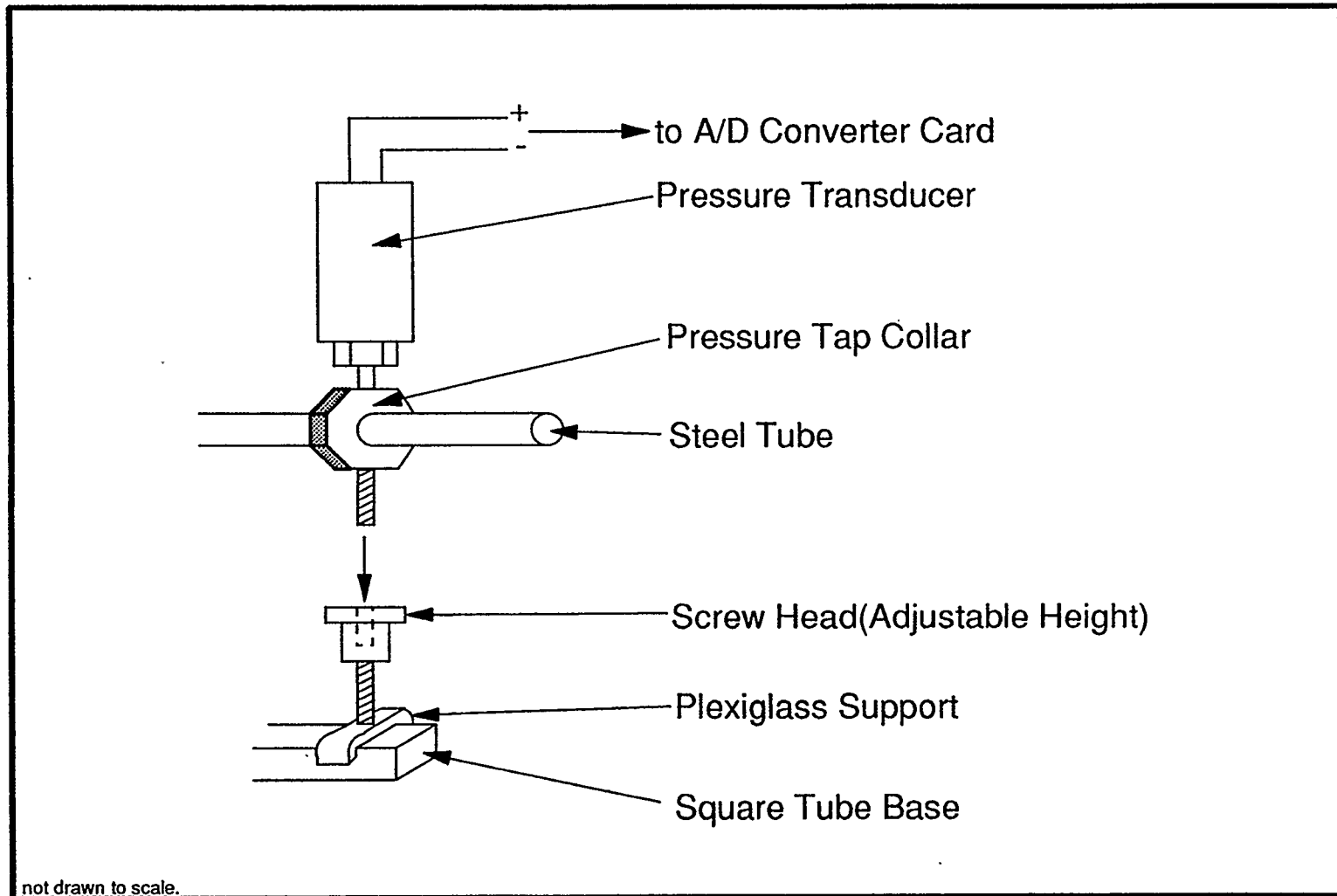
Figure 3.4 Arrangement of Support for the Test Tube.

To ensure that the test tubes were in the horizontal plane when making experimental measurements, the supports used all along the length of the tubes had screw heads, which could be used to adjust the height of the tubes (as shown in figure 3.4).

3.1.4.1. Pressure Measurement (figure 3.4 and 3.5)

Pressure drop along the length of the tube was measured by ten pressure transducers (Barksdale CVD-2000, 0 to 120 psi). The positions for the pressure tappings (figure 3.8) were selected in such a way that they were closely spaced in the first half of the tube so that data could be gathered to study the development of the hydrodynamic entrance region. At each pressure tap location, two holes, 1.5 mm in diameter, were drilled diametrically opposite and a teflon collar was placed over them (figure 3.5). The teflon collar has a sealed circular chamber overlapping the two holes which was also connected to the pressure transducer. This arrangement allowed the measurement of average pressure across the cross section where the pressure tap was located. Drilling of the holes resulted in the formation of burrs inside the tubes which were cleaned carefully to avoid any unintentional distortion of the flow and unreliable pressure readings.

To Pressure
Transducer

"O" Rings
(1mm diam.)

Steel Tube

Direction of Flow

Teflon Pressure
Tap Collars

33   70

6
25

not drawn to scale.

All Dimensions in mm.
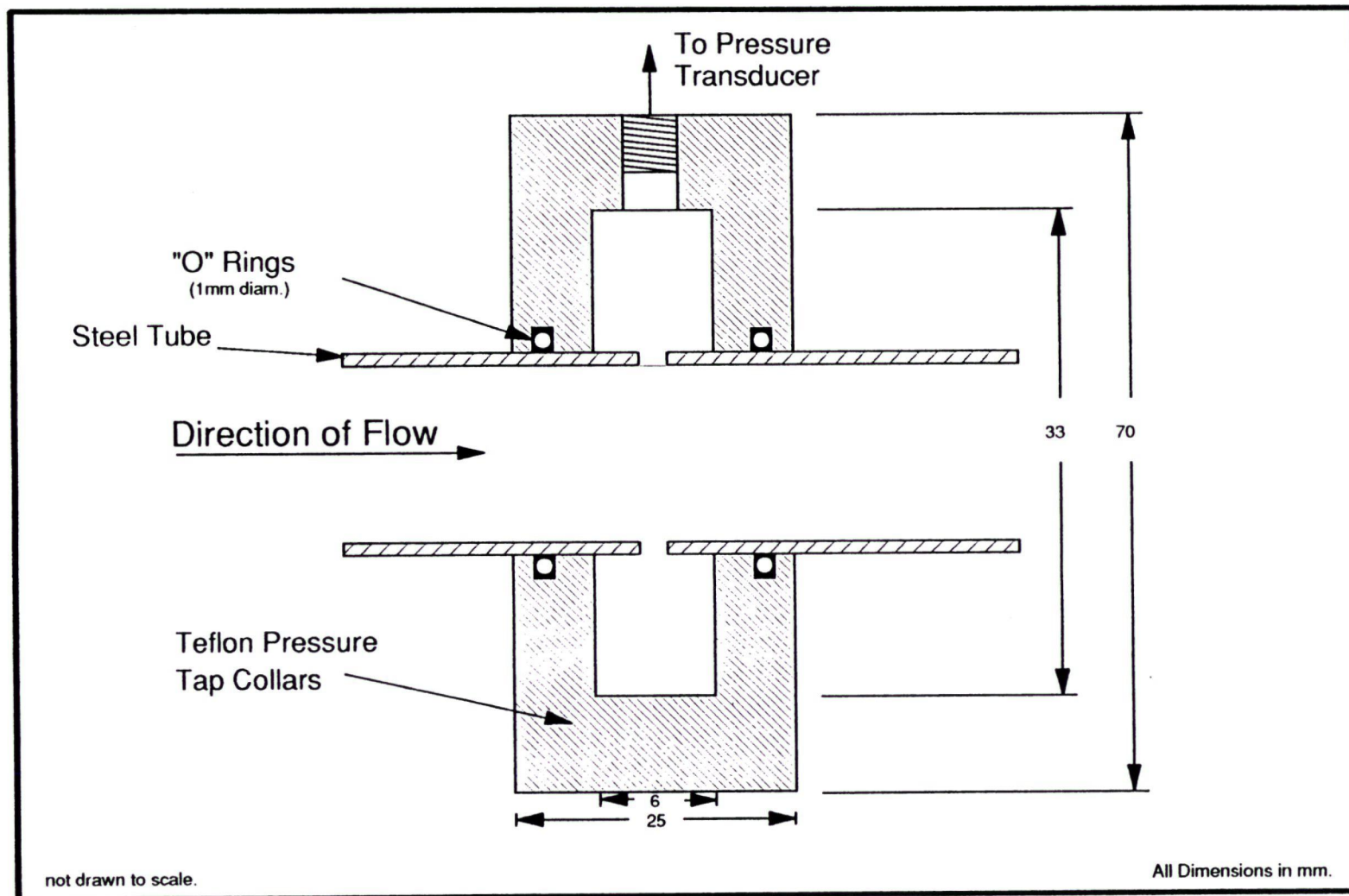
Figure 3.5 Inside View of a Pressure Tap.

3.1.4.2. Temperature Measurement (figure 3.6)

For heat transfer measurements 'T'-type 30 gauge copper-constantan thermocouples were attached at 8 different locations axial locations on the surface of the tube. Two thermocouples were attached diametrically opposite at the same axial location.

Bare thermocouple probes could not be attached directly to the tube surface as the DC current passing through the tube for constant flux heating would have distorted the readings. To overcome this problem, a Beryllium Oxide (BeO) disc, 6.35 mm in diameter and .76 mm thick was attached on the surface of the tube. The disc offers excellent thermal conductivity and electrical resistivity. Its normal use is in the cooling of power transistors. The following procedure for thermocouple installation was employed:

- A drop of heat sink compound was placed on the tube at the correct spot.

- The BeO disc was put on the spot over the drop of heat sink compound and a little more of the compound was put on it.

- Teflon tape was wrapped around the tube up to this spot.

- The thermocouple was placed in position, so that its tip was embedded in the heat sink compound on the BeO disc and wrapped with a further
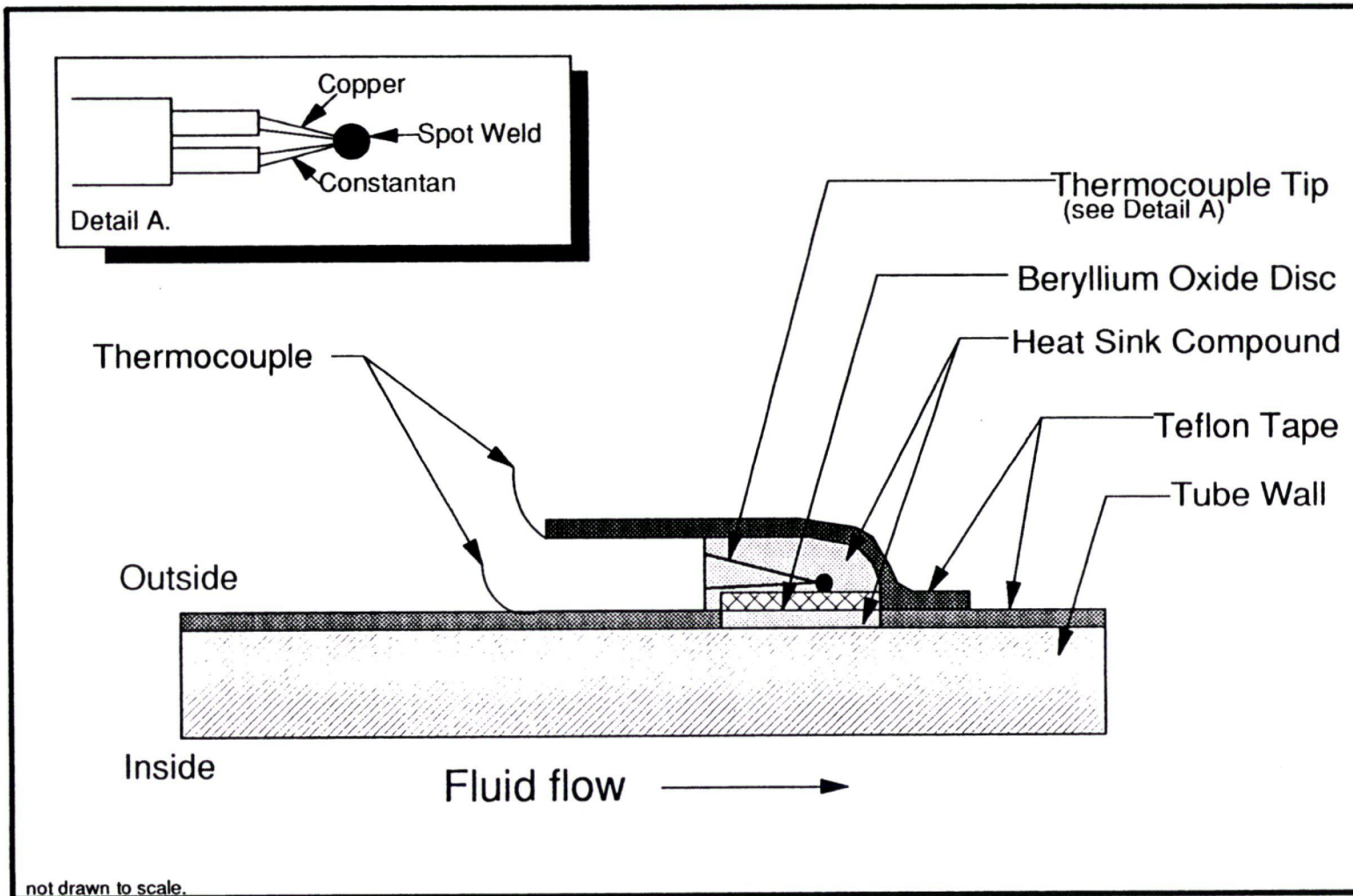
Figure 3.6 Thermocouple Attachment Technique.

layer of teflon tape to hold it in place.

3.1.5. Constant Flux Heating

Heating of the tube was done by DC power. A 13.5 kW DC welder which could work in constant current or constant voltage mode was used for this purpose. The electrical resistance of the tube generated heat, which was transferred to the solution flowing through the tube.

For passing DC power through the test tube, Copper plates were soldered on to the tube at both ends and the leads from the DC power supply were clamped tightly to them (figure 3.1).

The test section was electrically isolated from rest of the flow system by placing phenolic discs in between the copper plates and the flow calming/flow mixing chamber at the two ends of the tube. Phenolic is not only an electrical and thermal insulator but can also withstand operating temperatures of up to 150°C, hence it was considered suitable for use in our experimental set up as runs were to be carried out in the temperature range of 20 °C-50 °C.

The tube was wrapped with teflon tape all along the length to insulate it

against heat losses to the ambient. In addition, a rubber insulation, which is used for low temperatures, was used on top of the teflon tape to ensure that the heat losses were minimised.

3.1.6. Flow Measurement

Mass flow rate of the solution flowing through the system was measured by weighing a sample collected over a known period of time. A Mettler PC 1616 weighing scale and a stop watch were used for this purpose.

3.1.7. Data Acquisition System

Relatively short runs at high flow rates made the manual collection of data at a large number of points impossible. Consequently, an on line data acquisition system was used which was directly connected to the computer, where with the help of a software data files were generated. The software also enabled on-line graphical monitoring of the run conditions which proved useful for keeping track of any abnormalities during the course of a run. Also, since we were interested in collecting data at steady state, the graphical display was used to determine when they had been reached and thus eliminated collection of data in the unsteady state.

The signals from the 10 pressure transducers, 18 thermocouples and the voltage and current output from the DC power supply were fed to two Analog to digital conversion cards. With the help of a computer interface card, these signals were transmitted to the computer where the data acquisition software interpreted the signals and provided the output in engineering units. Data were collected at a frequency of 4 Hz. The software received 4 readings per second from each input device, calculated the average and wrote the final value to a file.

3.2. Experimental Techniques

3.2.1. Preparation of Polymer Solution

The polymer solution was prepared in the 1.15 m³ polyethylene tank according to the following procedure which was strictly adhered to in preparing the solutions for all runs:

The tank was filled up to the half level with tap water. Since the tap water temperature in Calgary is around 5°C, the water was allowed to stand in the tank for about two days to bring it to room temperature.

The addition of polymer to water was a time consuming process. Rapid addition of powder to water leads to the formation of large chunks of gels which take a long time to go into solution. Polyox WSR 301 is in the form of an amorphous powder and has a very low bulk density. An improvised method of adding the powder to the water was devised, as shown in figure 3.7, to ensure that all of the powder went into the solution. The nozzle fitted to the bottle allowed only a small amount of powder to issue out in a steady stream. The bottle and funnel arrangement was placed under a jet of tap water with the funnel tip only a few millimetres away from the water surface in the tank. Once the powder started to come out of the nozzle, the bottle and funnel arrangement was moved in and out of the path of the water jet in a horizontal plane. It was in fact a manually controlled periodic motion which ensured that when the bottle was not in the path of the water jet, the jet fell on the powder sitting on the water surface, thus sending it into the water mass instantly. When the bottle was in the path of the water jet, the water spray from the top of the funnel wetted the powder which came out of the nozzle when the bottle was not in the path of the water jet. Thus the to and fro motion of the bottle resulted in all the powder being wetted the instant it came out of the nozzle. It also prevented the formation of gels of polymer mass which take a long time to go into solution and sometimes need to be broken up manually.

1. Place On Bottle (See No. 2)

Nozzle

Powder

2.

3. Motion of Bottle

Water Jet

Wall of Vessel

Water

Key:
- - -▶ Water
······▶ Powder
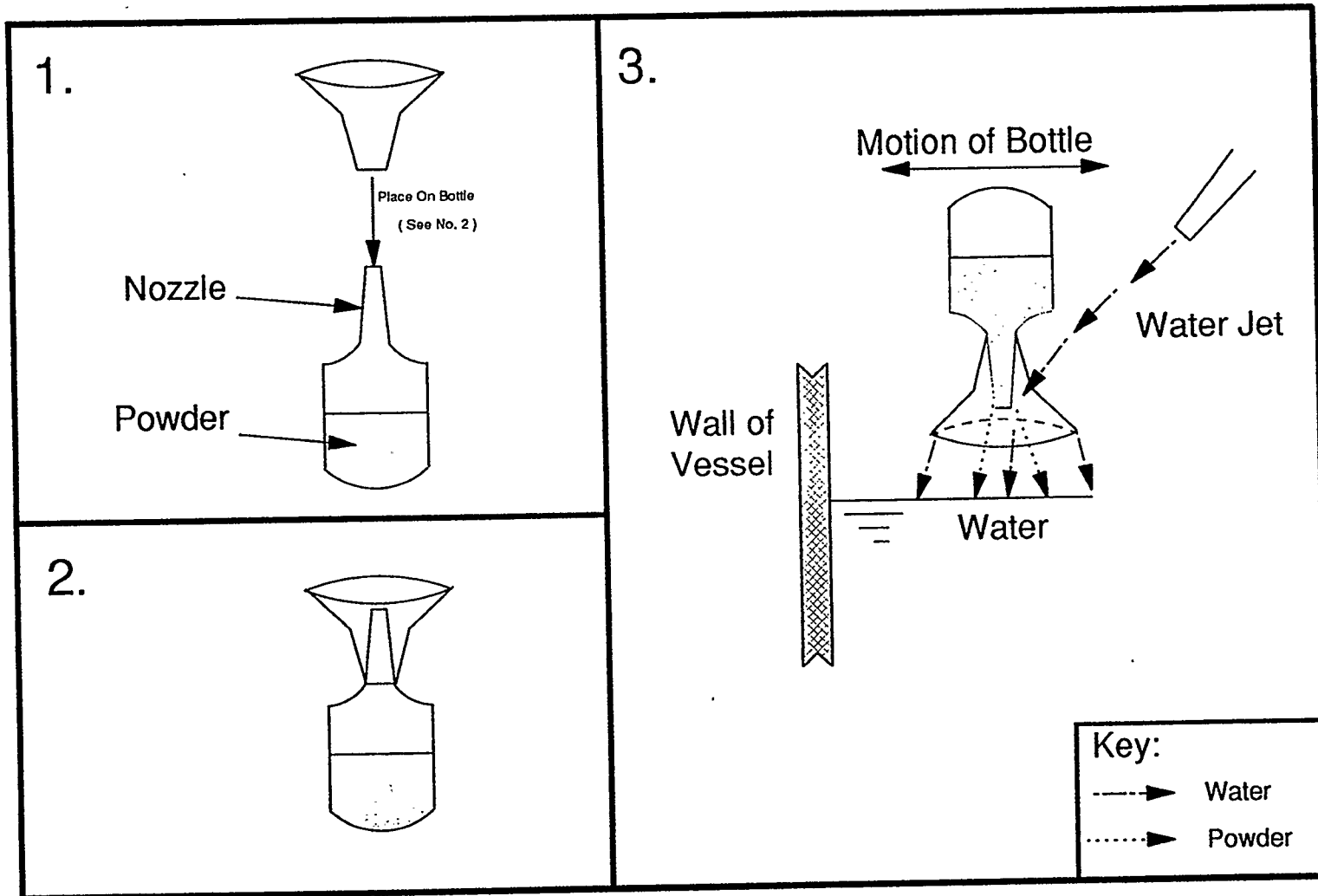
Figure 3.7 Solution Preparation Technique.

The powder was added to the water mass while the tank got filled up to about three fourths of its capacity. The polymer took about 36 to 48 hours to dissolve. During this period, air was gently bubbled through the tank from the bottom to provide agitation and ensure uniform mixing of the contents in the tank. This also helped in dislodging small gels of polymer which might have been sticking to the walls of the tank.

The water level in the tank was made up before the run to achieve the required concentration of polymer in the solution.

3.2.2. Experimental Run Procedure

The following sequence of operations was followed for every experimental run:

The polymer solution preparation tank was cleaned with water to remove any traces of the previous solution. A fresh polymer solution of required concentration was prepared. The pressure tank was cleaned and the flow system was purged with water to ensure that no polymeric material from previous run was remaining in the system. The flow calming and flow mixing chambers were drained to remove accumulated water. Before draining the prepared solution into

the pressure tank, air was bubbled through the solution preparation tank to ensure uniform concentration. After about an hour, the solution was drained to the pressure tank. The level of the liquid in the pressure tank was monitored through the sight glass and when the tank was filled to the top, the draining valve was closed and the line from the compressed air cylinder was connected to the pressure tank. The pressure regulator on the cylinder was set to the desired pressure. The desired output from the DC power supply in the constant voltage mode was selected. The pressure tank was pressurized by opening the valve from the compressed air cylinder. The needle valve just before the entrance to the test section was set for the desired flow rate. The valves at the end of the test section were set to allow draining of the solution during the initial parts of the run. The Data Acquisition System was put online to graphically monitor the run conditions. The valve at the bottom of the pressure tank was opened to let the solution flow through the system. The DC power supply was turned on to pass electric current through the wall tubes. A constant watch was kept on the graphical display to ensure that the pressure and temperature profiles had reached the steady state values. At steady state conditions, transfer of data to the data files was initiated and by adjusting the valves, the flow at the outlet of the system was directed to the tank on the weighing scale for a set period of time (using a stop watch) to measure the mass flow rate. The valves were then again switched to allow flow of the solution to the drain. Transfer of data to the data files was stopped. The

power supply was turned off and the valve at the bottom of the pressure tank was closed to complete one cycle of operation.
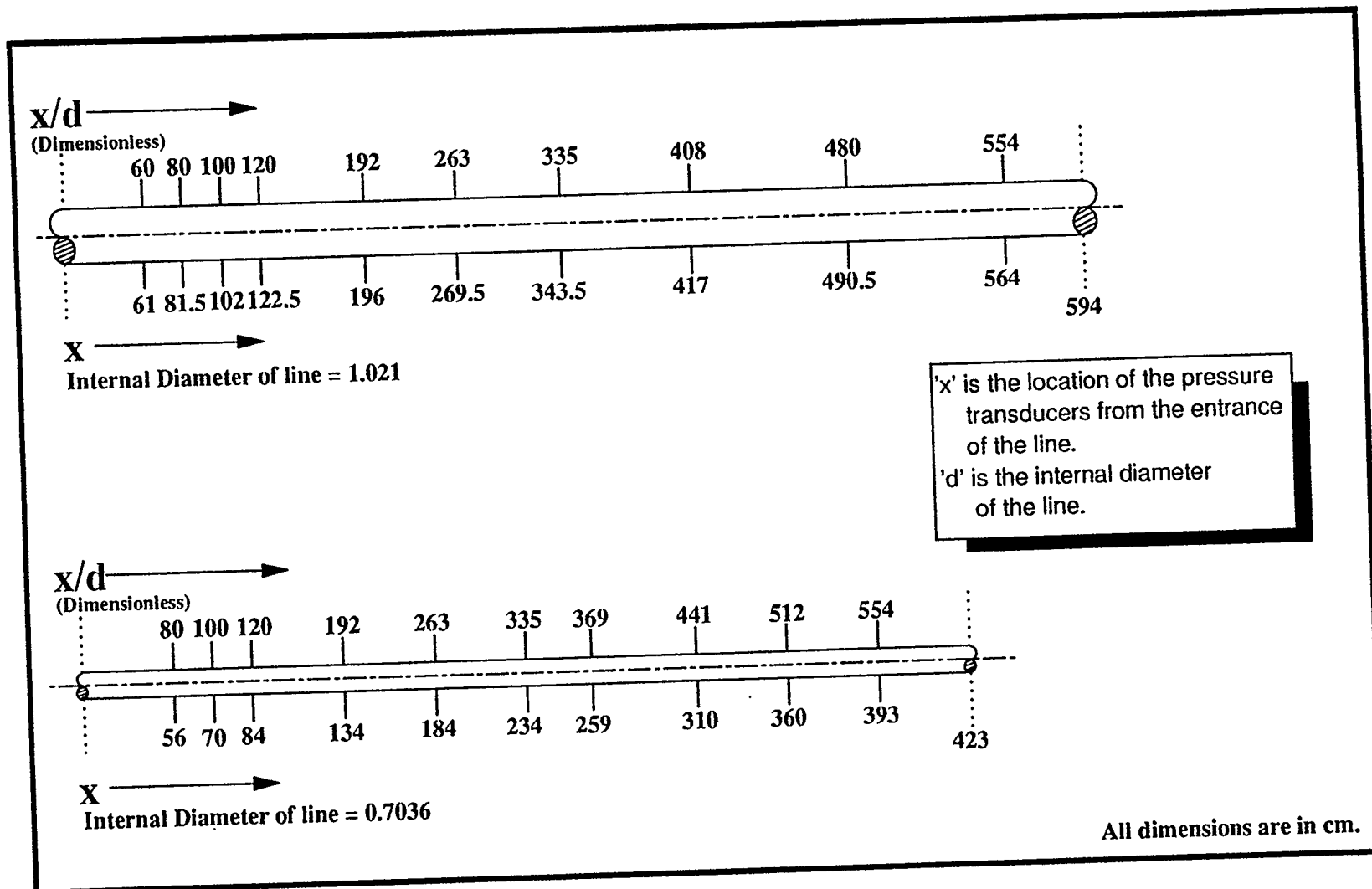
Figure 3.8 Location of Pressure Taps on Test Tubes.

4. VISCOSITY MEASUREMENTS

4.1. Nature of Drag Reducing Polymer Solutions

Fluids are classified on the basis of their response to applied shearing stresses in the laminar flow regime. Newtonian fluids exhibit a direct proportionality between shear stress and the induced rate of shear.

$$\tau = \mu \left(\frac{du}{dy} \right) \tag{4.1}$$

The constant of proportionality, μ, is the fluid viscosity. All those fluids that do not conform to the above equation are categorised as non-Newtonian fluids. For these fluids, the viscosity varies with the imposed conditions of shear and is called the apparent viscosity.

Drag reducing polymer solutions exhibit a decrease in apparent viscosity with an increase in shear stress. This is known as pseudo-plasticity, which is the most common type of non-Newtonian behaviour. In a plot of shear stress versus shear rate for a pseudo-plastic solution, the slope of the tangent at the origin is the apparent viscosity at zero rate of shear and the slope of a straight line drawn asymptotically to the curve at high values of shear rate is called the limiting

viscosity at infinite shear.

4.2.1. Viscosity Measurement Procedure

Viscosity measurements were carried out using two concentric cylinder viscometers to cover a broad range of shear rates. A Contraves Low Shear viscometer was used for shear rates from 0.204 sec^{-1} to 128.5 sec^{-1}. A Contraves High Shear 6 viscometer was used for shear rates from 297.0 sec^{-1} to 1340 sec^{-1}.

To study the effect of concentration and temperature on the shear viscosity of Poly(ethylene oxide) solutions in water, viscosity measurements were carried out for 20, 50, 100 and 200 ppm solutions at 25, 35 and 45°C. In addition, the viscosity of tap water which was used for preparing the solutions, was also measured at the above three temperatures for comparison of results. Two separate solutions of 200 ppm concentration were prepared and their viscosity was measured at the above three temperatures to verify the repeatability of the measurements.

Tap water contains dissolved gases which come out of the solution at high temperatures and can change the viscosity of water by a considerable extent. The tap water used for making the solutions was degassed beforehand. Only a few

bubbles were observed during the viscosity measurements at high temperatures which did not affect the viscosity of the solutions.

4.2.2. Viscosity Measurement Results

Measurement of shear viscosity constitutes an important part of the data interpretation for dilute polymer solutions. At low shear rates, the viscosity of the solutions decreases with an increase in shear rate. Though at high shear rates the viscosity of the solutions tends towards an asymptotic value, the effect of temperature is very pronounced due to the susceptibility of the polymer solutions to thermal degradation at higher temperatures.

The choice of viscosity to be used in the calculation of Reynolds number for characterising the flow of drag reducing polymer solutions has been a point of much debate over the last decade (Hartnett, 1982). In our heat transfer experiments, constant flux heating at the wall was used. This led to a non uniform temperature distribution in the radial direction at the same axial position during flow experiments. Since in our experiments the outer wall temperatures were measured, the apparent viscosity at the wall was considered appropriate for calculation of the Reynolds number. To take into account the effect of temperature on viscosity, measurement of viscosity at different temperatures

covering the range of temperatures encountered in our experiments was done. Figures 4.1 through 4.4 show the results of these measurements which show the effect of temperature and concentration on viscosity of Poly(ethylene oxide) at different shear rates.

The viscosity measurement results shown in figures 4.1 through 4.4 are consistent, with the viscosity of the solutions increasing with an increase in concentration. At low shear rates, the viscosity of the solution decreases with an increase in shear rate. At higher shear rates, the viscosity tends to approach an asymptotic value indicating that at these shear rates the solutions are approximately Newtonian by conventional viscometric methods. The viscosity of the polymer solutions is also seen to be a function of shear rate, which is typical of non-Newtonian fluids. Figure 4.5 shows the repeatability of the measurements with two 200 ppm solutions.

A number of models have been proposed over the years which try to predict the viscosity behaviour of the drag reducing polymer solutions. A list of these equations is provided in Table 4.1. An iterative least squares regression routine was used to fit these constitutive equations to our experimental data (figures 4.6 through 4.8). It was observed that the second and higher degree polynomials fit the experimental data well at low and moderately high shear rates
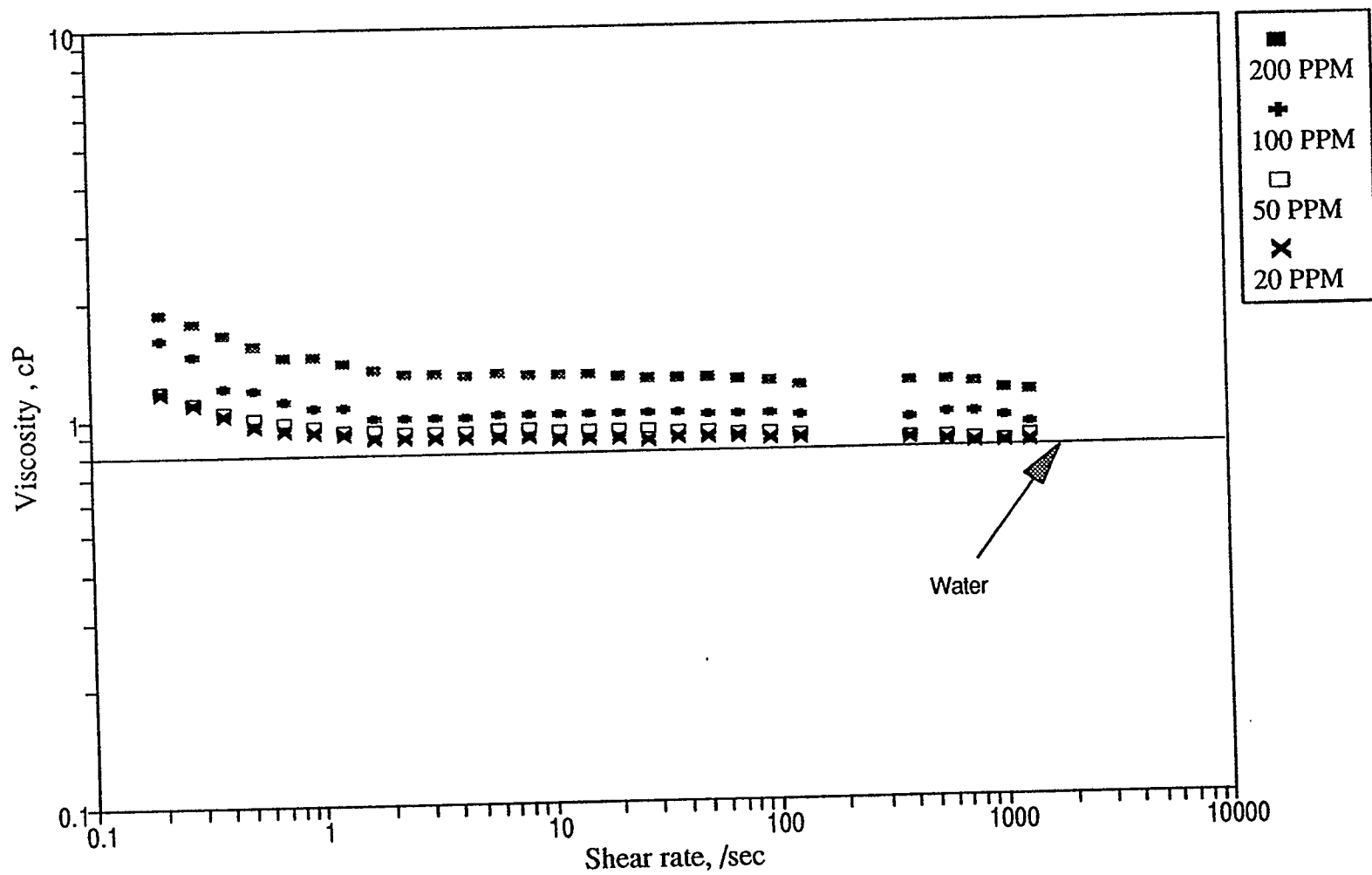
Figure 4.1. Viscosity At 25 Deg. Celcius
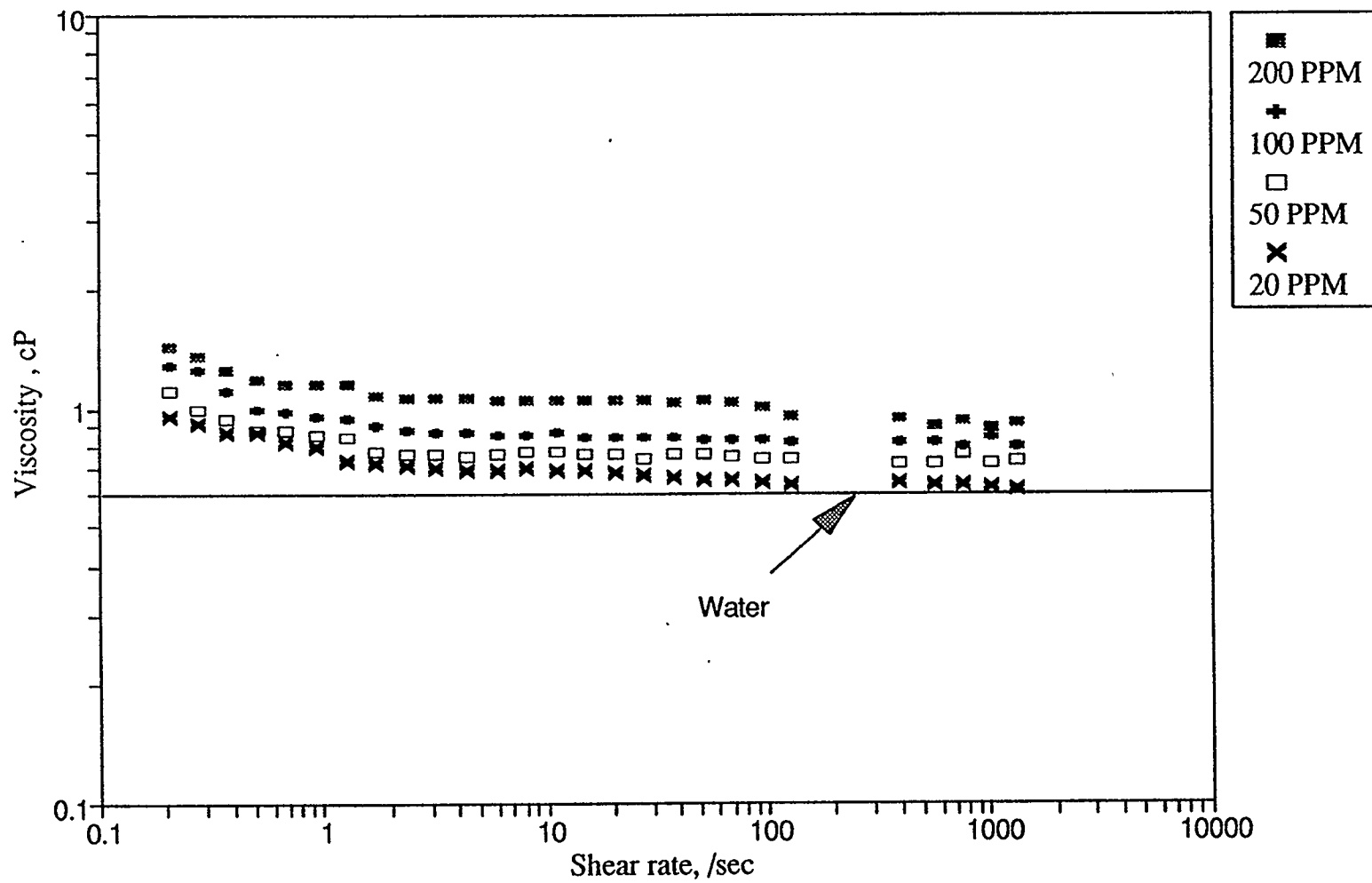
Figure 4.2. Viscosity At 35 Deg. Celcius
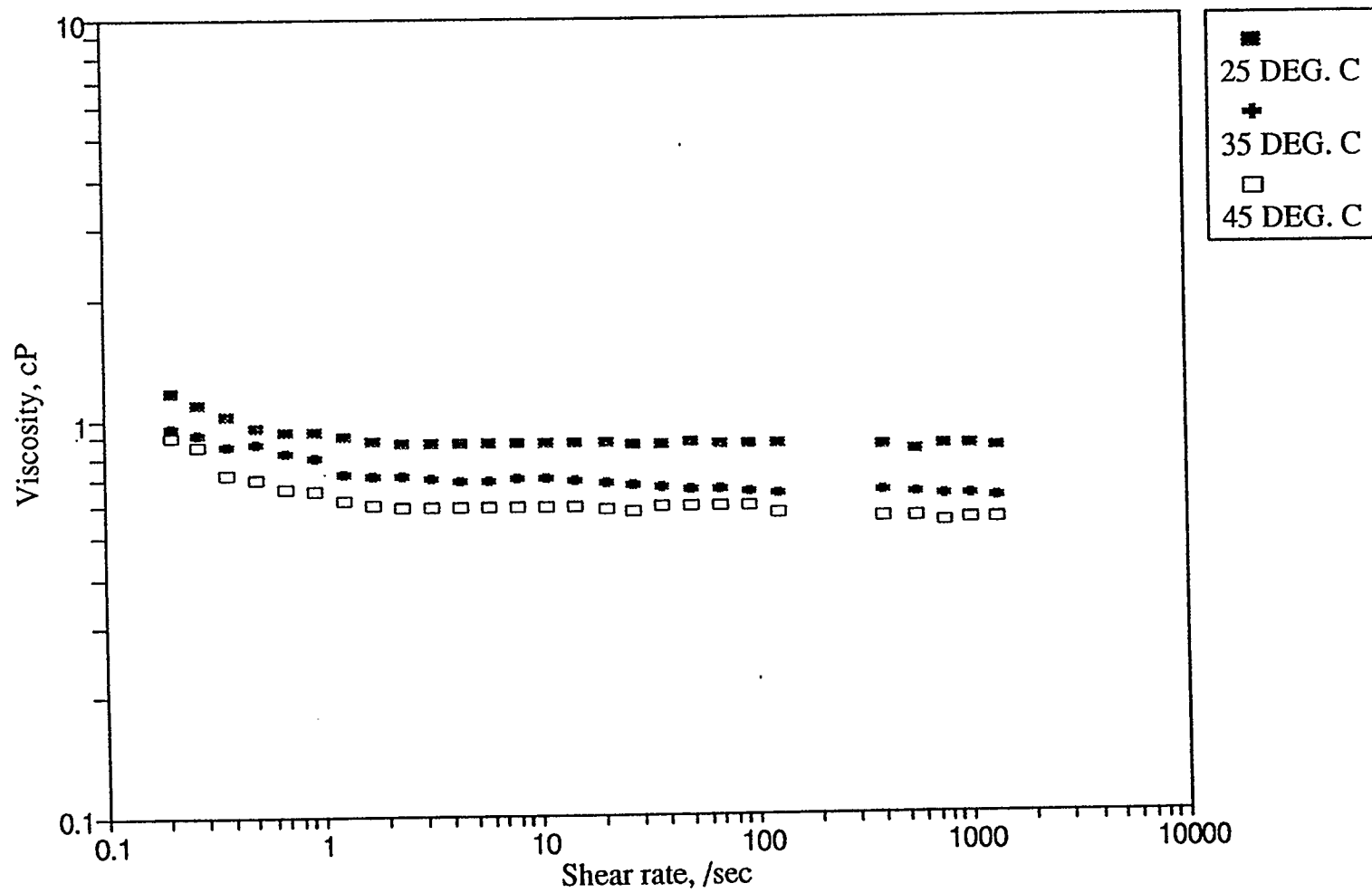
Figure 4.3. Effect of Temperature on Viscosity of 20 ppm Solution
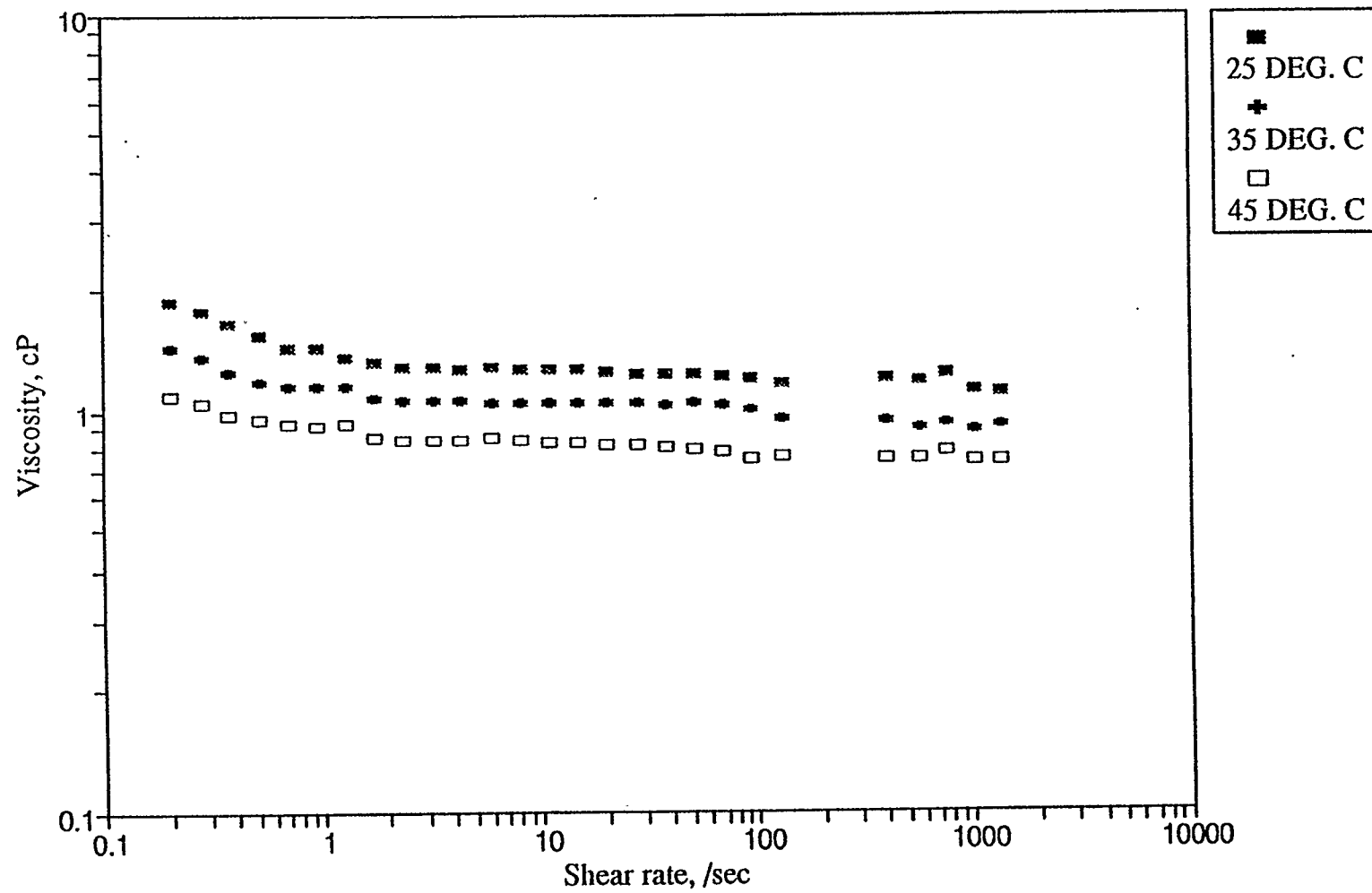
Figure 4.4. Effect of Temperature on Viscosity of 200 ppm Solution
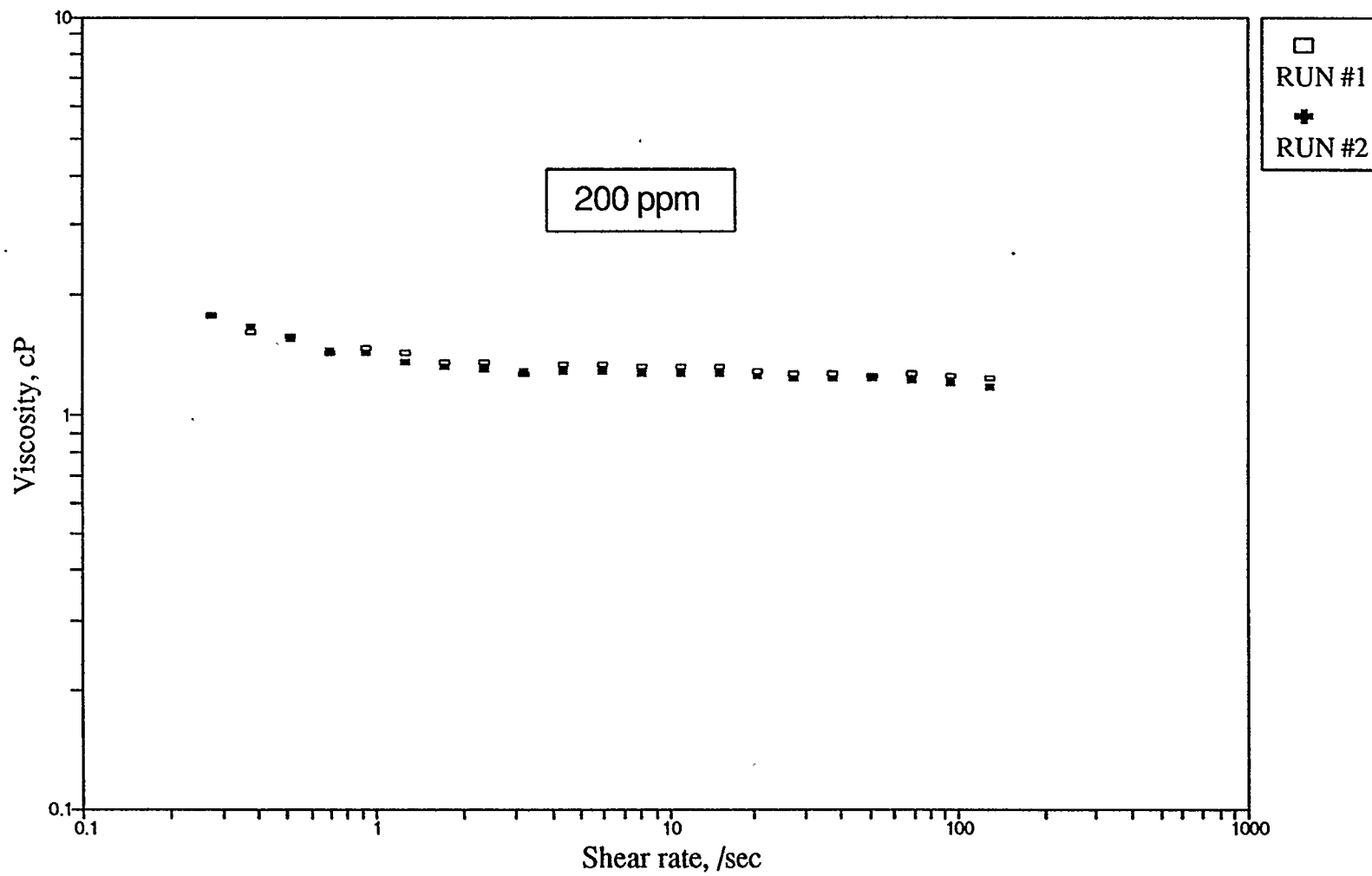
Figure 4.5. Repeatability of Viscosity Measurements

(figure 4.6). Third and higher degree polynomials tended to predict a solution viscosity which was lower than the viscosity of the pure Newtonian solvent at higher shear rates. The second order polynomial predicted a viscosity which increased with shear rate at high shear values (figure 4:6). The Carreau and Cross models fit the data best with the viscosity tending towards an asymptotic value which is slightly higher than the pure solvent viscosity at high shear rates (figures 4.7 and 4.8). A comparison of the sum of least squares of errors for all models was made (figure 4.9) and it was observed that the Carreau model and the Cross model give the best fit curves. Though the third, fourth and fifth degree polynomials show the least error in data fitting, they cannot be used for viscosity correlations as they tend to fail at high shear rates.

TABLE 4.1

Viscosity Models for Dilute Polymer Solutions (Elbirli et al. 1978[1])

MODEL	EQUATION
Linear Polynomial	$a + bx + cx^2 + ...$
Beuche - Harding, 1958	$y = a/(1 + b(cx)^{1/2})$
Cross, 1966	$y = a + b/(1 + cx^d)$
Sabia, 1963	$y = a/(1 + (bx)^c)^{((y/a)-d)}$
Sutherby, 1966	$y = a + b((arc\ sinh(cx)/cx)^d$
Eyring, 1936	$y = a(arc\ sinh(bx))/bx$
Powell - Eyring	$y = a + b(arc\ sinh(cx))/(cx)$
Mieras, 1973	$y = a/(1 + ((bxy)/a)^2)^c$
Carreau, 1972	$y = a + (b-a)/(1 + (cx)^2)^d$

---

[1]*except Carreau Model*
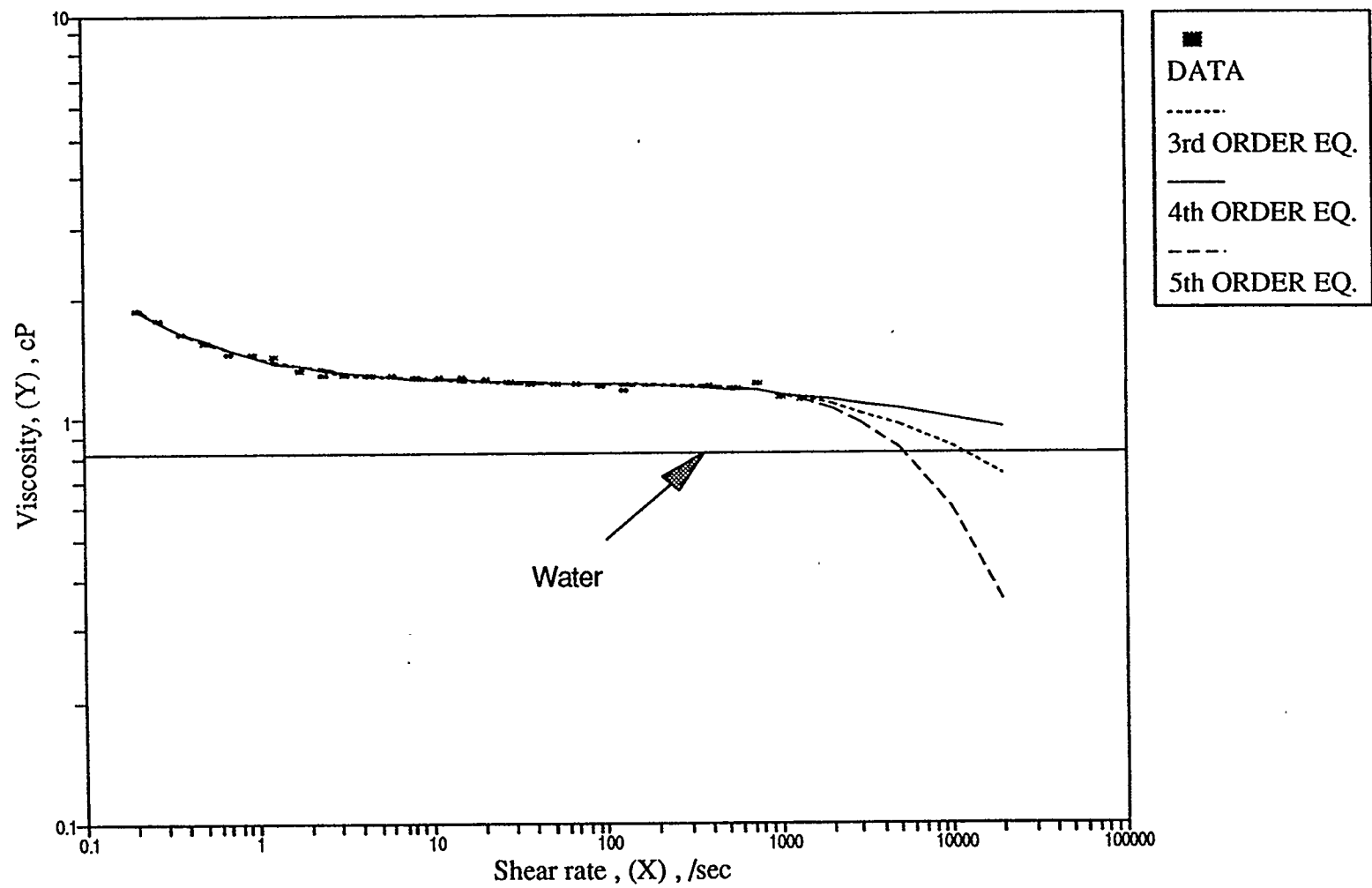
Figure 4.6. Curve Fit For Viscosity Data, 200 ppm, 25 Deg. C (Set I)
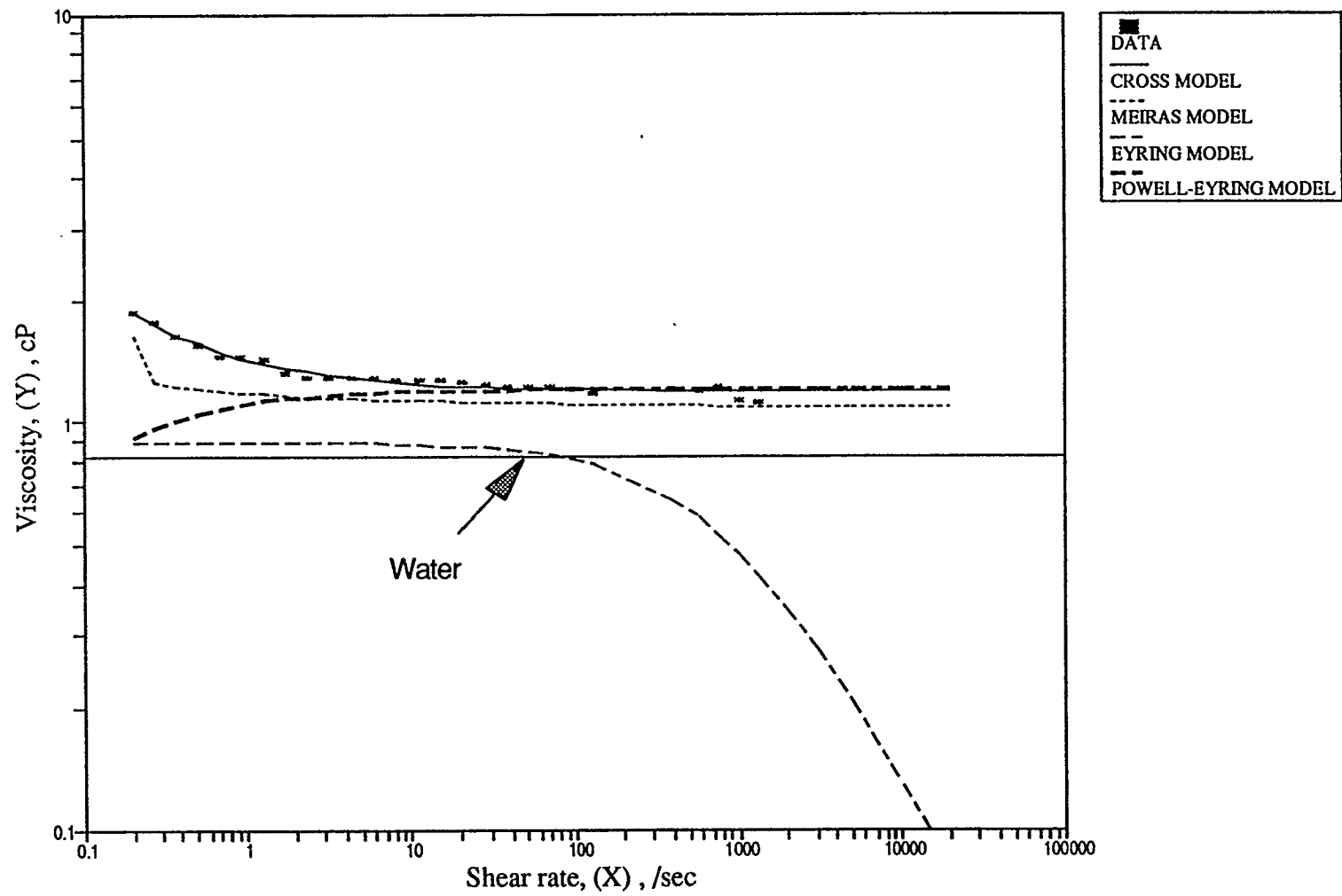
Figure 4.7. Curve Fit For Viscosity Data , 200 ppm, 25 Deg. C (Set II)
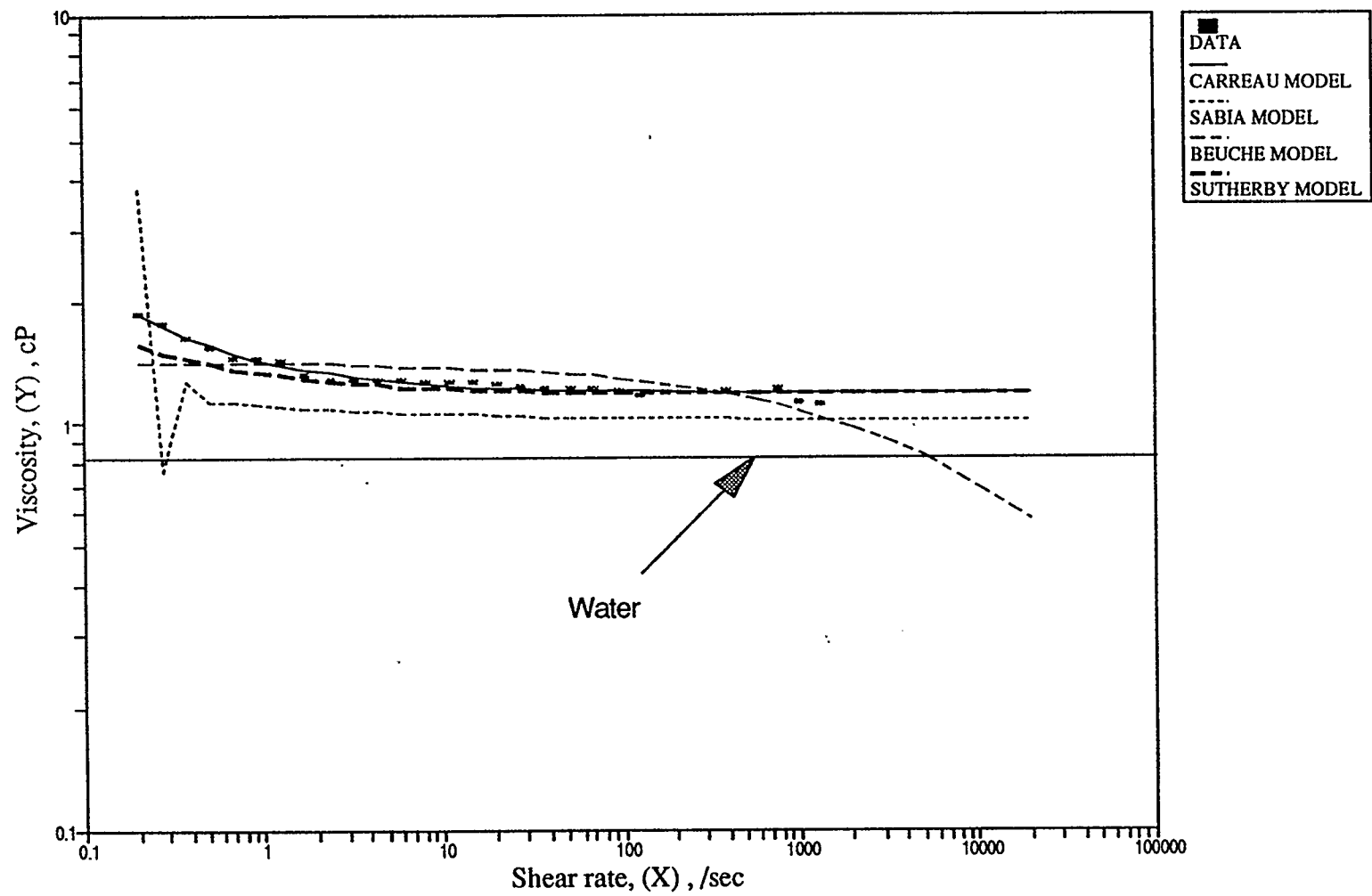
Figure 4.8. Curve Fit For Viscosity Data, 200 ppm , 25 Deg. C (Set III)
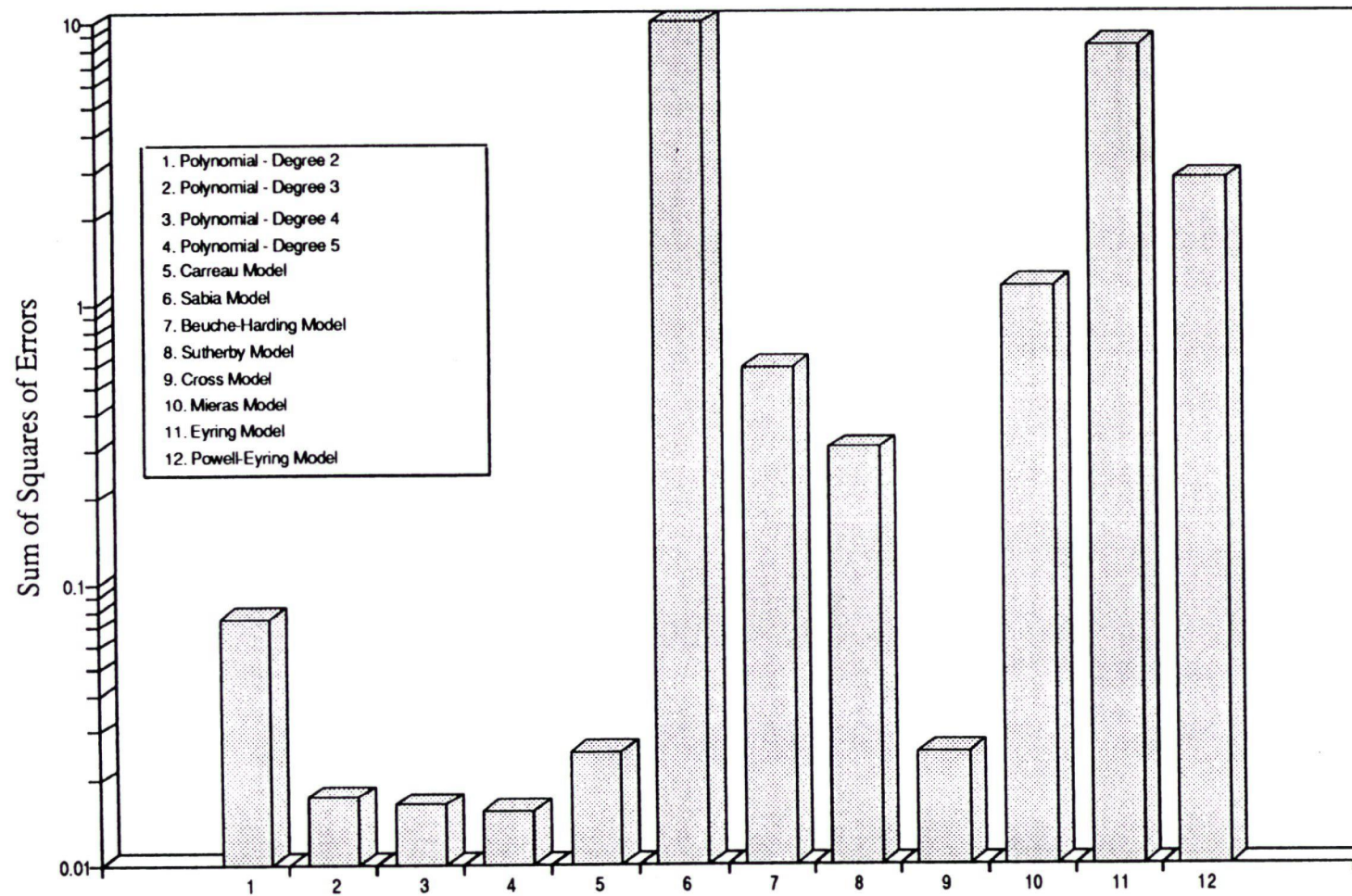
Figure 4.9. Error Analysis For Viscosity Curve Fit

5. RESULTS AND DISCUSSION

Experimental runs were carried out with tap water and three different concentrations (20, 100, 200 ppm) of Poly(ethylene oxide) WSR 301 in tap water. Pressure drop and temperature measurements were done for different flow rates in 7.04 mm and 10.21 mm inside diameter SS 304 tubes, as described in the Experimental Set-up and Procedures section.

Due to unavailability of standard equipment to measure viscosity at high shear rates, several investigators (Matthys, 1985) have used custom built capillary viscometers to carry out the measurements in those shear rate ranges. Such equipment was not available for the current study and thus viscosity measurements were carried out at low and moderately high shear rates using commercially available concentric cylinder viscometers. As discussed in the Viscosity Measurements section, the Carreau model showed a very good fit to the experimental data and predicted an asymptotic viscosity at higher shear rates. But to avoid correlation of experimental data on the basis of a viscosity calculated from a constitutive equation rather than an experimentally determined one, friction and heat transfer results were compared for different mass flow rates. The mass flow rates were maintained in such a way that fully developed turbulent flow was achieved for all the experimental runs.

5.1. Friction Results

The friction factors for the experiments were calculated based on the method described in Appendix III. The friction factors for water in our calibration runs were obtained within 5% of the values predicted by experimental correlations listed in Appendix IV. Calculations for the smaller diameter tubing with a pipe roughness factor of 0.0062 yielded friction factor values within 16% of those predicted by the Moody chart for Re = 15,000 to 20,000 (Perry's Handbook, 1984).

The friction factor is plotted against mass flow rate in figures 5.1 and 5.2 for water and 20, 100 and 200 ppm polymer solutions for flow through 7.04 mm ID (D1) and 10.21 mm ID (D2) tubes respectively. Considerably lower friction factors are observed for the polymer solutions as compared to water. It is observed that at a given constant flow rate, drag reduces with an increase in the concentration of the polymer in solution. The effect of concentration on drag reduction seems to become more apparent with an increase in the flow rate.

For Newtonian fluids, flow through two different diameter pipes is considered similar if the Reynolds number of the flow is the same; in other words, the same friction factor is obtained for flow through different diameter
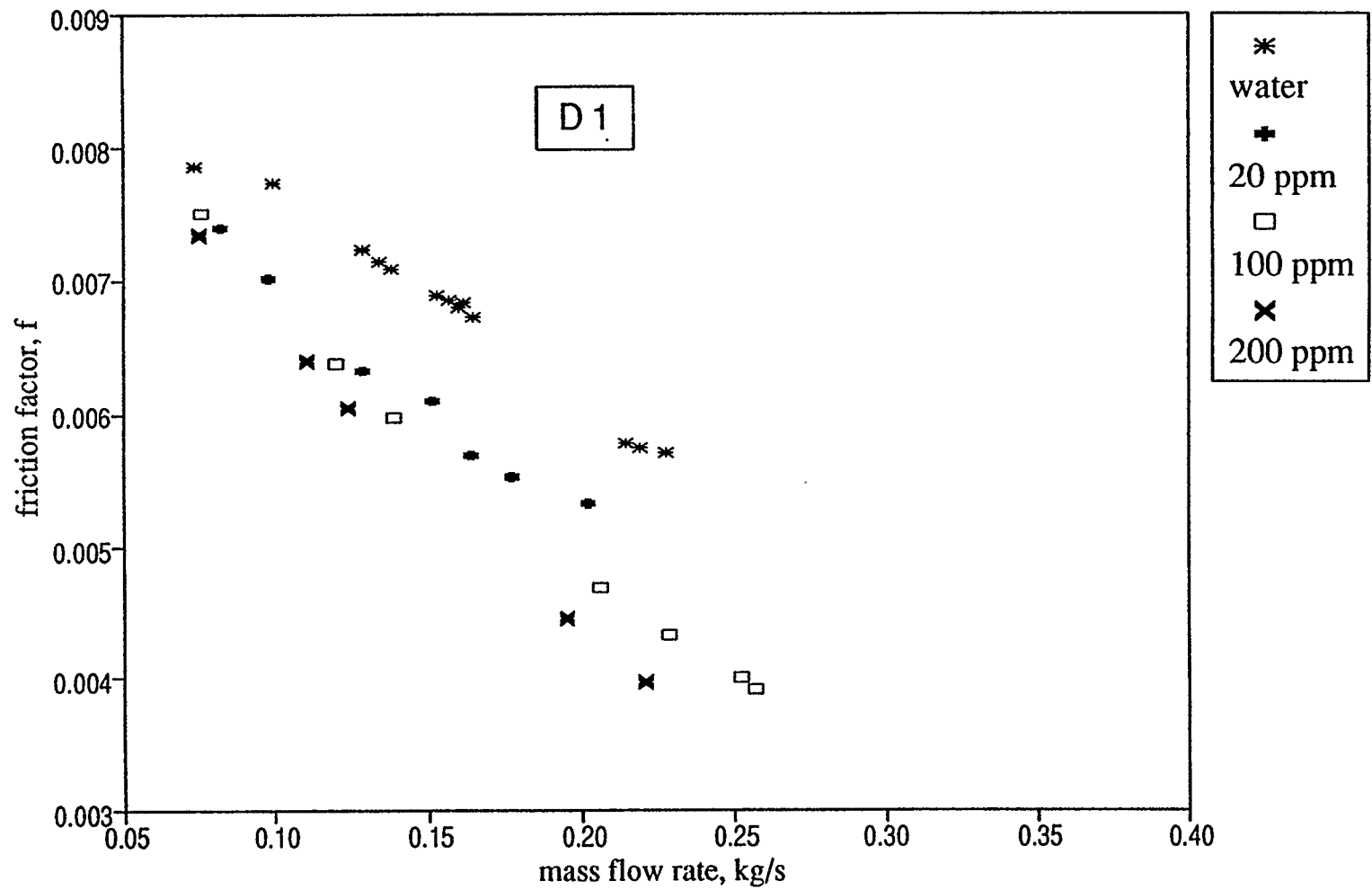
Figure 5.1. Friction Factor Diagram for D 1
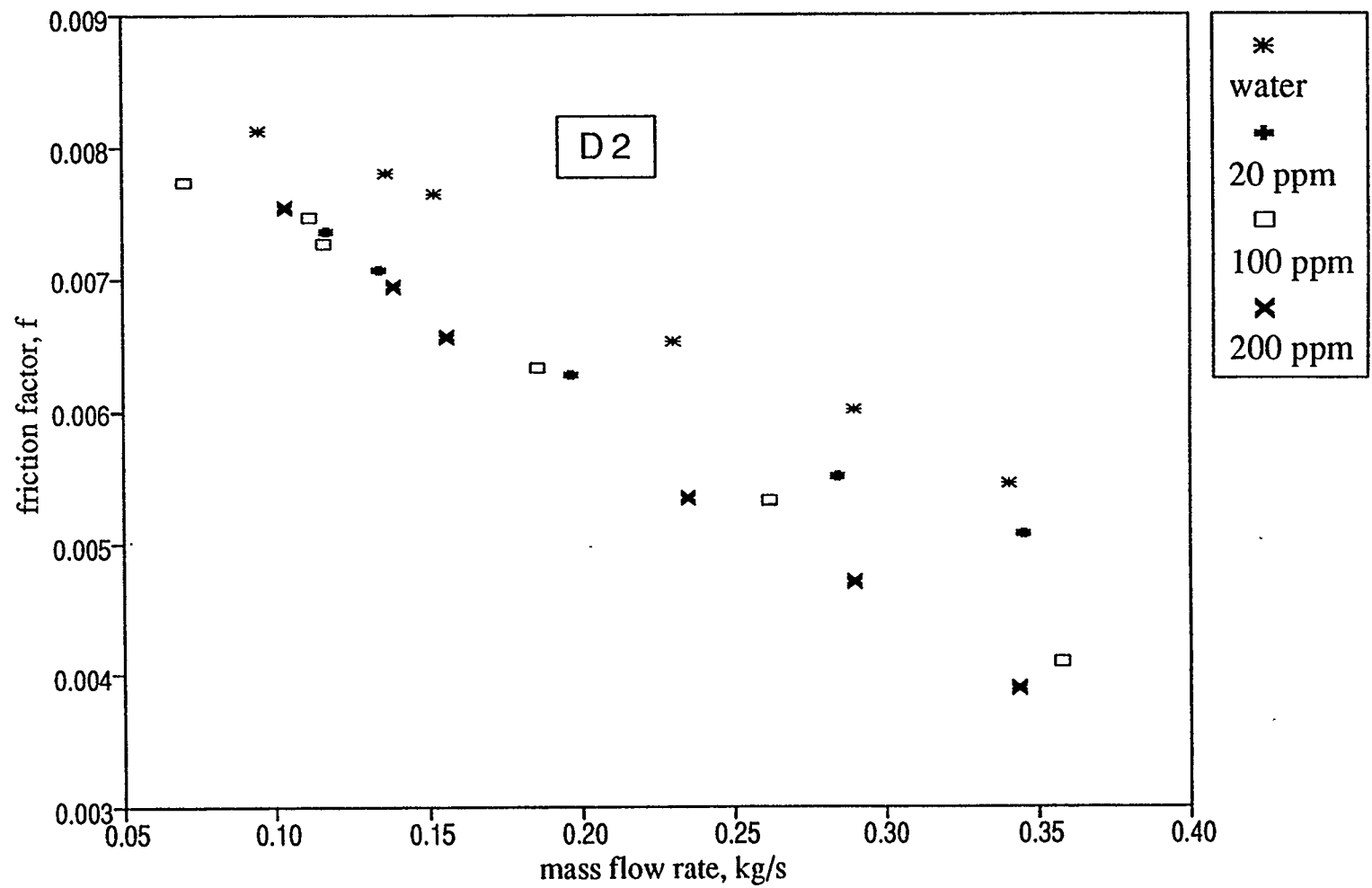
Figure 5.2. Friction Factor Diagram for D 2

pipes for similar flow conditions. Reynolds number is defined as,

$$Re = \frac{D\,u_m\,\rho}{\mu} = \frac{4m}{\pi D \mu} \qquad (5.1)$$

$$Re\left(\frac{\pi\mu}{4}\right) = \frac{m}{D} \qquad (5.2)$$

For a given solution, viscosity, μ, is constant. Hence, m/D is also a measure of similar flows through different diameter pipes.

A "*diameter effect*" (see Literature Review) is associated with drag reducing solutions, as a result of which similar flows in different diameter pipes do not lead to the same friction factor. This is observed from figures 5.1 and 5.2 where at a mass flow rate of 0.2 kg/s (m/D = 28.426) in D1 tube, a friction factor of 0.00425 is obtained while at a mass flow rate of 0.29 kg/s (m/D = 28.426) in D2 tube, a friction factor of 0.0045 is obtained. Hence, it can be inferred by comparing the two graphs that to achieve the same levels of drag reduction, a higher value of m/D is required in a larger diameter pipe.

Figures 5.3 and 5.4 show that lower values of shear stress at the wall
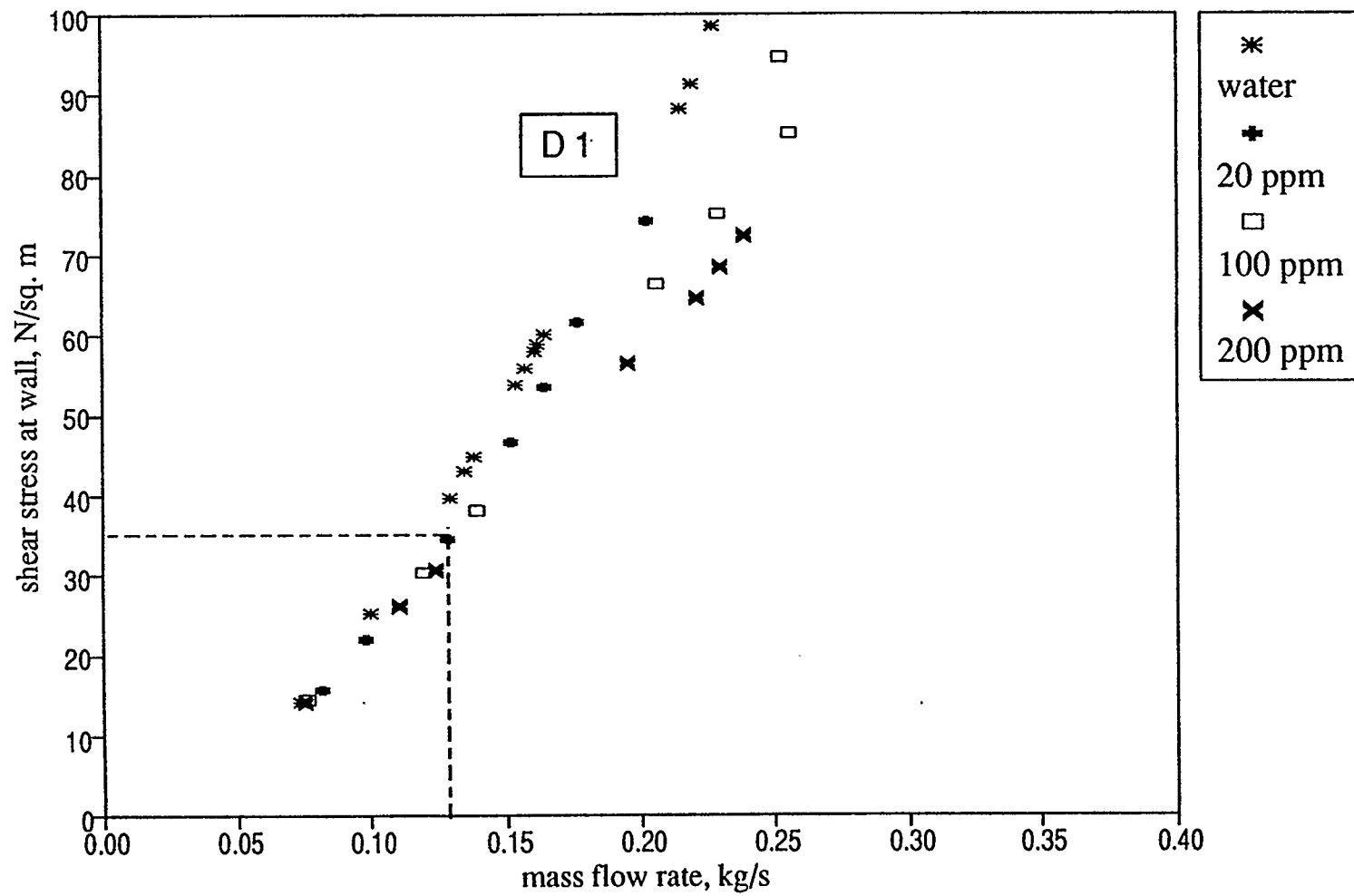
Figure 5.3. Effect of shear Stress at the Wall on Mass Flow Rate (D 1)
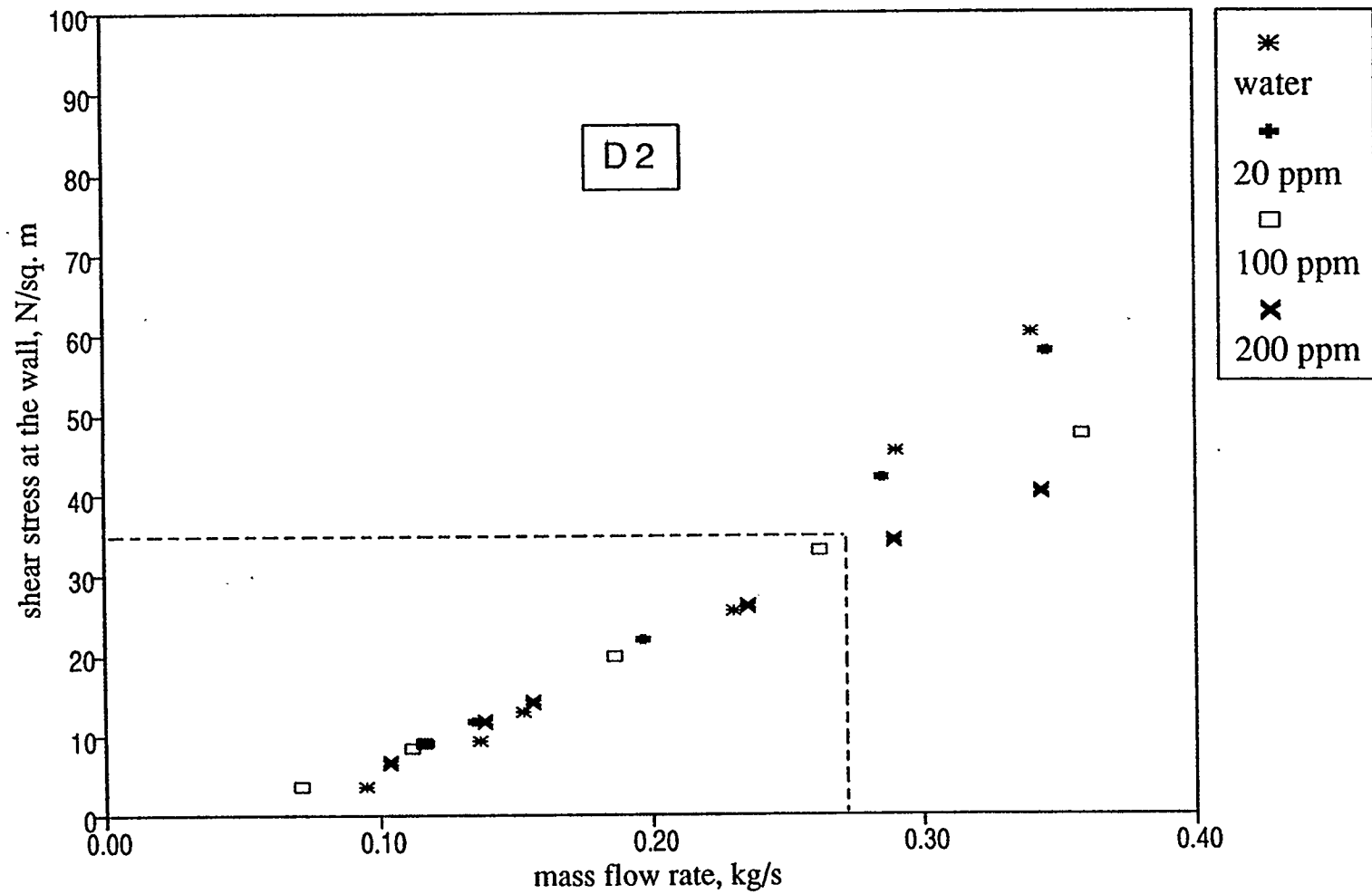
Figure 5.4. Effect of Shear Stress at the Wall on Mass Flow Rate (D 2)

correspond to low flow rates and the curves for all concentrations seem to approach the value for water. At higher values of shear stress, the curves for the polymer solutions tend to move away from that of water showing an increase in mass flow rates (hence drag reduction) with an increase in concentration at a given value of the shear stress. The value of shear stress at the wall at which the curves for the polymer solutions begin to move away from that of water is observed to be the same in both the tubes. This confirms the findings of Gadd (1968) who observed that a critical value of shear stress at the wall should be exceeded for the drag reduction effect to manifest itself. This critical value is found to be independent of the diameter of the tube. This observation provides support to the theory that the interaction of the polymer molecules with the turbulent fluctuations in the boundary layer flow produces the drag reduction effect (Lumley, 1973). The intensity of turbulent fluctuations can be scaled based on the shear stress value at the wall (Tritton, 1990), i.e., same shear stress at the wall in different diameter pipes would lead to similar turbulent fluctuations in the boundary layer which are equal in magnitude.

The same levels of shear stress are only achieved in larger diameter pipes at higher flow rates as seen in figures 5.3 and 5.4. Hence, the drag reduction effect is generally seen at higher flow rates in larger diameter pipes.This is also evident from figure 5.5 where friction factors for 200 ppm solution are plotted
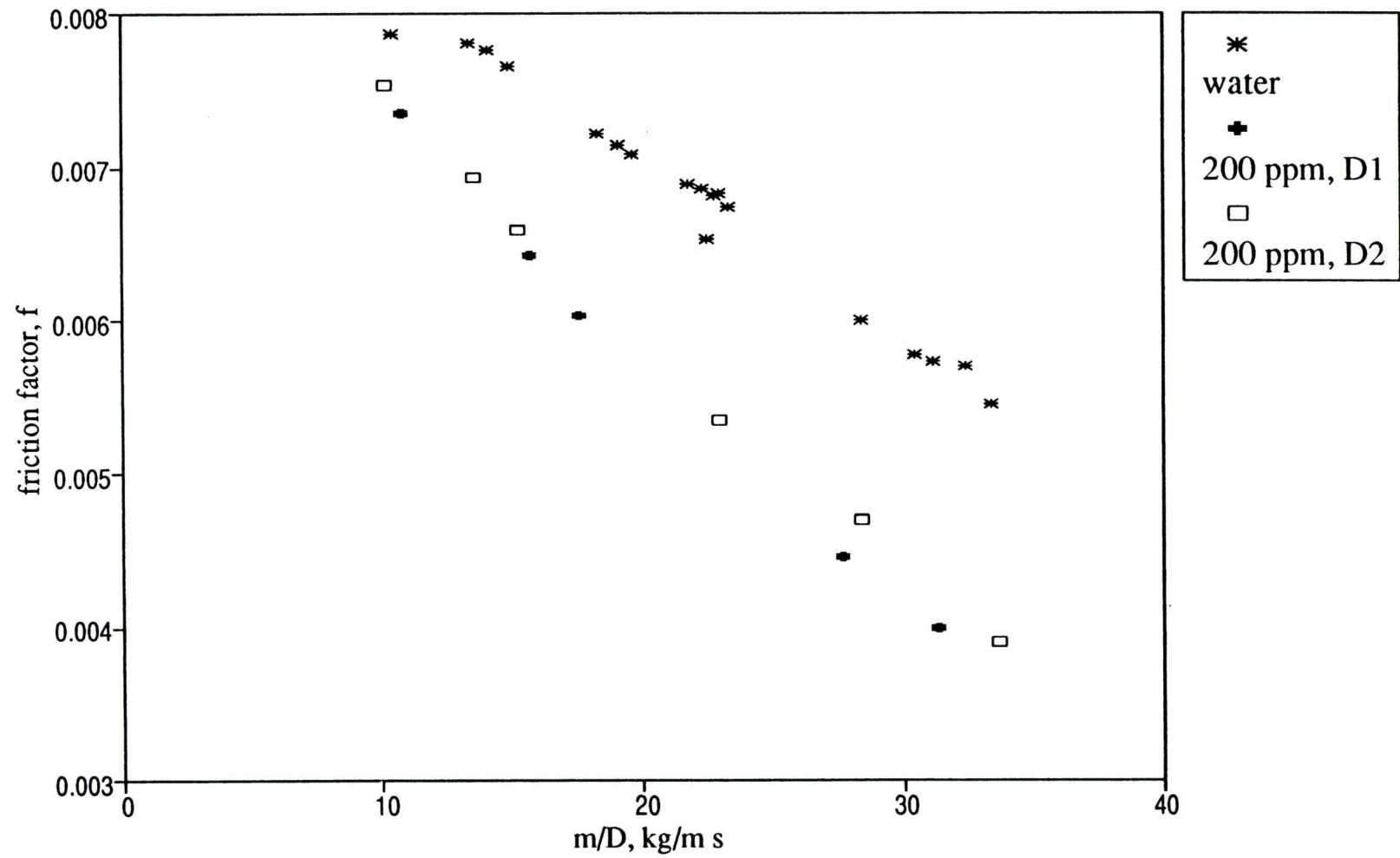
Figure 5.5. Friction Factor versus m/D for 200 ppm Solution

against m/D for the two diameter pipes used in our study. Since m/D is equivalent to the Reynolds number if the viscosity of the fluid is constant, the friction factors for water (Newtonian fluid) fall on a single curve. Different curves for 200 ppm solution are obtained due to the 'diameter effect'.

Though it cannot be concluded definitely from figures 5.1 through 5.4, there appears to be an effect of mechanical degradation on the 20 ppm solution. Mechanical degradation leads to the breaking up of the molecule chains and as a result of this, they lose their drag reducing effectiveness. The friction factors for the 20 ppm solution tend towards that of water at higher flow rates (figures 5.1 and 5.2). Such effect is not seen on 100 and 200 ppm solutions for the flow range examined. The effect of mechanical degradation would become evident for the lower concentration earlier than the more concentrated solutions (Matthys, 1991). At higher shear stress values at the wall, the mass flow rate for the 20 ppm solution tends towards that of water indicating the degradation effects (figures 5.3 and 5.4).

To demonstrate an idea of the extent of drag reduction achieved in our experimental set up, a comparison of drag reduction values for polymer solutions over water at the same flow rates is done in figures 5.6 and 5.7 using equation
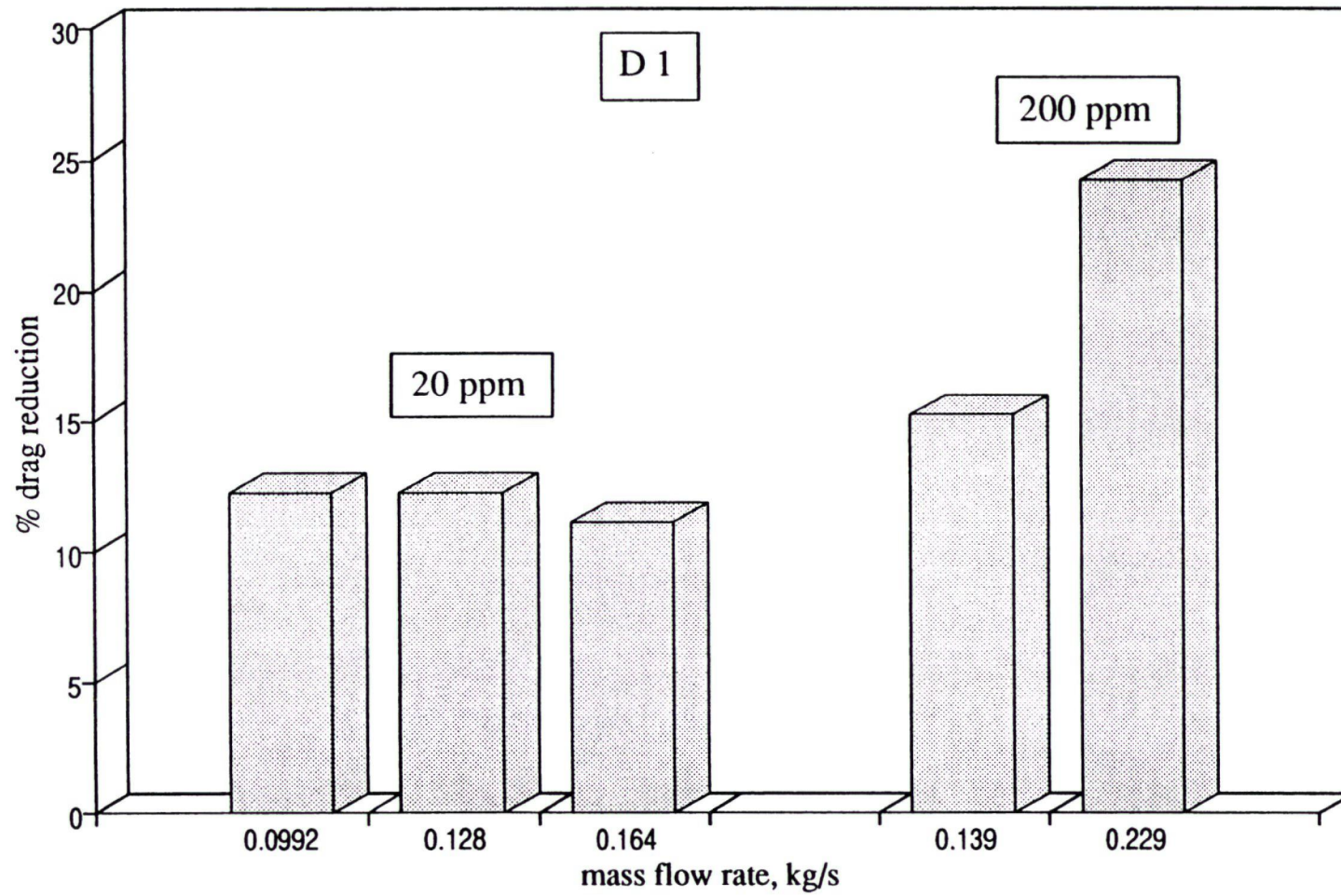
Figure 5.6. Drag Reduction Results For D 1
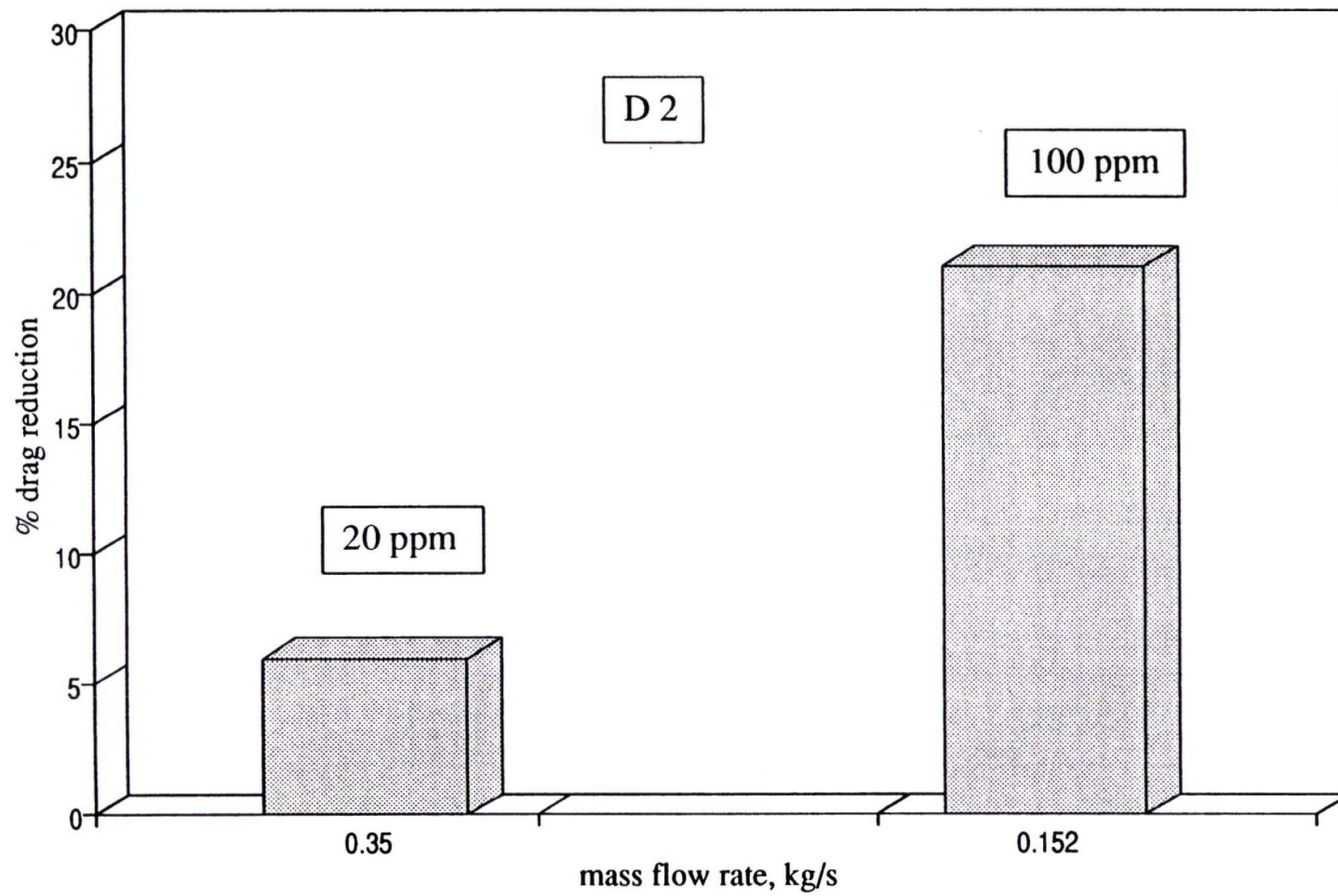
Figure 5.7. Drag Reduction Results For D 2

1.2 from Chapter 1. Since flow rates were randomly selected in the turbulent region during the runs, comparisons could only be done at a few flow rates. Drag reduction ranging from 6% (20 ppm solution, 10.211 mm ID, figure 5.7) to 23% (200 ppm solution, 7.0358 mm ID, figure 5.6) is observed.

5.2. Heat Transfer Results

The heat transfer coefficient is defined by an equation of the form;

$$h_x = \frac{q}{(T_{i,w} - T_{b_x})} \qquad (5.3)$$

where q is the rate of heat flux at the wall, $T_{i,w}$ is the inside wall temperature and T_b is the bulk temperature. It is very difficult to measure the inside wall temperature of an electrically heated tube in an experiment, so a more convenient way to express the heat transfer coefficient is (Ghajar and Yoon, 1988),

$$h_x = \frac{q}{(T_{ow} - T_{in}) - (T_{ow} - T_{iw}) - (T_{b_x} - T_{in})} \qquad (5.4)$$

The quantity, $T_{o,w} - T_{in}$ can be measured experimentally. The other terms in the

denominator can be calculated using the heat conduction equation in the cylindrical coordinates (Appendix II) and energy conservation equation (Appendix II). This is done as follows;

$$T_{o,w} - T_{i,w} = \frac{Q[2D_o^2 \ln(D_o/D_i) - (D_o^2 - D_i^2)]}{4\pi(D_o^2 - D_i^2)\kappa_s L} \tag{5.5}$$

and,

$$T_{b_x} - T_{in} = \frac{Q_x}{mC_p} \tag{5.6}$$

where κ_s is the thermal conductivity of the tube. The value of κ_s was calculated as a function of temperature using data shown in Appendix Va. Properties of water used in calculation of the heat transfer coefficients from experimental correlations (Appendix IV) are listed in Appendix Vb.

Direct current electrical heating of the steel tube produces an approximately constant heat flux. As a result of this, the bulk temperature of the fluid and both the inside and outside wall temperatures increase almost linearly with distance. Slight non-linearities will be caused due to variation in material properties as a result of these temperature increases. The viscosity of the fluid will also change

along with local Reynolds and Prandtl numbers due to an increase in the temperature of the fluid as it passes through the tube. Hence local heat transfer coefficients will also vary along the length of the tube due to these property changes, though the main effect would be of the changing fluid viscosity as thermal conductivity and specific heat capacity of liquids do not change appreciably with temperature.

An increase in the tube wall temperature between entry and exit to the test section causes an increase in the thermal conductivity and electrical resistivity of the tube. Hence the heat generated in the wall will be a function of the axial location and the temperature difference between inside and outside wall will vary as well. In fact, the heat generated in the wall and the conductivity of the metal varies in the radial direction as well due to the radial gradient of temperature in the wall.

The expression for the difference in temperature between inside and outside wall of the tube (equation 5.5) was developed assuming no heat loss. As a further simplification, radial gradients of temperature were assumed to be much larger than the axial ones. This assumption was based on the fact that typical rise across the length of the smaller tube was about 5°C (1.186°C/m) compared to about 1°C (803°C/m) across the wall. Temperature drop across the beryllium oxide disc was

assumed to be negligible as it has a very high thermal conductivity (272 W/m °C at 27 °C). Further, the variation of heat flux in the radial direction was assumed to be negligible as the thermal conductivity of SS 304 increases by approximately 0.8% for a 10°C rise in temperature.

Local heat transfer coefficients were calculated using the above method for the same constant heat flux at the wall (28.9 kW/m^2) for the two different diameter tubes used in the experiments. A discussion of the results obtained is given hereunder.

A comparison of the local heat transfer coefficients for 20, 100 and 200 ppm solutions and water at the same mass flow rate in D1 tube is shown in figure 5.8. The plot clearly shows the effect of increasing polymer concentration on heat transfer, with the local heat transfer coefficients going down with an increase in concentration. It appears that the presence of polymer molecules in solution causes an additional resistance to heat transfer leading to lower local heat transfer coefficients than for the pure solvent flow. The greatest reduction in heat transfer is obtained in the entrance region of the tube with the heat transfer coefficient for 200 ppm solution being lower than that for water by almost 45% at $x/D = 73$. The difference decreases to 25% beyond $x/D = 400$. This can be explained based on the fact that as the solution enters the test section from the flow calming section,
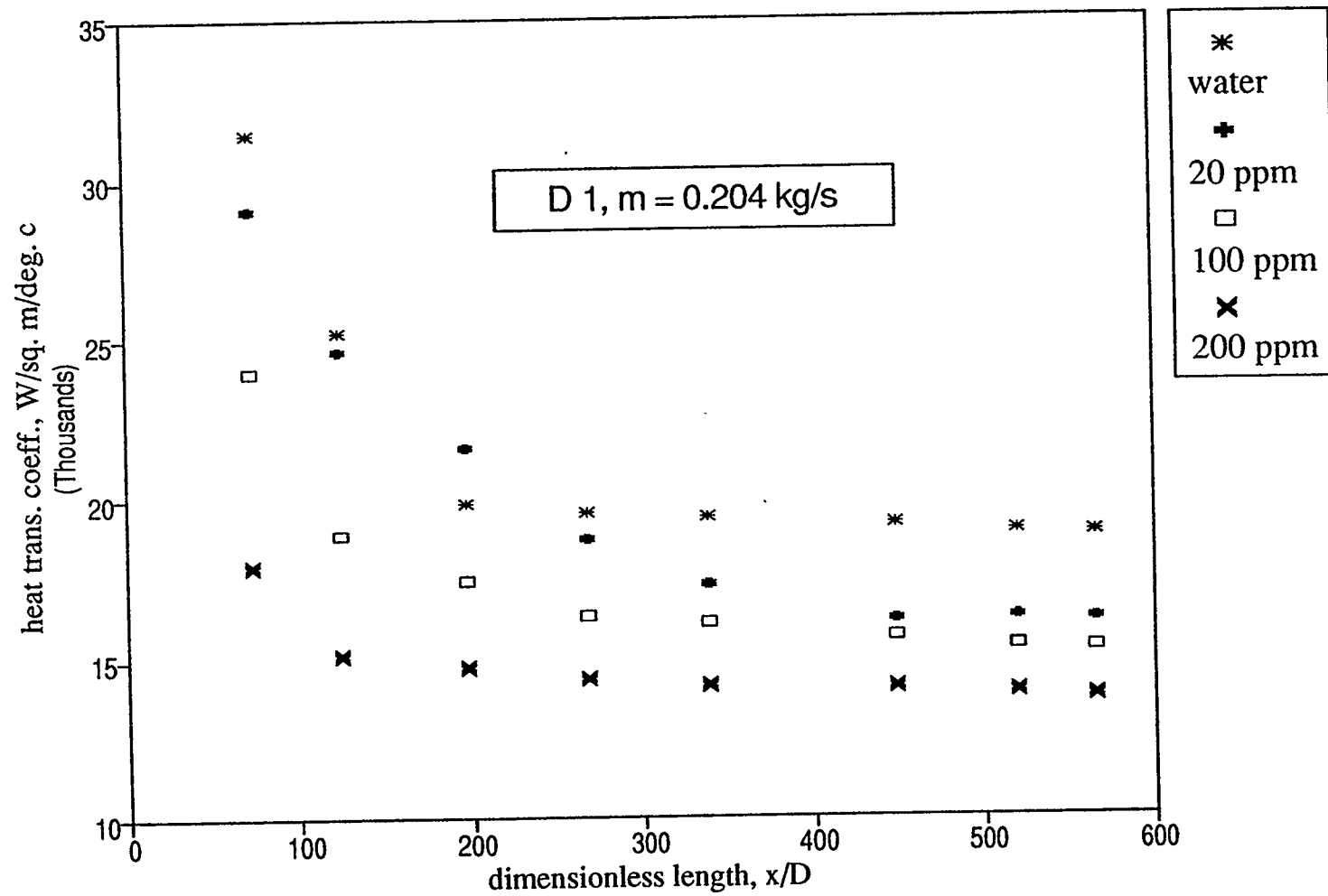
Figure 5.8. h versus x/D For Water and Polymer Solutions (m = 0.204 kg/s)

the streams break contact with the wall of the tube. A jet is formed which flows into the stagnant fluid in the tube (figure 5.9). The jet first contracts and then expands to fill the entire cross-section and downstream from the point of contraction, the normal velocity distribution is eventually reestablished. Due to the separation of the flow from the wall, vortices appear (Kays and Crawford, 1980) and this subjects the polymer molecules to high shear stresses at the wall in the entrance region. As discussed earlier in the case of drag reduction, where the dependence of drag reduction on the shear stress at the wall was shown, high shear stress values at the wall causes the polymer molecules to produce the enhanced heat transfer reduction effect in the entrance region which increases with an increase in the polymer concentration. As the solution moves further down the tube, the velocity profile is reestablished and the shear stress at the wall stabilizes at a lower value thus leading to a decreased heat transfer reduction effect. Due to the use of only a few thermocouples in the entrance region, the effect of polymer concentration on the thermal entrance length could not be studied.

Figure 5.10 is a plot of local heat transfer coefficients for water at different flow rates. It is observed from the plot that water has a thermal entrance length of approximately 100 - 120 diameters. Thermal entrance length for water has been reported to be 50 - 70 diameters (Hartnett, 1982).
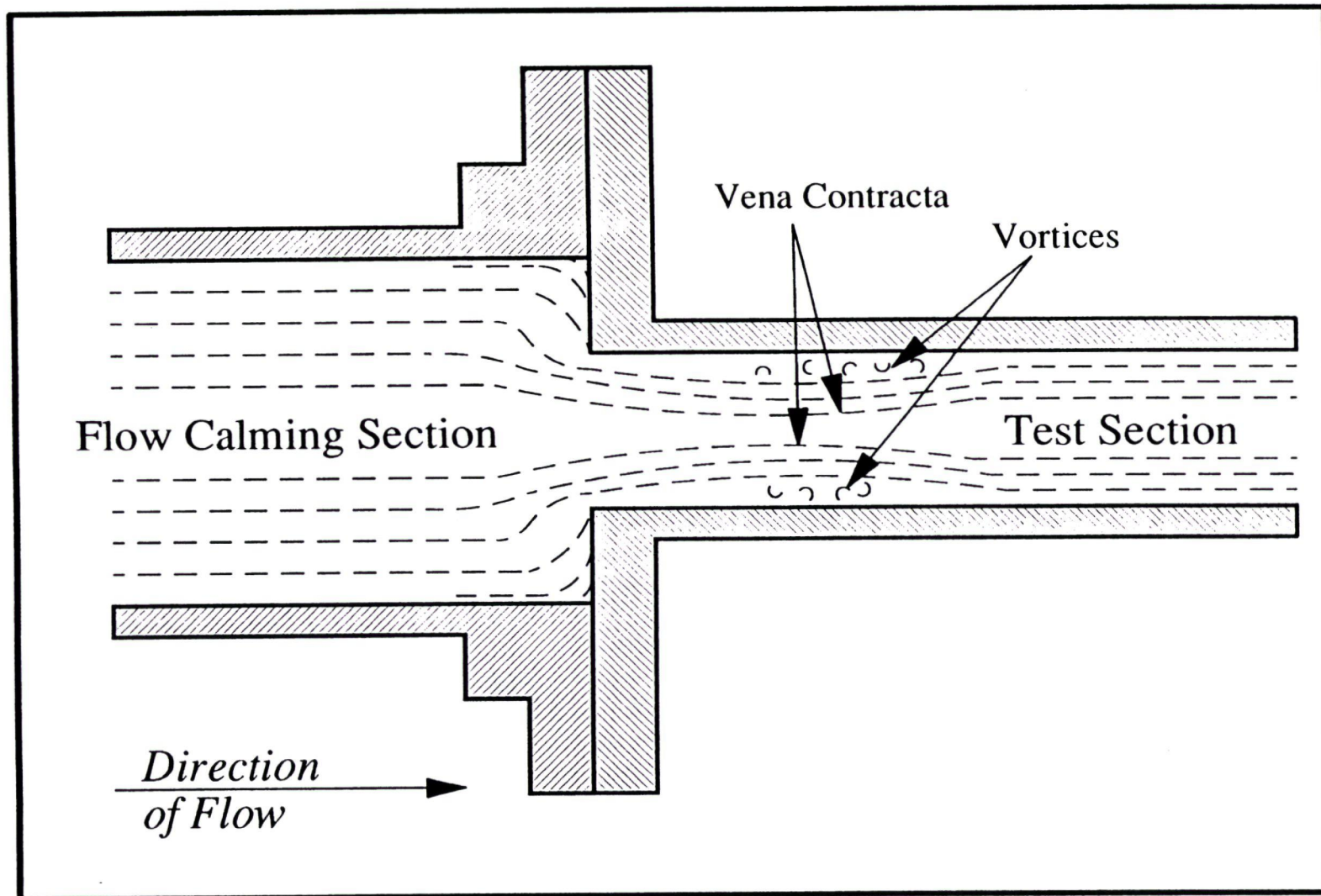
Figure 5.9 Structure of flow near the entrance of the test section
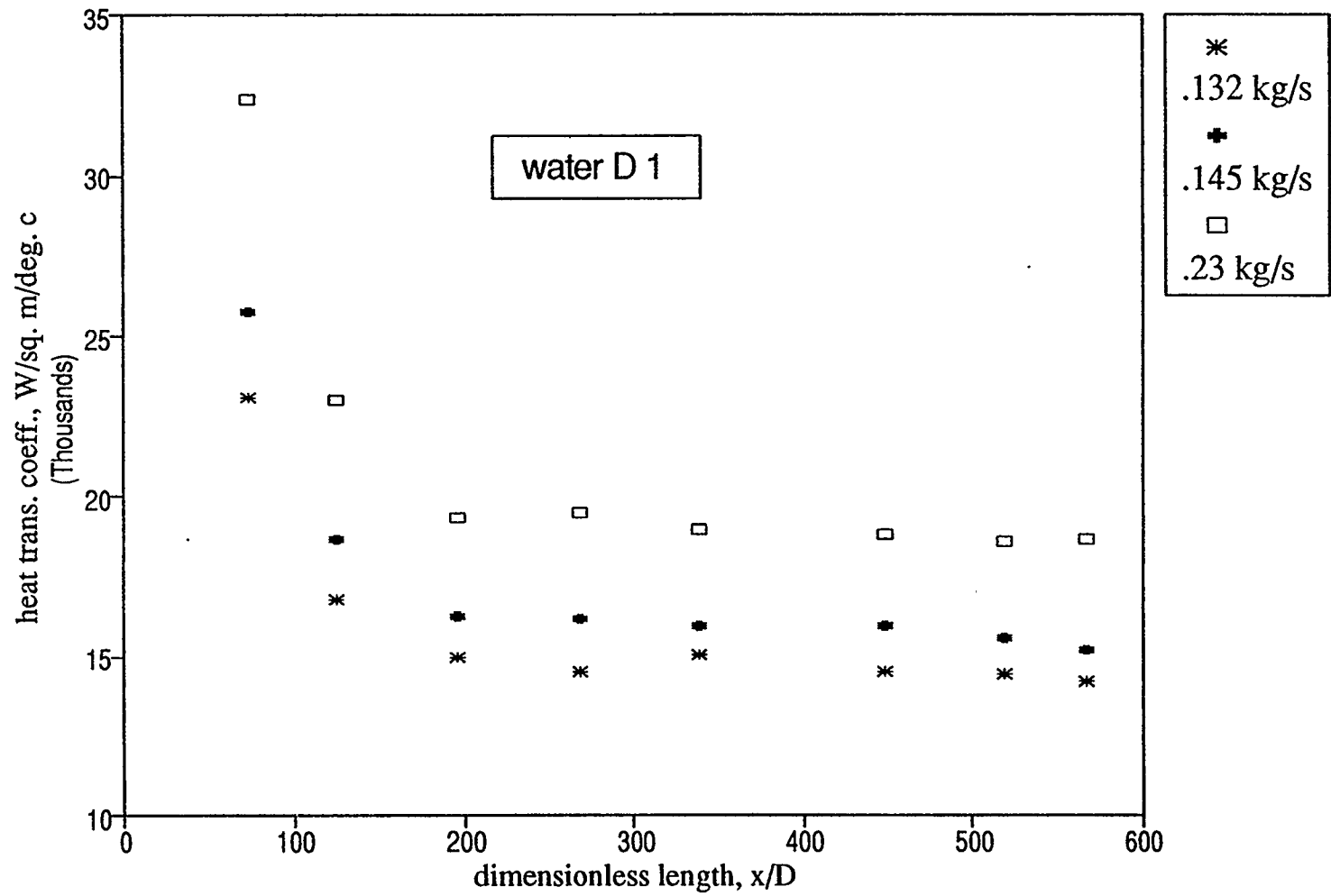
Figure 5.10. h versus x/D (water, D1) For Different Flow Rates

A comparison of heat transfer coefficients for different concentrations of polymer solution and water at one particular x/D (330), at different flow rates (or, shear stress at the wall) (figure 5.11) leads to some interesting observations. This plot for heat transfer reduction shows similar trends as figures 5.3 and 5.4 which are plots to show the effect of shear stress on the drag reduction. At lower flow rates, when the shear stress at the wall is low, the heat transfer coefficients for all concentrations of polymer solution tend towards that of water. As the flow rate increases and once the threshold value of shear stress at the wall is exceeded, the presence of polymer molecules in the solution affects the heat transfer coefficients and the curves for the polymer solution tend to move away from that of water. The 200 ppm solution shows the maximum heat transfer reduction effect, which means that an increase in flow rate does not result in a corresponding increase in the heat transfer coefficients as the polymer molecules are creating an added resistance to the heat transfer probably in a thermal boundary layer containing stretched polymer molecules and suppressed turbulence. The critical value of shear stress at which the heat transfer reduction effect appears to manifest itself (figure 5.11) is found to be approximately the same at which the drag reduction effect becomes apparent (figure 5.3). Hence the role of shear stress at the wall (i.e., intensity of turbulent fluctuations) in producing the drag reduction and heat transfer reduction effect is confirmed.
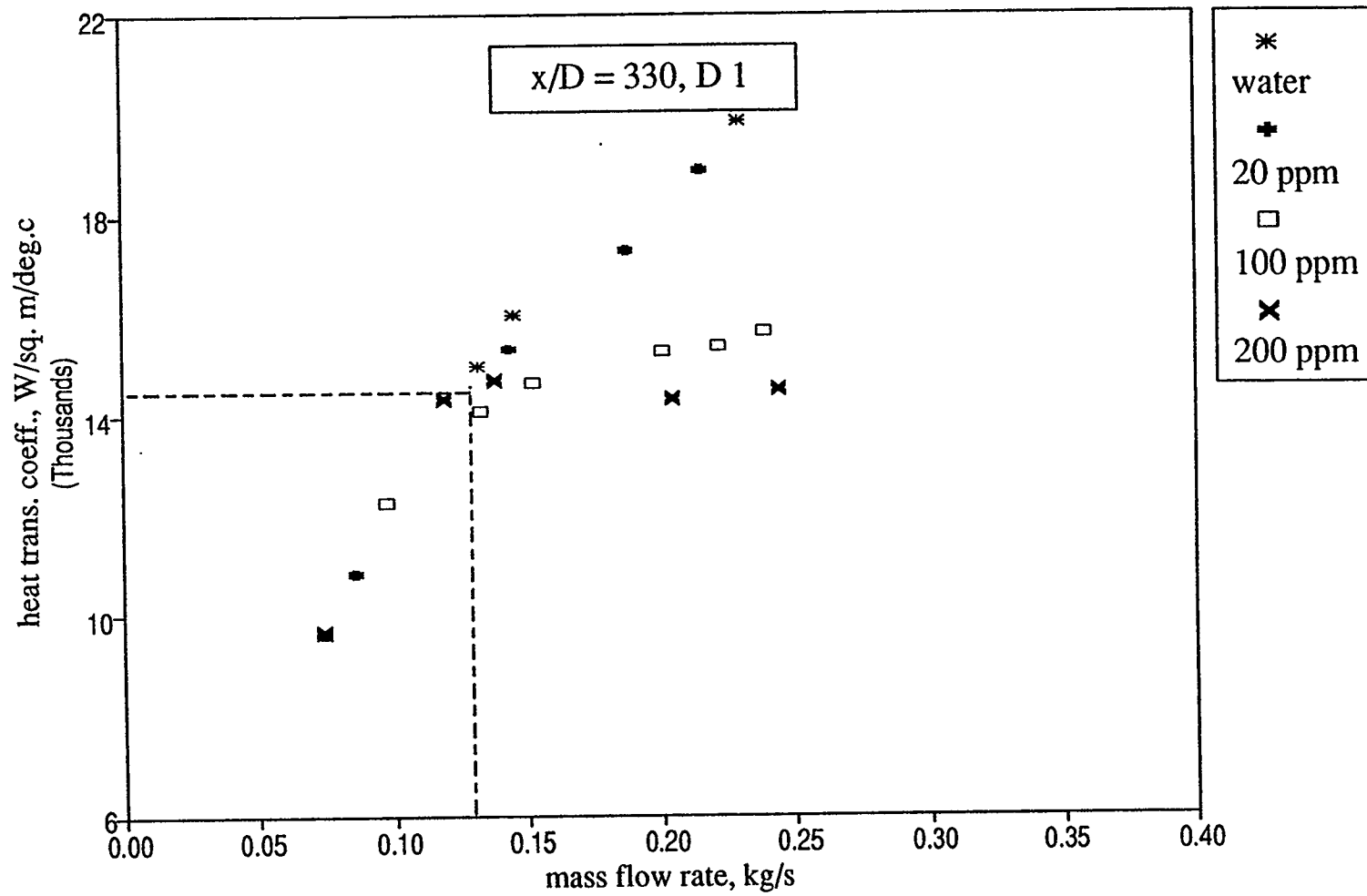
Figure 5.11. h versus Mass Flow Rate (x/D = 330, D 1)

Figure 5.12 confirms that at a low flow rate, where the shear stress is below the critical value, 100 ppm and 200 ppm solutions show very similar heat transfer behaviour.

Figures 5.13 and 5.14 compare heat transfer coefficients for different flow rates in 7.04 mm and 10.21 mm ID tubes respectively for 200 ppm polymer solution. It is observed that an increase in flow rate leads to a corresponding increase in the heat transfer coefficients due to an increase in the rate of convective heat transfer. Considerably lower heat transfer coefficients are obtained for the larger diameter tube.

Figure 5.15 shows the difference in heat transfer under similar flow conditions in two pipes for the 200 ppm solution. Like m/D, hD is also an approximate measure of heat transfer for a given fluid under same heating conditions in different diameter pipes (assuming constant thermal conductivity for the fluid). The hD values for D2 are bigger than those for the D1, indicating a less heat transfer reduction due to the 'diameter effect' in the bigger diameter tube. The above results could not be compared with water as data was not available at the same flow rates.

It appears from the above observations that extensional viscosity of the
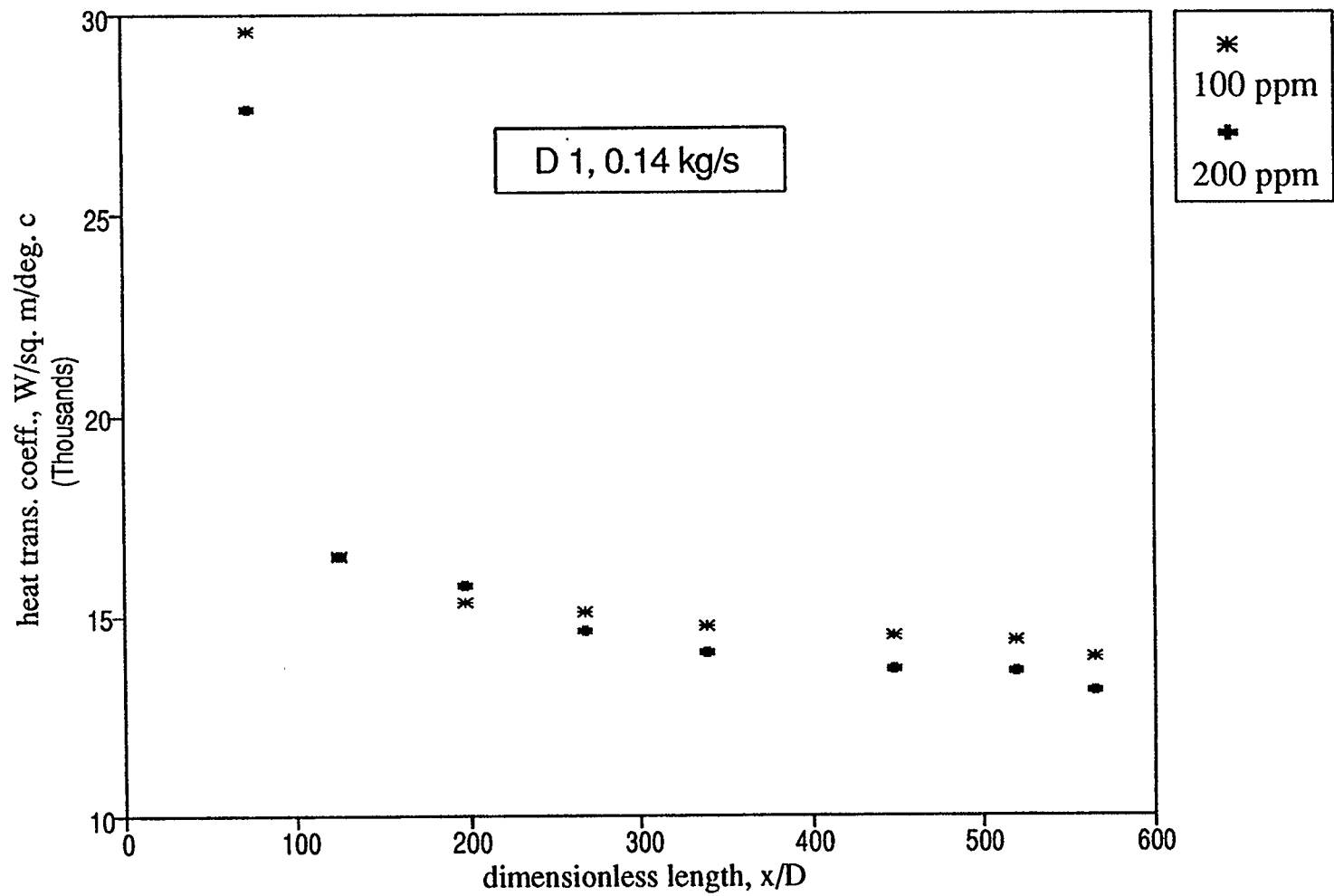
Figure 5.12. h versus x/D for low flow rates (100 & 200 ppm Solutions)
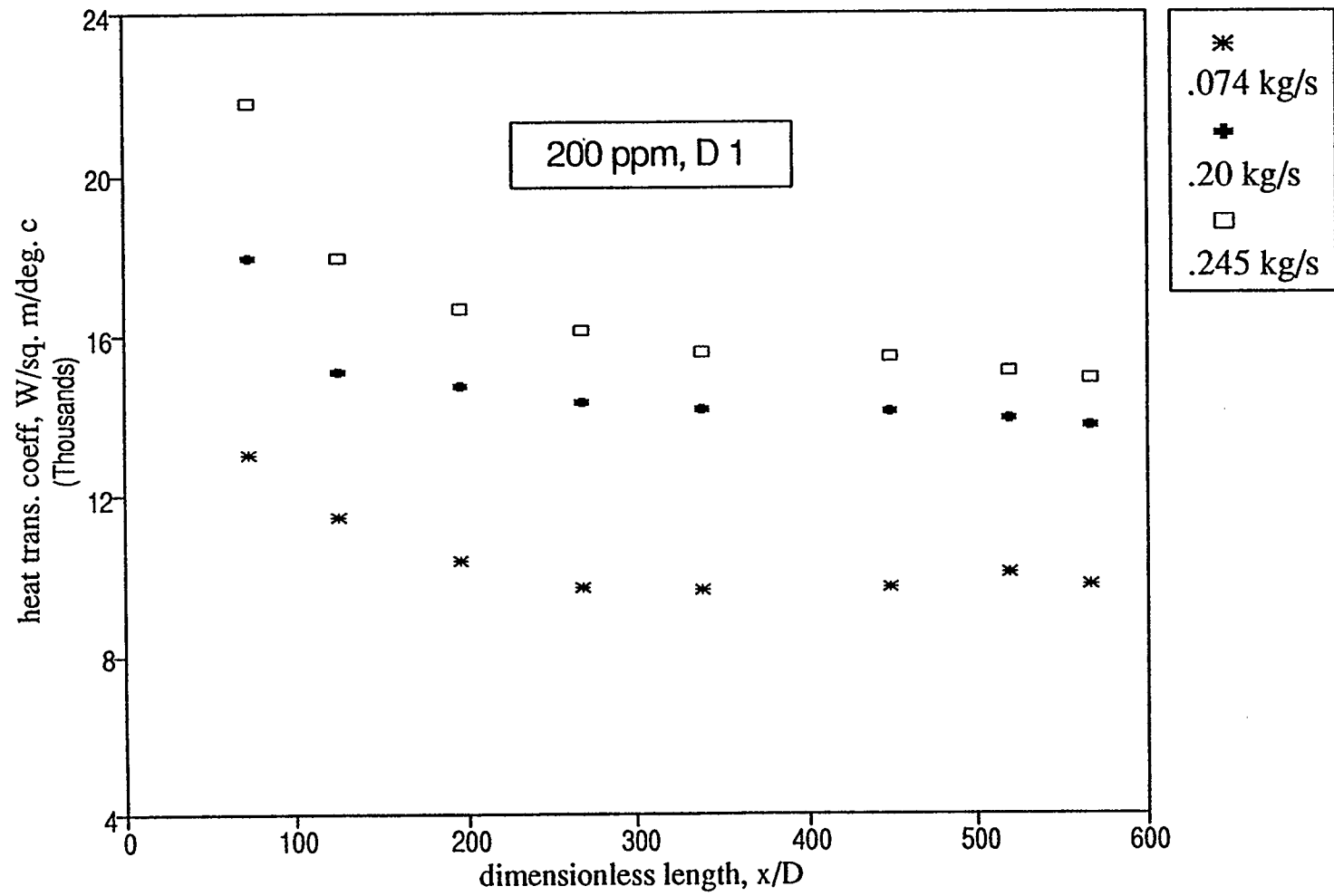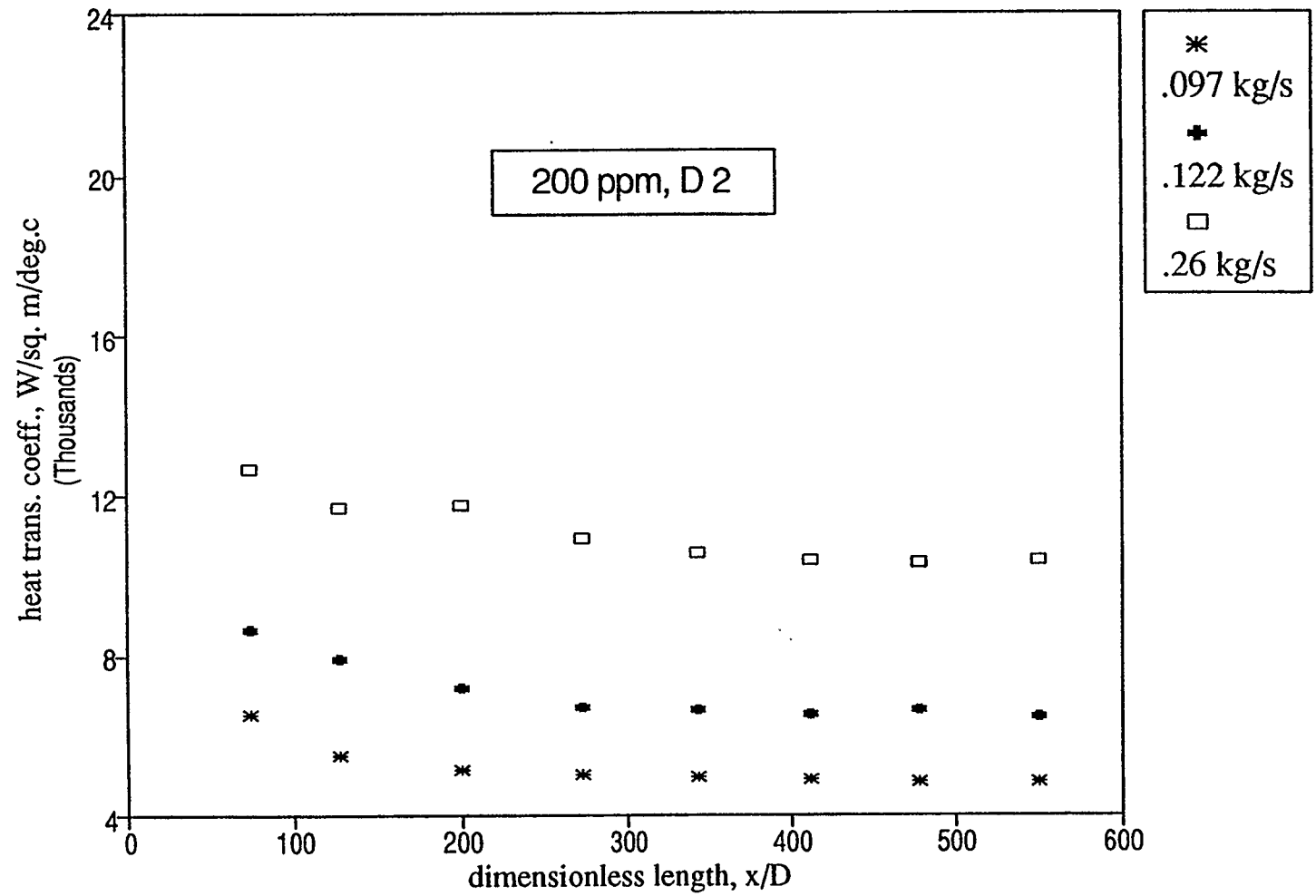
Figure 5.13. h versus x/D for Different Flow Rates (D 1)

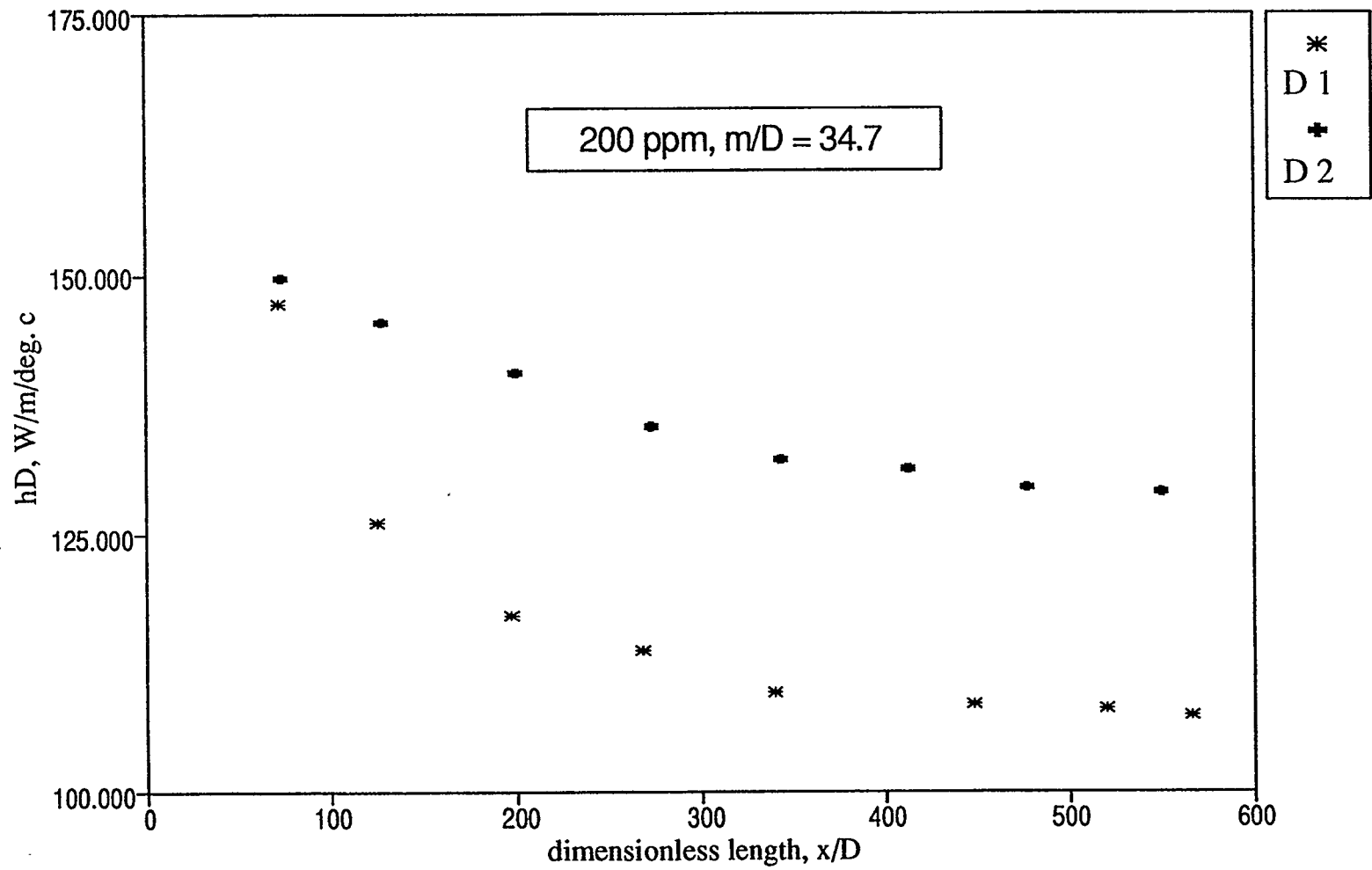Figure 5.14. h versus x/D For Different Flow Rates (D 2)

Figure 5.15. hD versus x/D for 200 ppm Solution

polymer molecules in solution plays an important part in producing the drag reduction and heat transfer reduction effect. If indeed it is the property of the polymer molecules in solution to resist stretching due to the action of turbulent shear forces, in the boundary layer flow, that results in the above discussed effects, then the polymer molecules should be effected in the same way irrespective of the diameter of the pipe if the shear stress near the wall is the same. In other words, if the same shear stress at the wall (i.e., same intensity of turbulent fluctuations) is maintained in two different diameter pipes for the flow of polymer solution, then similar drag and heat transfer reduction effects should be obtained. To test this hypothesis, shear stresses at the wall were calculated from the pressure drop data collected during the experimental runs. Data from pressure transducers in the fully developed flow region, which were far away from the entrance and the exit to the test section, were used in the calculations. One set of heat transfer and friction data, each for 20, 100 and 200 ppm solutions at the same shear stress at the wall in both the tubes was chosen. Drag reduction and heat transfer reduction were calculated by comparing these runs with the water runs at the same flow rates.

$$DR = \left(1 - \frac{\tau_{w_a}}{\tau_{w_s}}\right) \times 100 \qquad (same\ flow\ rate) \qquad (5.7)$$

$$HTR = \left(1 - \frac{h_{i_a}}{h_{i_s}}\right) \times 100 \qquad (same\ flow\ rate) \qquad (5.8)$$

Heat transfer coefficient, h_i is obtained by calculating the area under the curve in the plot of h_x versus x/D. The results obtained are shown in Table 5.1.

It is seen from Table 5.1 that the drag reduction ratios are observed to go down in all the cases with an increase in diameters. The heat transfer reduction is seen to go up for the 20 ppm solution but goes down for 100 and 200 ppm solutions with an increase in diameter. The above results are plotted graphically in figures 5.16 and 5.17.

In the above calculation, friction factor and heat transfer coefficients for water were calculated from empirical correlations as data were not available. Average heat transfer coefficient values were obtained from the calculation of area under the curve for local heat transfer coefficient versus x/D plot, which is an approximate method of calculation.

Figure 5.17 is a plot of DR/HTR ratio for the two diameters at the same shear stress for three different concentrations. Interestingly enough, the value of

DR/HTR ratio for the two diameters is very close to 1 for all concentrations. This may be due to the fact that the shear stress values for all the three sets of data are very close, indicating that there may be an analogy between heat and momentum transfer for drag reducing polymer solutions. The Reynolds analogy which assumes that the eddy diffusivities for heat and momentum transfer are approximately equal as the fundamental mechanism of heat and momentum transport are the same, does not does not hold for drag reducing polymer solutions when comparison is made at the same Reynolds number. It seems that from the above that there may be a basis to derive an analogy between momentum and heat transport in drag reducing fluids if comparison of results is made at same shear stress value at the wall. This may also be used in predicting the 'diameter effect' for these solutions. Though more data are not available currently to test this hypothesis, the trends shown by these results are quite encouraging and justify further investigation.

Table 5.1

Conc. (ppm)	τ_w (N/m^2)	Dia	DR	HTR	DR/HTR	$\left(\dfrac{DR_1/HTR_1}{DR_2/HTR_2}\right)$
20	33	(1)	17.888	6.9989	2.556	1.097
		(2)	17.251	7.3995	2.331	
100	29	(1)	16.930	9.36	1.8088	1.186
		(2)	13.710	8.988	1.5254	
200	30	(1)	19.438	10.302	1.8868	1.054
		(2)	17.580	9.82	1.7902	
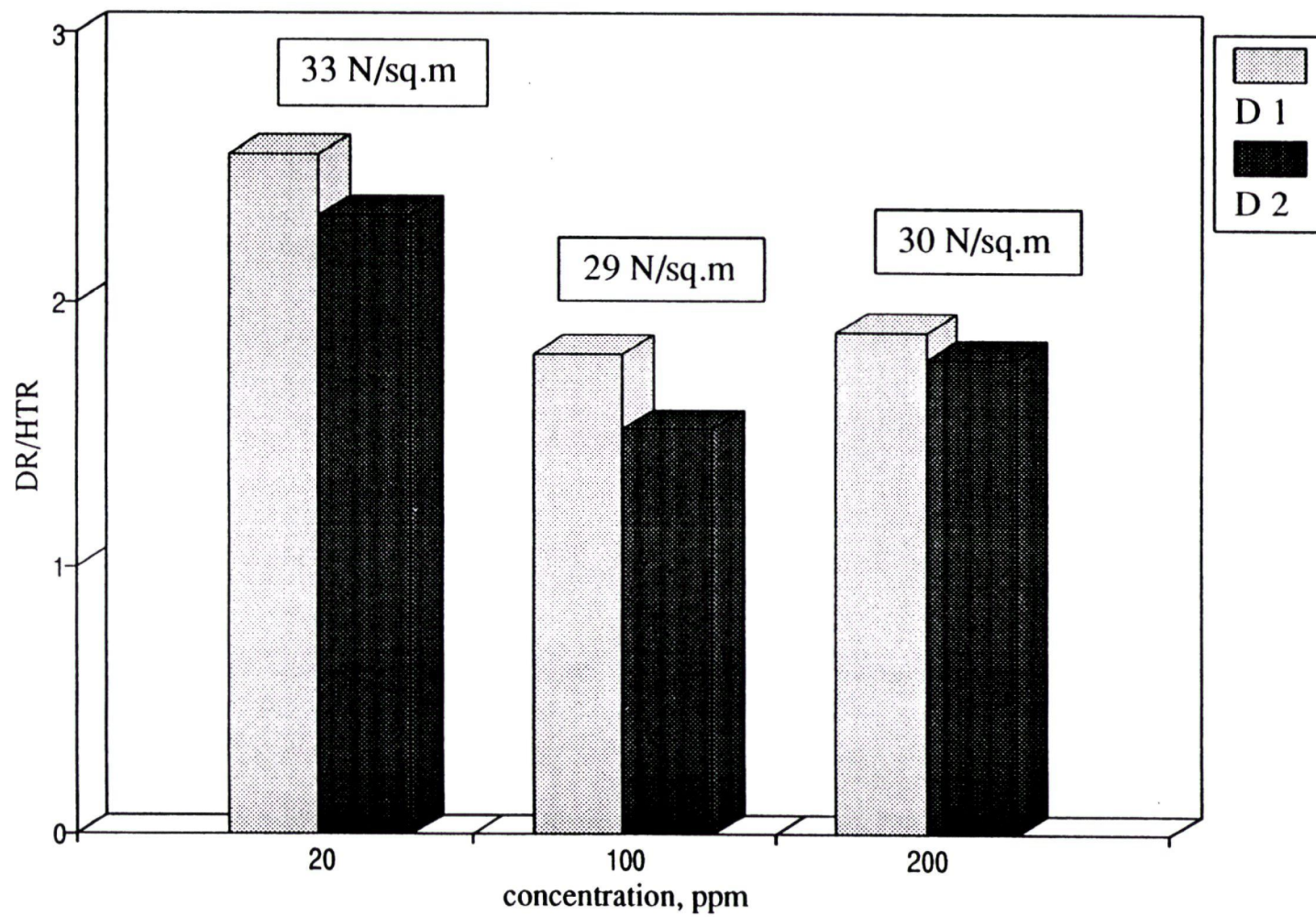
Figure 5.16. DR/HTR For 20, 100 and 200 ppm Solutions
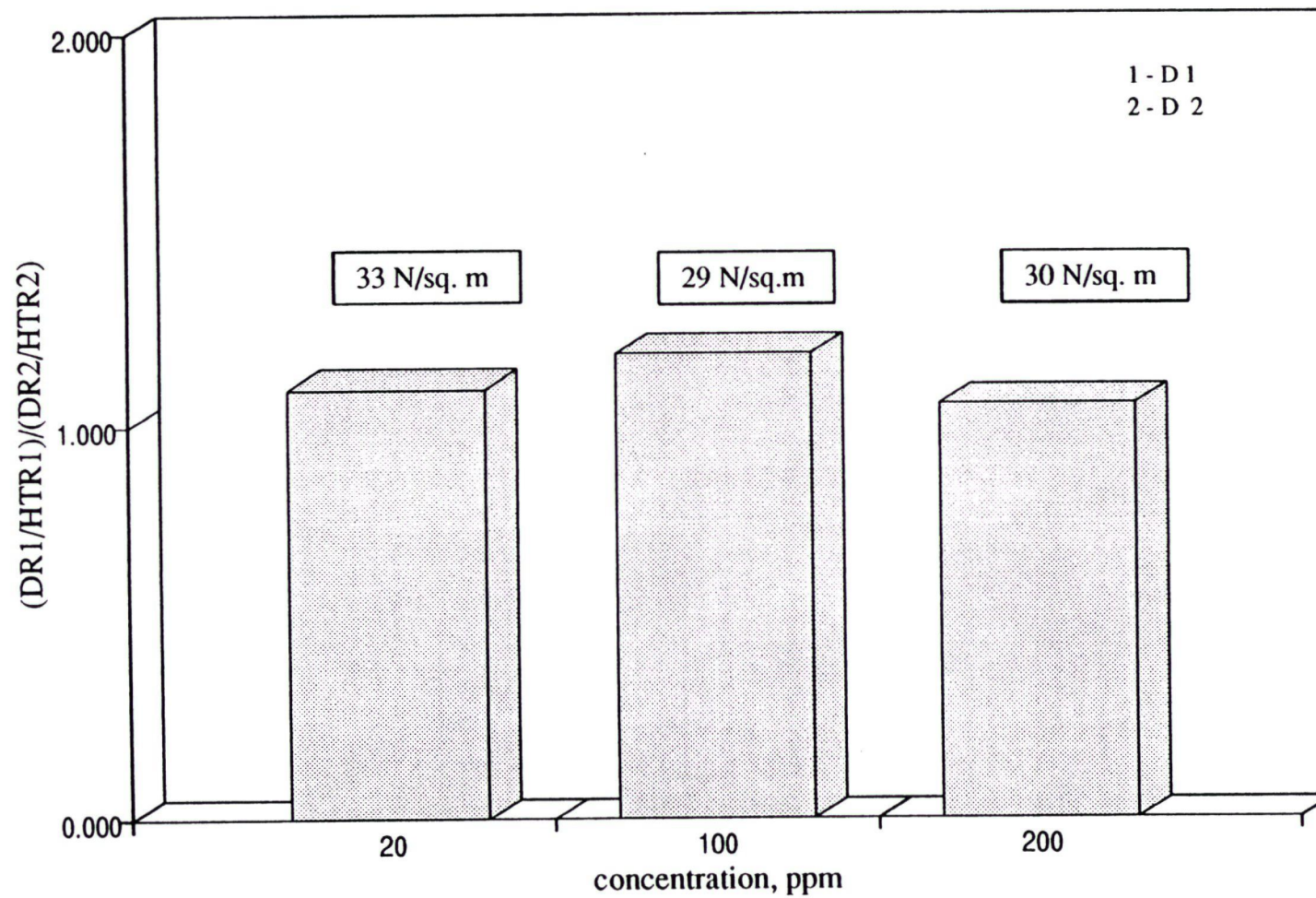
Figure 5.17. Drag Reduction to Heat Transfer Reduction Ratios for 20, 100 & 200 ppm Solutions

6. CONCLUSIONS AND RECOMMENDATIONS

An experimental study on momentum and heat transfer to dilute Poly(ethylene oxide) solutions has been completed. Experimental runs were carried out with and without constant heat flux input at the wall for three (20, 100 and 200 ppm) concentrations of polymer in solution and water in two SS 304 tubes of internal diameter 0.00704 m and 0.01021 m respectively. Pressure drop and temperature data were collected all along the length of the test tubes.

Viscosity measurements for these solutions were carried out at different shear rates and three temperatures in two concentric cylinder viscometers covering low and moderately high shear rates. Available correlations in literature to predict viscosity behaviour of dilute polymer solutions were tested on our data.

The following conclusions were drawn:

1.   Viscosity of dilute polymer solutions decreases with an increase in shear rate and tends towards an asymptotic value at higher shear rates. It is also a function of temperature with viscosity of a 20 ppm Poly(ethylene oxide) solution in water decreasing by about 30% for a 20°C rise in temperature.

2.   The Carreau model and Cross model fit the viscosity data best and predict

a viscosity at higher shear rates that tends towards an asymptotic value. Linear polynomials fit the experimental data well at low shear rates but tend to predict a solution viscosity which is lower than the pure Newtonian solvent viscosity at higher shear rates.

3.   An effect of increasing concentration of polymer in solution on friction factor and local heat transfer coefficients was observed. It was shown that an increase in concentration of the polymer in solution leads to an increase in drag reduction and lower heat transfer coefficients , with the effect becoming more apparent at higher flow rates.

4.   The findings of Meyer (1966) were confirmed that a critical value of shear stress at the wall has to be exceeded for the drag reduction effect to become apparent. A similar dependence of heat transfer reduction on shear stress at the wall was observed.

5.   Maximum reduction in heat transfer was observed in the entrance section of the test tube. Since in our experimental set up, hydrodynamic boundary layer and thermal boundary layer develop simultaneously, high shear stress values near the entrance of the tube might be effecting the polymer molecules and producing this increased reduction in heat transfer.

6.   A new hypothesis for predicting the 'diameter effect' on friction and heat transfer reduction was proposed, which is based on the concept of extensional viscosity (Dodge, 1959). This theory visualizes the polymer molecules absorbing energy and getting stretched due to the action of shear forces in the region near the wall. A comparison of friction and heat transfer results at the same values of shear stress at the wall should show similar trends for a given concentration of polymer in solution. The hypothesis was tested on a single set of data for 20, 100 and 200 ppm solutions and encouraging trends were observed.

Recommendations for future work are:

1.   Though extreme care was taken in preparing and homogenising the polymer solutions, the concentration of the solutions was not analyzed before the runs. A method for determining the exact concentration of the solution needs to be devised for proper correlation of friction and heat transfer results for different concentrations.

2.   Modifications in the experimental set up need to be carried out so that the same solution is tested in different diameter pipes for friction and heat transfer studies. This will eliminate the error that may have crept in due to non uniform concentration of the solutions.

3.   Further tests should be carried out at constant shear stress at the wall in different diameter pipes for different concentrations of polymer solutions. This will prove to be an effective test of the hypothesis that the polymer molecules are effected by the shear stress at the wall.

4.   More thermocouples should be used in the thermal entrance region to study the development of the thermal boundary layer for different concentration solutions.

5.   Accurate viscosity measurements should be carried out at higher shear rates to provide a sound basis for correlating the experimental results with Reynolds number of the flow.

REFERENCES

Astarita, G., Greco, Jr., G., Nicodemo, L.;"A phenomenological; interpretation and correlation of drag reduction", AIChE J., 15(4):564, 1969.

Berman, N.S. and George, W.K.;"Onset of drag reduction in dilute polymer solutions", Phys of Fluids, 17:250, 1974

Bird, R.B., Armstrong, R.C. and Hasseger, O.;"Dynamics of polymeric liquids", Vol 1:Fluid Mechanics, J. Wiley, New York, 1977

Burger, E.D., Chorn, L.G. and Perkins, T.K.;"Studies of drag reduction conducted over a broad range when flowing Prudhoe Bay crude oil", J. Rheol., 24(5):603, 1980.

Carreau, P.J.;"Rheological equations from molecular network theories", Trans. Soc. Rheol., 16:99, 1972

Cottrell, F.R., Merrill, E.W., Smith, K.A.;"Intrinsic Viscosity and axial extensions ratio of random-coiling macromolecules in a hydrodynamic shear field", Polymer, 8:287, 1970

Darby, R. and Chang, H.D.;"Generalized correlation for friction loss in drag reducing polymer solutions", AIChE J., 30(2):274, 1984.

Darby, R. and Pivsa-art, S.;"An improved correlation for turbulent drag reduction in dilute polymer solutions", Can. J. of Chem. Eng., 69:1395, 1991.

De Loof, J.P., De Lagarde, B., Petry, M. and Simon, A.;"Pressure drop reduction in large industrial ducts by macromolecular additives", Proc. 2nd Int. Conf. on Drag Reduction, Cranfield, England, 1977.

Deissler, R.G.;"Turbulent heat transfer and friction in the entrance regions of smooth passages", Trans ASME, 77:1221, 1955.

Dimant, Y. and Poreh, M.;"Heat transfer in flows with drag reduction", Adv. Heat Transfer, 12:77, 1976.

Dodge, D.W.;"Fluid systems", Ind. and Eng. Chemistry, 51:839, 1959.

Elbirli, B. and Shaw, M.T.;"Time constants from shear viscosity data", J. of Rheol., 22(5):561, 1978.

El'Perin, I.T., Smol'skii, B.M. and Leventhal, L.I.;"Decreasing the hydrodynamic resistance of pipelines", Int. Chem. Eng., 7:276, 1967

Fabula, A.G.;"Fire-fighting benefits of polymeric friction reduction", J. Basic Eng., Trans, ASME, Series D, 93(4):453, 1971.

Gadd, G.E.;"Reduction of turbulent friction in liquids by certain additives", Nature, 212:874, 1966.

Gadd, G.E.;"Turbulence damping and drag reduction produced by certain additives in water", Nature, 206:463, 1965.

Gadd, G.E.;"Differences in normal stress in aqueous solutions of turbulent drag reducing additives", Nature, 212:1348, 1966.

Gampert, B. and Wagner, P.;"reduced turbulence production by increased elongational viscosity", Recent contributions to fluid mechanics, ed. Haase, W., Springer, Berlin-New York, 1982.

Golda, J.;"Hydraulic transport of coal in pipes with drag reducing additives", Chem. Eng. Commun, 43:53, 1986.

Greene, H.L., Mostardi, R.F. and Wokes, R.F.;"Effects of drag reducing polymers on initiation of arteriosclerosis", Polym. Eng. Sci., 20:499, 1980.

Gupta, M.K., Metzner, A.B. and Hartnett, J.P.;"Turbulent heat transfer characteristics of viscoelastic fluids", Int. J. Heat Mass Transfer", 10:1211, 1967.

Hartnett, J.P. and Cho, Y.I.;"Non-Newtonian fluids in circular pipe flow", Adv. Heat Transfer, 15:59, 1982.

Hoyt, J.W.;"The effect of additives on fluid friction", Trans ASME, J. Basic Eng., 94:258, 1972.

Huang, T.T.;"Similarity laws for turbulent flow of dilute solutions of drag reducing polymers", The Phy. of Fluids, 17(2):298, 1974.

Interthal, W. and Wilski, H.;"Drag reduction experiments with very large pipes", Colloid Polym. Sci., 263:217, 1985.

Johnson, B. and Barchi, R.H.;"Effect of drag reducing additives on boundary layer turbulence", J. Hydronautics, 2:108, 1968.

Kays, W.M. and Crawford, H.R.;"Convective heat and mass transfer", McGraw Hill, 1980.

Khabakhpasheva, E.M. and Perepelitsa, B.V.;"Turbulent heat transfer in weak polymeric solutions", Heat transfer-Sov. Res., 5:117, 1973.

Kulicke, W.M., Kotter, M. and Grager, H.;"Drag reduction phenomenon with special emphasis on solutions", Advances in Polymer Science, 89:1, 1989.

Little, R.C.;"Flow properties of polyox solutions", Ind. Eng. Chem. Fundam., 8:520, 1969.

Lumley, J.L.;"Turbulence in non-newtonian fluids", Phys of Fluids, 7:335, 1964.

Lumley, J.L.;"Drag reduction by additives", Ann. Rev. Fluid Mech., 1:367, 1969.

Lumley, J.L.:'Drag reduction in turbulent flow by polymer additives", J. Polym. Sci. Macromol. Rev., 7:263, 1973.

Matthys, E.F. and Sabersky, R.H.;"A method of predicting the diameter effect for heat transfer and friction of drag reducing fluids", Int. J. Heat Mass Transfer, 25(9):1343, 1982.

Matthys, E.F. Ahn, H. and Sabersky, R.H.;"Friction and heat transfer measurements for clay suspensions with polymer additives", J. Fluids. Eng., 109(3):307, 1987.

Matthys, E.F.;"Heat transfer, drag reduction and fluid characterization for turbulent flow of polymer solutions:recent research needs", J. of Non-Newtonian Fluid Mech., 38:313, 1991.

Merrill, E.W. and Shaver, R.G.;"Turbulent flow of pseudoplastic polymer solutions in straight cylindrical tubes", AIChE Journal, 5:189, 1959.

Meyer, W.A.;"A correlation of the frictional characteristics for turbulent flow of dilute viscoelastic non-newtonian fluids in pipes", AIChE J., 12:522, 1966.

Neilsen, E.N.;"Polymer Rheology", Marcel Dekker Inc., New York , 121, 1977.

Ng, K.S., Hartnett, J.P. and Tung, T.T.;"Heat transfer of concentrated drag reducing viscoelastic polyacrylamide solutions", AIChE Heat Trans. Conf., 17th, 74, 1977.

Patterson, G.K. and Zakin, J.L.;"Prediction of drag reduction with a viscoelastic model", AIChE J., 14:434, 1968.

Peterlin, A.;"Molecular model of drag reduction by polymer solutes", Nature, 227:598, 1970.

Perry, R.H. and Green, D.;"Perry's Chemical Engineers's Handbook", Chapter 5, 1984.

Savins, J.G.;"Drag reduction characteristics of solutions of macromolecules in turbulent pipe flow", SPE J., 4:203, 1964.

Savins, J.G.and Seyer, F.A.;"Drag reduction scale up criteria", Phy. of Fluids, 20(10), Pt II:S78, 1977.

Sellin, R.H.J., Hoyt, J.W. and Scrivener, O.;"The effect of drag reducing additives on fluid flows and their industrial applications", Part 1, J. Hydraulic Res., 20::29, 1982.

Sellin, R.H.J. and Ollis, M.;"Effect of pipe diameter on polymer drag reduction", Ind. Eng. Chem. Prod. Res. Dev., 22:445, 1983.

Singh, R.P., Singh, J., Deshmukh, S.R. and Kumar, A.;"Novel applications of drag reducing polymers in agriculture", Drag Reduction in Fluid Flows, Sellin, R.H.J. and Moses, R.T.(Eds), Ellis, Horwood, Chichester, 223, 1989.

Smith, K.A., Keuroghlian, P.S., Virk, P.S. and Merrill, E.W.;"Heat transfer to drag reducing polymer solutions", AIChE J., 15:294, 1969.

Toms, B.A.;"Some observations on the flow of linear polymer solutions through

straight tubes at large reynolds numbers", Proc. 1st Int. Congr. on Rheology, North Holland, Amsterdam, 1948.

Tritton, D.J.,"Physical fluid dynamics", Oxford Science Publication, 2nd ed., 1990.

Tulin, M.P.;"Hydrodynamic aspects of macromolecular solutions", Proc. 6th Symp. on Naval Hydrodynamics, ONR CR-136, P3, Washington, 1966.

Virk, P.S.;"The toms phenomenon: turbulent pipe flow of dilute polymer solutions", Fluid Mech., 30:305, 1967.

Virk, P.S.;"The ultimate asymptote and mean flow structure in toms phenomenon", ASME J. Appl. Mech., 37:488, 1970.

Virk, P.S.;"Drag reduction in rough pipes", J. Fluid Mech., 45:225, 1971.

Virk, P.S.;"Drag reduction fundamentals", AIChE J., 21:625, 1975.

Walsh, M.;"Theory of drag reduction in dilute high polymer flows", Int. Shipbuilding Prog., 14:134, 1967.

Wells, C.S. and Walters, R.R.;"An experimental study of turbulent diffusion of drag reducing polymer additives", J. Hydronautics, 5:65, 1971.

Yoo, S.S. and Hartnett, J.P.;"Thermal entrance lengths for non-newtonian fluids in turbulent pipe flow", Lett. Heat Mass Transfer, 2:189, 1975.

Yoon, H.K. and Ghajar, A.J.;"A method for correlating the diameter and concentration effects on friction and heat transfer in drag reducing flows", Paper AIAA-88-2622, AIAA, Washington, D.C., 1988.

APPENDIX I

CALIBRATIONS

Before actual runs were performed on the experimental set up, calibration

runs were carried out to determine the accuracy of the measurement techniques

and the Data Acquisition System.

A.1. Temperature Measurement

To study the response time and accuracy of the thermocouples, the inlet of

the test section was connected to the cold water (5°C) and hot water (60°C)

supply lines through two valves in such a way that it allowed instant switching

from one line to the other. Such an arrangement was useful in studying the

response of the thermocouples to step change in input.

The procedure adopted for this study is outlined below:

Cold water was allowed to run through the system for some time to let the

thermocouples reach a steady state value. This could be observed by graphically

monitoring the run conditions on the computer. At this moment, data transfer to

the files was initiated. After a few seconds, by quickly operating the valves, the

cold water line was shut off and hot water was allowed to pass through the

system. The system was allowed to reach a steady state and transfer of data to files was stopped.

It was observed (figure A1) that the thermocouple installed at the inlet of the test section to measure the bulk fluid temperature took about 100 seconds to reach the final steady state after the step input. The thermocouple at the outlet of the test section took slightly more time to reach the final steady state (figure A2), which is understandable, as the moment when the cold water line was shut off and hot water circulated through the system, the test section still contained cold water. This introduced a time lag in the response of the thermocouple at the outlet of the test section. Also, it read lower than the thermocouple at the inlet at steady state because of the heat losses to the ambient from the copper plates soldered to the two ends of the test section.

The response of the thermocouples was tested for a step change of 55°C in temperature. During actual heat transfer experiments, the heat flux input at the wall resulted in a wall temperature rise of about 10-12°C for the low flow rates. Hence the steady state was achieved much quickly in this case.

In comparison with the thermocouples at the ends of the test section, the ones on the wall of the tube followed almost the same responses (figure A3).
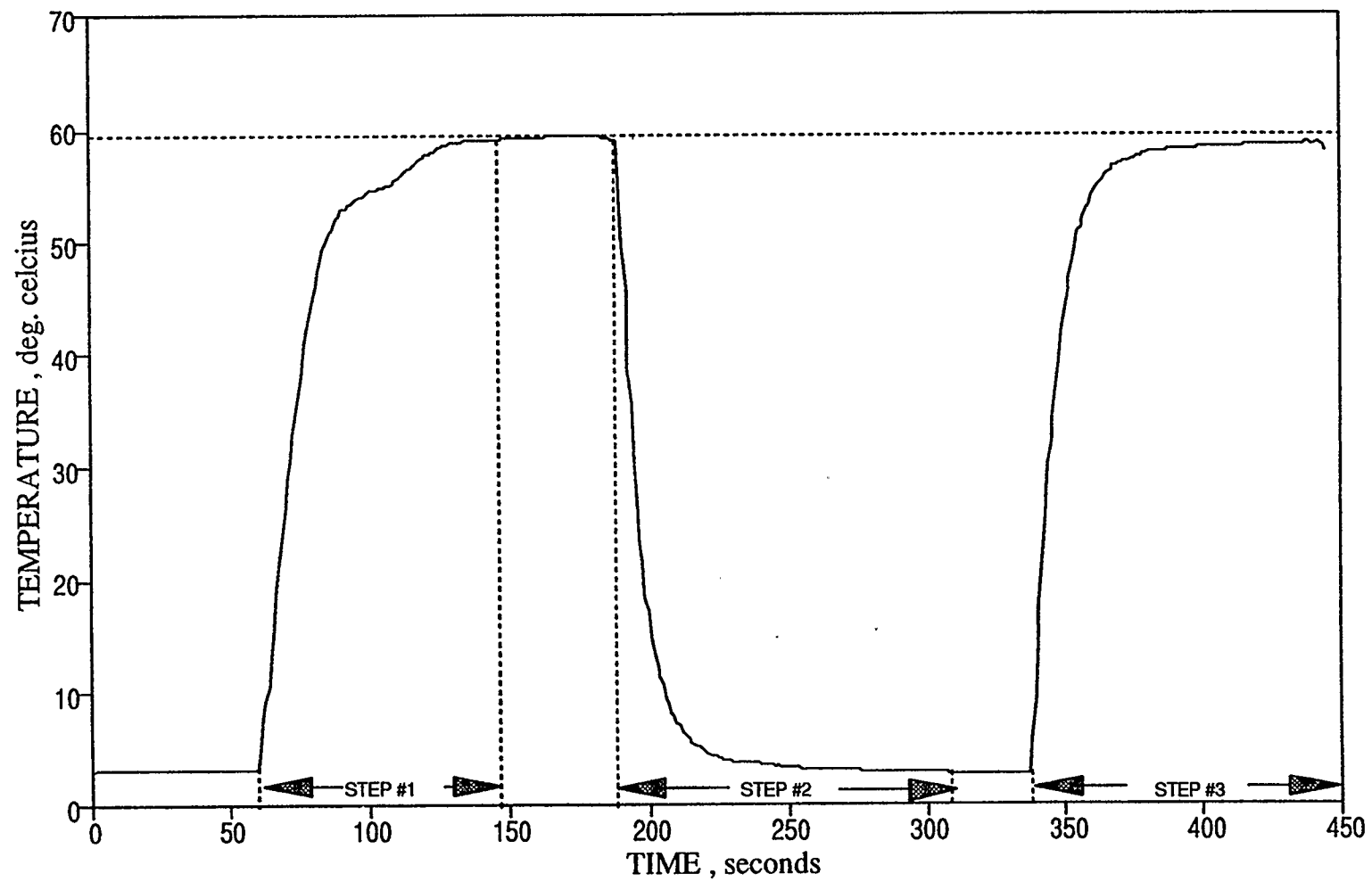
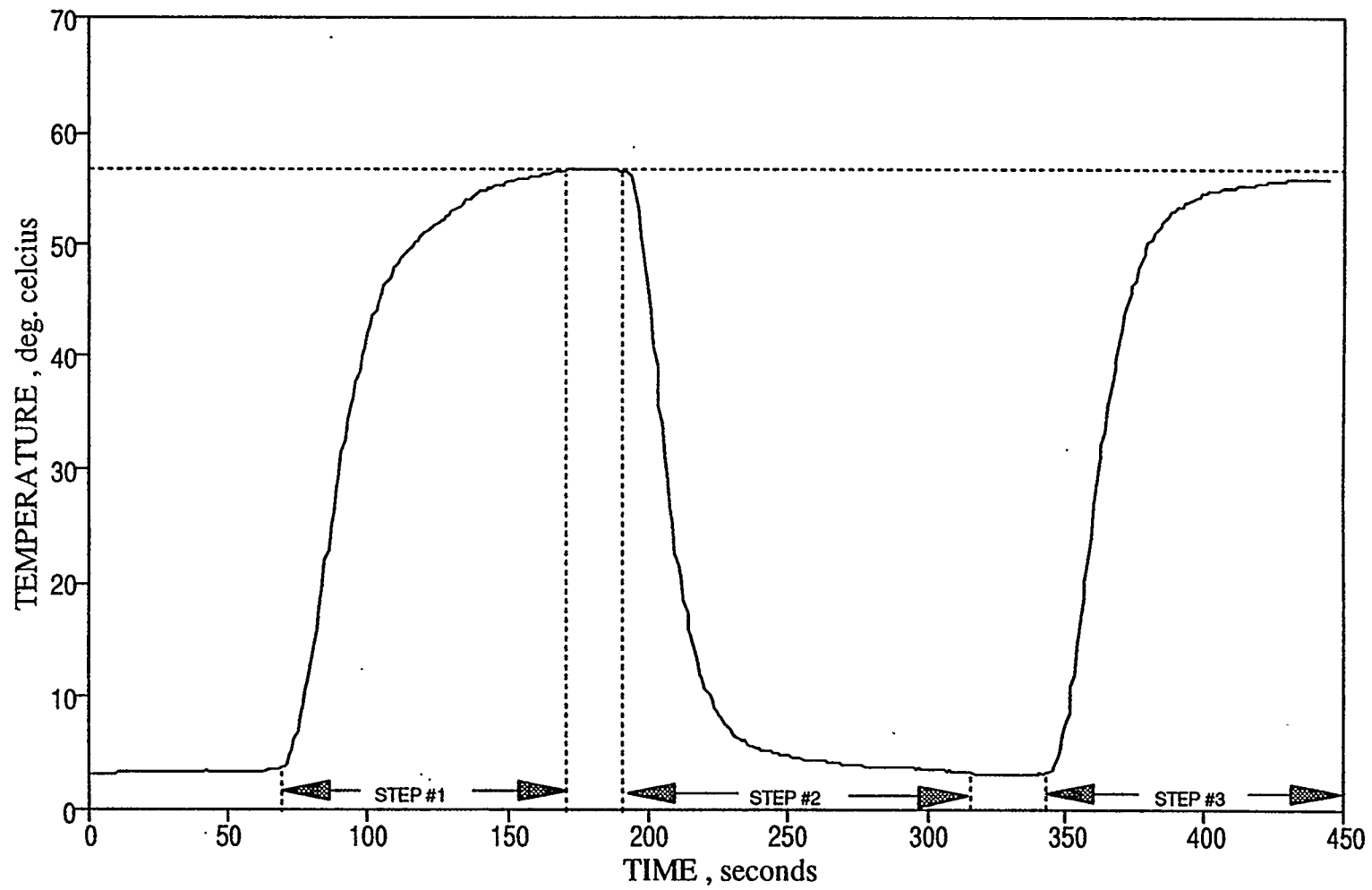Figure A1. Thermocouple Response to Step Change in Input (at inlet)

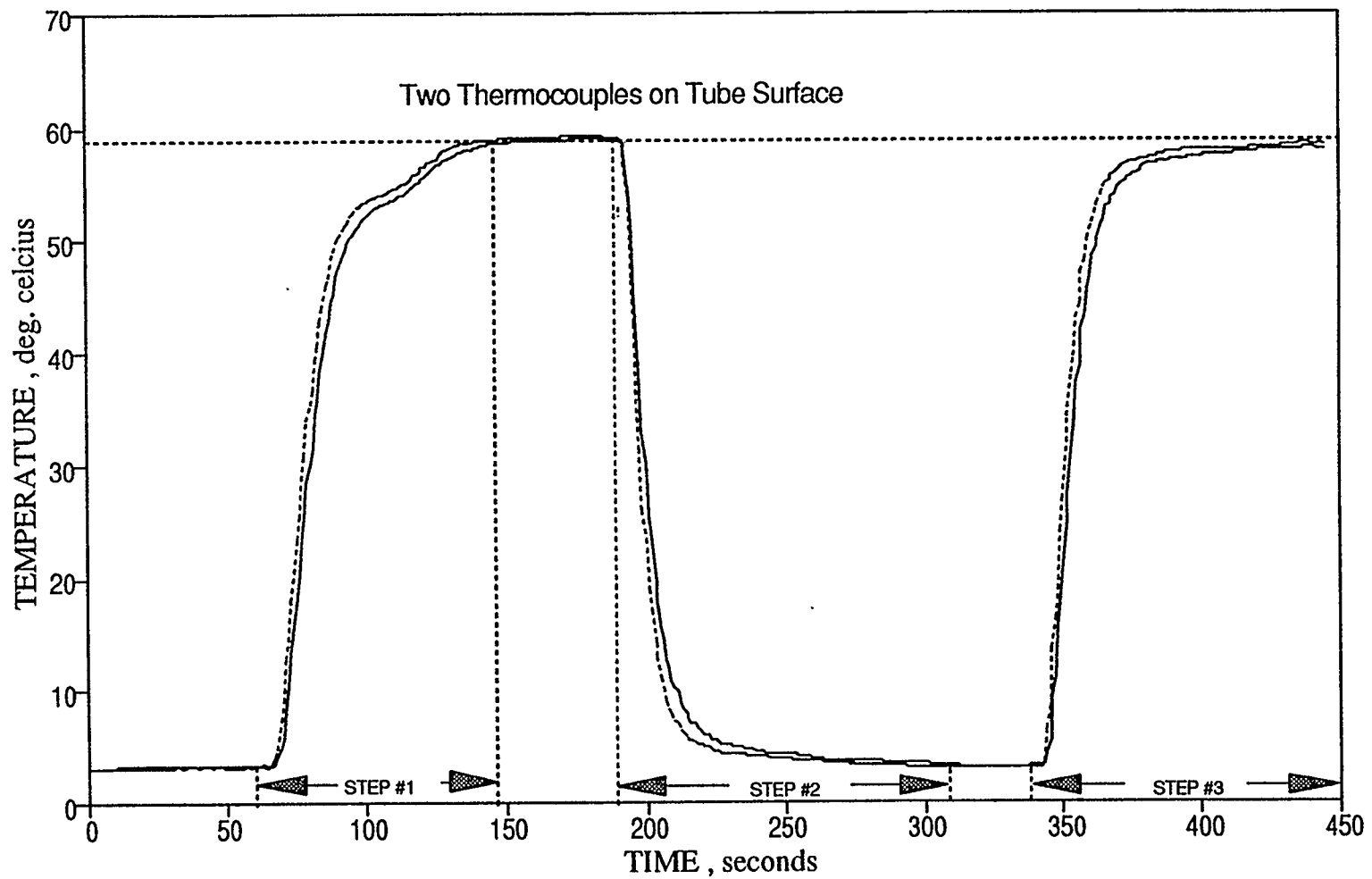Figure A2. Thermocouple Response to Step Change in Input (at outlet)

Figure A3. Thermocouple Response to Step Change In Input (on tube surface)

Another calibration run was done by passing water at room temperature through the system. All the thermocouples read the temperature within 0.5°C of each other.

The above analysis enabled determination of the response time of the thermocouples. Hence in all heat transfer measurements, a sufficient time delay (about 90-100 seconds) was allowed prior to data collection, to ensure that all thermocouples were reading steady state temperatures. In addition to this, a visual monitoring of the run conditions on the computer was also done during all the runs to ensure data acquisition at steady state .

A.2. Energy Balance

Runs were carried out with water at different wall heat flux inputs to ascertain the validity of the law of conservation of energy for our system. The power output from the DC welder (a measure of the heat input at the wall) was calculated from the voltage and current signals measured by the data acquisition system. The amount of heat removed from the system by water was calculated by measuring the flow rate and monitoring the temperatures at the inlet and outlet of the test section. It was observed that the heat losses to the ambient were minimum and the data acquisition system was able to verify the heat balance

within ±2.0%, which is within the limits of experimental error (figure A4).

The power output from the DC power supply was constant (±0.5%) and ripple-free, which was essential for maintaining constant heat flux conditions at the wall (figure A5). It was monitored for all runs by using the Data Acquisition System which received the voltage and current signals from the DC power supply. The software enabled online calculation of power input from the DC welder, which could be visually monitored during the runs on the computer screen.

A.3. Pressure Measurement

The 10 pressure transducers used for the experimental set up were statically calibrated against a digital manometer at 7 pressure levels, covering the range of operating pressures used during the actual runs. The pressure transducers had linear responses (figure A6). The calibration curves for individual transducers were incorporated in the Data Acquisition software. During the experimental runs, voltage signals from the pressure transducers were converted to absolute pressures
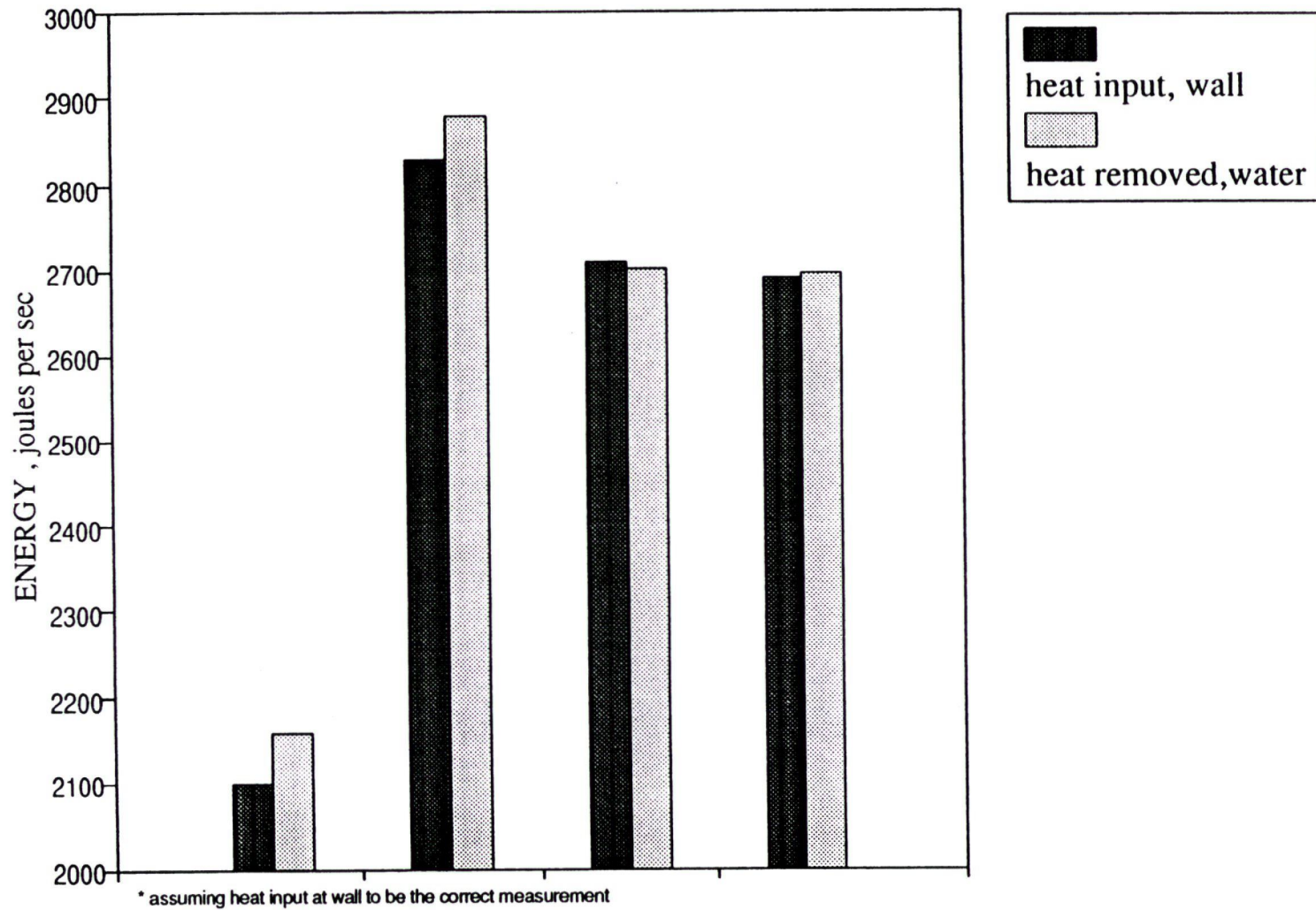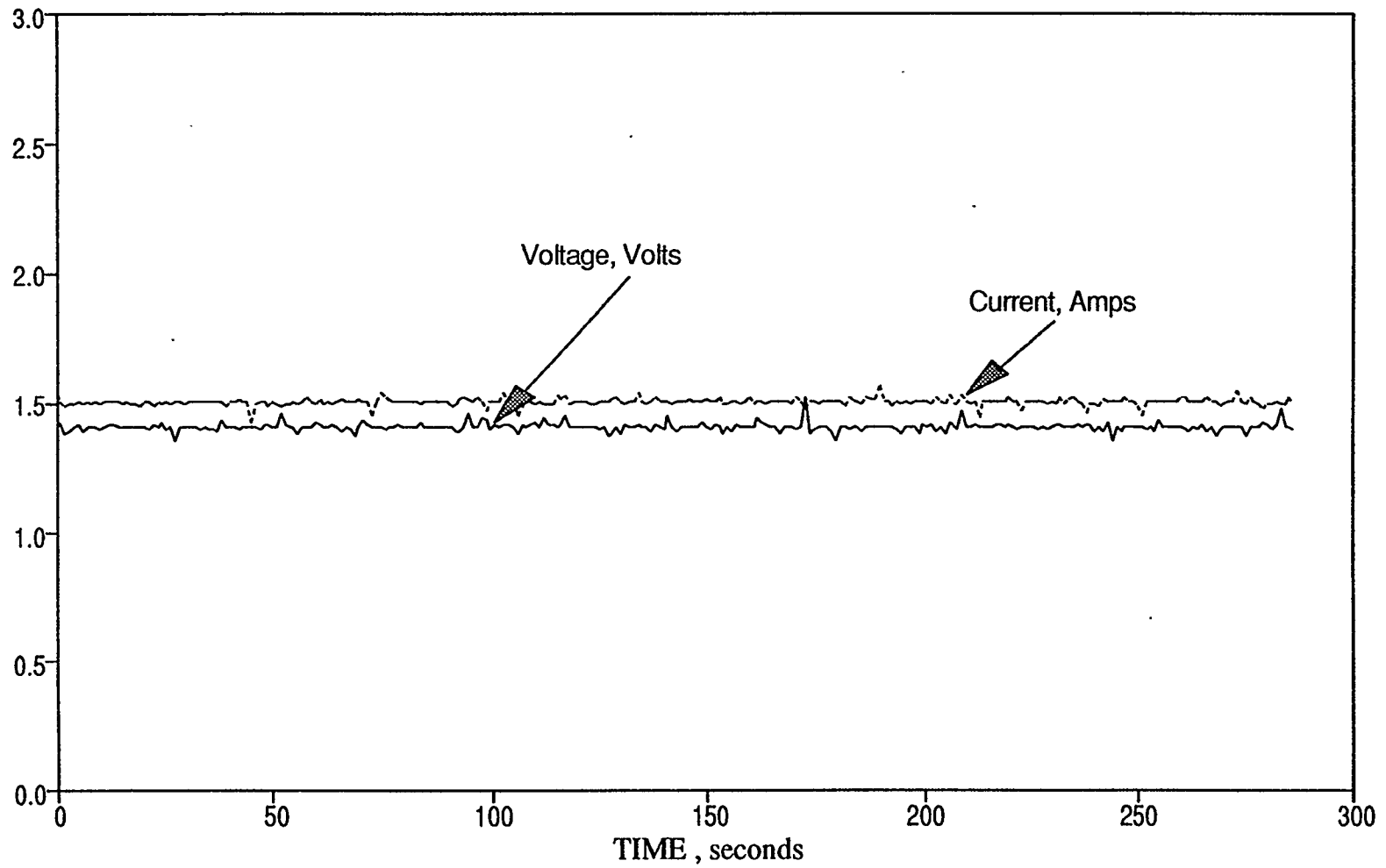
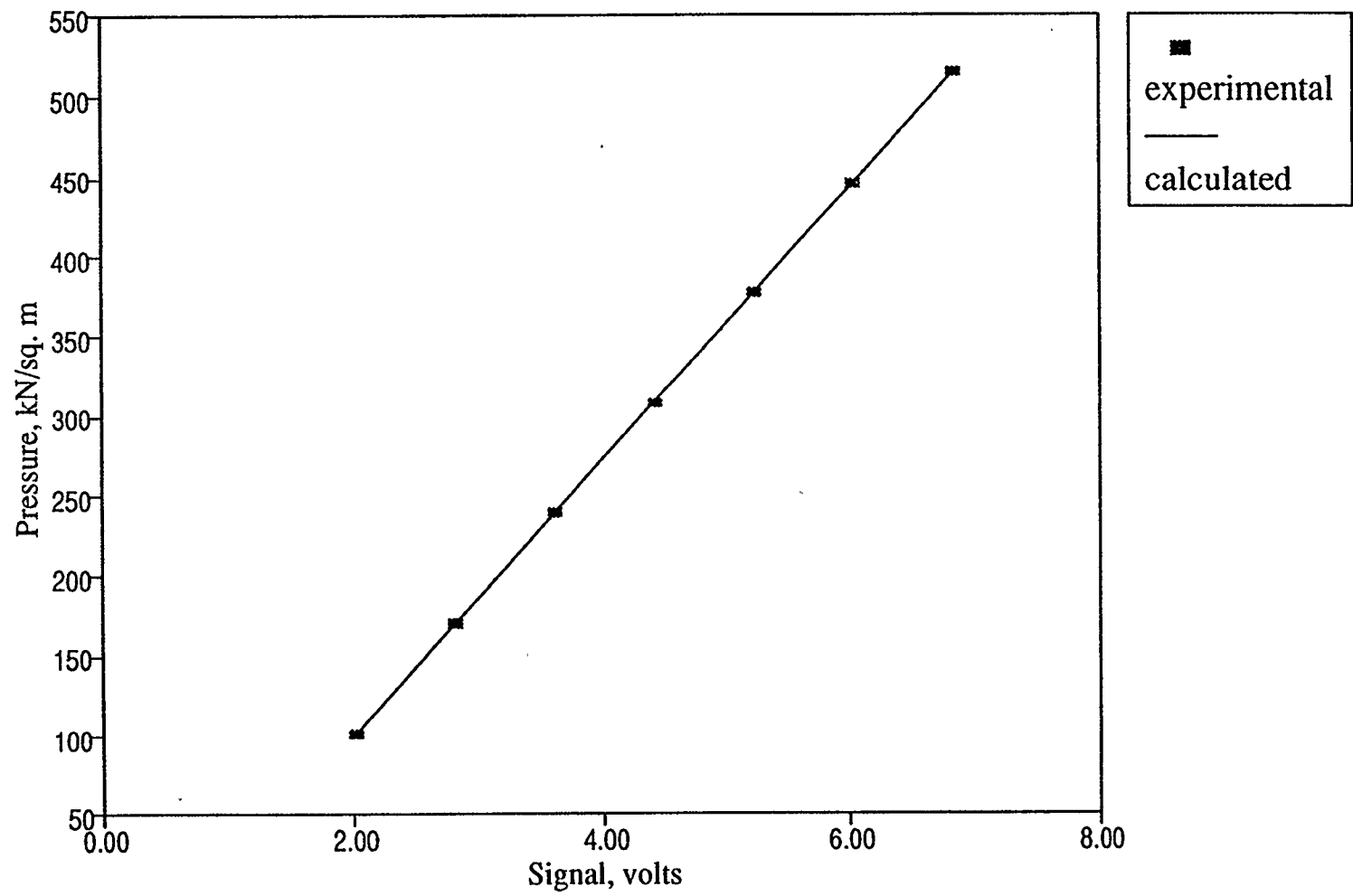Figure A4. Energy Balance On Test Section

Figure A5. DC Welder Output

Figure A6. Typical Pressure Transducer Calibration Curve

and written to files.

Air pressure from a compressed air cylinder was used to provide the driving force to make the solutions flow through the system. A pressure regulator on the air cylinder maintained the constant pressure in the pressure tank. The changing liquid level in the 1.6 m high pressure tank could lead to corresponding change in the test section pressure head. To study this fluctuation, a run was carried out in which the water level in the pressure tank was allowed to go down by 0.75 m at a constant pressure head. It was observed that the reading from the first transducer on the test section changed by 0.4% (figure A7). During actual runs the liquid level in the tank would go down by about 5 cm. Hence it was safe to assume that constant pressure head (flow rate) was maintained during the runs.

A.4. Friction Results for Water

Runs with water were done at different flow rates to enable friction factor calculations at different Reynolds numbers. A comparison of the experimental results with the values predicted by the empirical correlations available in the literature showed a good agreement within 4% (figure A8).
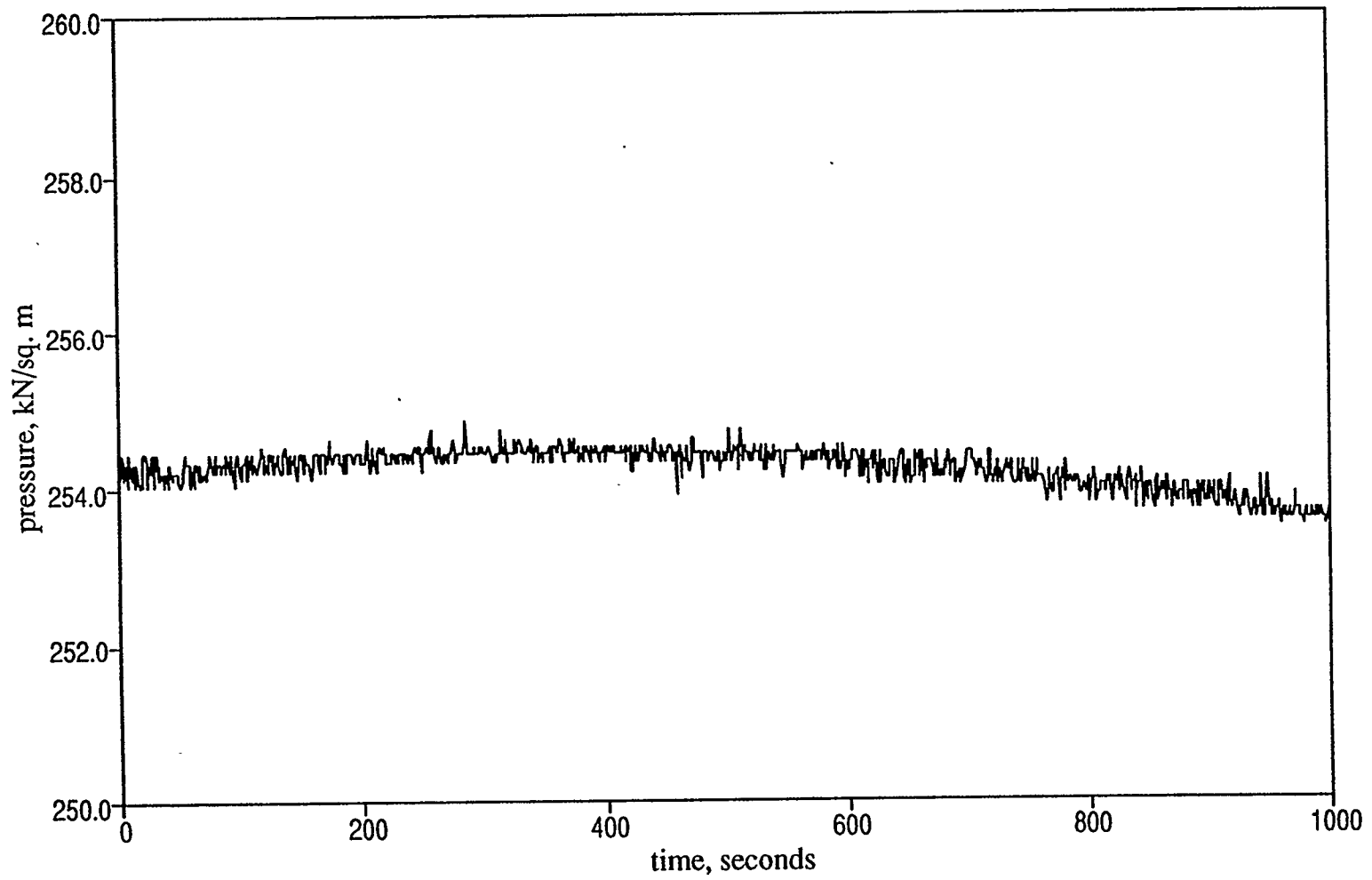
Figure A7. Effect of Changing Liquid Level in The Pressure Tank on Pressure Readings
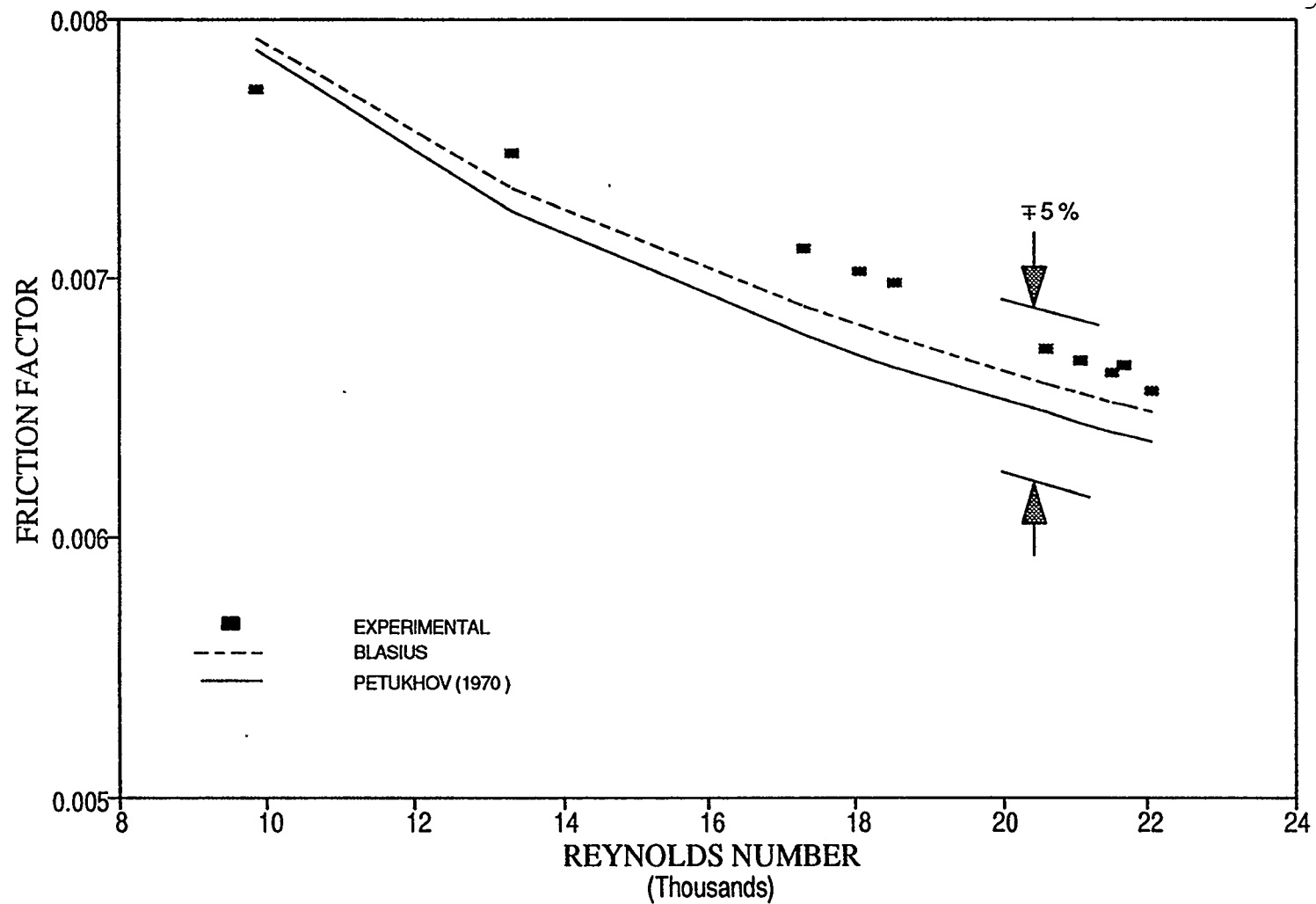
Figure A8. Friction Results For Water

A.5. Heat Transfer Results for Water

Average heat transfer coefficients (Nusselt number) for water runs at different flow rates were compared with those predicted by empirical correlations available in the literature. There is a difference of about 20% in the values of heat transfer coefficients predicted by correlations. Our values of heat transfer coefficients for water seem to be predicted well by the Sleicher and Rouse correlation. An agreement within ± 10% is observed (figure A9).
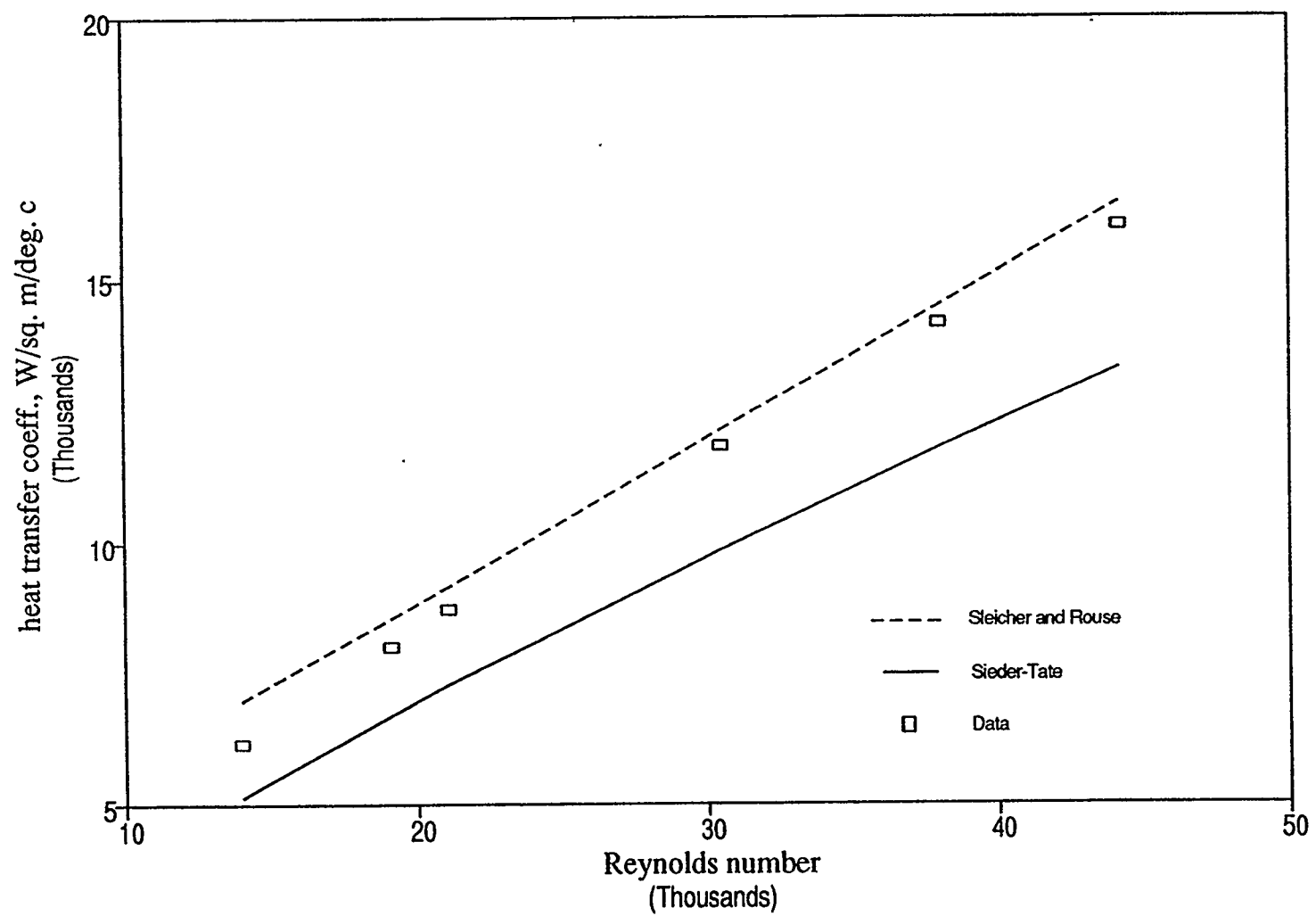
Figure A9. Heat Transfer Results For Water

APPENDIX II

To calculate the temperature difference across the tube wall, heat conduction is considered. The general energy equation is of the form,

Input + Generation = Output + Accumulation

Assuming steady state conditions, the equation takes the form,

Generation = Output - Input

In cylindrical coordinates,

$$\nabla\left[(k_s(r,x))\,\nabla T\right] = -Q(r,x) \qquad (1)$$

or,

$$\nabla k_s(r,x)\nabla T + k(r,x)\nabla^2 T = -Q(r,-x) \qquad (2)$$

where Q is the heat generated per unit volume of the steel tube. Both k and Q can be functions of r and x. As a simplification, radial heat temperature gradients are assumed to be much larger than the axial ones (as discussed in Chapter 5). Also, since the thickness of the tube wall is very small, k and Q are assumed to be constant in the radial direction. Hence, the equation finally reduces to the form,

Integrating,

$$\frac{\partial^2 T}{\partial r^2} + \frac{1}{r}\frac{\partial T}{\partial r} = -\frac{Q}{k_s} \qquad (3)$$

$$\frac{\partial T}{\partial r} = -\frac{Qr}{2k_s} + \frac{C_1}{r} \qquad (4)$$

Integrating once again,

$$T = -\frac{Qr^2}{4k_s} + C_1 \ln(r) + C_2 \qquad (5)$$

The boundary conditions are as follows;

1. At $r = r_{ow}$, $\qquad T = T_{ow}$

2. At $r = r_{iw}$, $\qquad k_s\frac{\partial T}{\partial r} = Q_1$

where,

$$Q_1 = Q\left[\frac{\pi\left(r_{ow}^2 - r_{iw}^2\right)L}{2\pi r_{iw}L}\right] \qquad (6)$$

Equating the boundary condition 2 and equation 4,

$$\frac{Q_1}{k_s} = -\frac{Qr}{2k_s} + \frac{C_1}{r} \tag{7}$$

or,

$$
\begin{aligned}
C_1 &= \frac{Q_1 r_{iw}}{k_s} + \frac{Q}{2k_s} r_{iw}^2 \\
&= \frac{Q}{2\pi k_s L}\left[\frac{r_{ow}^2}{r_{ow}^2 - r_{iw}^2}\right]
\end{aligned}
\tag{8}
$$

From boundary condition 1 and equation 5,

$$
\begin{aligned}
C_2 &= T_{ow} + \frac{Q r_{ow}^2}{4k_s} - C_1 \ln(r_{ow}) \\
&= T_{ow} + \frac{Q r_{ow}^2}{4k_s} - \frac{Q}{2\pi k_s L}\left[\frac{r_{ow}^2}{r_{ow}^2 - r_{iw}^2}\right]
\end{aligned}
\tag{9}
$$

Substituting equations (9) and (10) in equation (5),

$$
\begin{aligned}
T - T_{ow} &= \frac{Q}{4\pi k_s L} + \frac{Q}{2\pi k_s L}\frac{r_{ow}^2}{r_{ow}^2 - r_{iw}^2}\ln\left(\frac{r}{r_o}\right) \\
&= \frac{Q}{4\pi k_s L}\left[1 + \frac{2r_{ow}^2}{r_{ow}^2 - r_{iw}^2}\ln\left(\frac{r}{r_{ow}}\right)\right]
\end{aligned}
\tag{10}
$$

At $r = r_{iw}$, $T = T_{iw}$, hence equation (11) takes the form,

$$T_{iw} - T_{ow} = \frac{Q}{4\pi k_s L}\left[1 + \frac{2r_{ow}^2}{r_{ow}^2 - r_{iw}^2}\ln\left(\frac{r_{iw}}{r_{ow}}\right)\right] \tag{11}$$

Expressing in terms of the outer and the inner wall diameters,

$$T_{ow} - T_{iw} = \frac{Q\left[2D_o^2\ln(D_o - D_i) - (D_o^2 - D_i^2)\right]}{4\pi(D_o^2 - D_i^2)k_s L} \tag{12}$$

APPENDIX III

Friction factor calculations

The friction factor, f, is defined as the ratio of the wall shear stress to the velocity head. It is given as,

$$f = \frac{\tau_w}{\rho u_m^2/2g_c} = \frac{2g_c\tau_w}{\rho u_m^2} \tag{A1}$$

This equation can be derived if we consider steady state flow in a horizontal tube. The fluid is incompressible and has a fully developed flow pattern. If a circular, axially concentric element of radius r and length dL is considered to be at the centre of the tube (figure A10) then the shear force acting on the rim of the element is the product of shear stress and the cylindrical area. The force balance on the element leads to,

$$\Sigma F = \pi r^2 P - \pi r^2(P+dP) - (2\pi r dL)\tau = 0 \tag{A2}$$

Fluid element in steady flow through tube
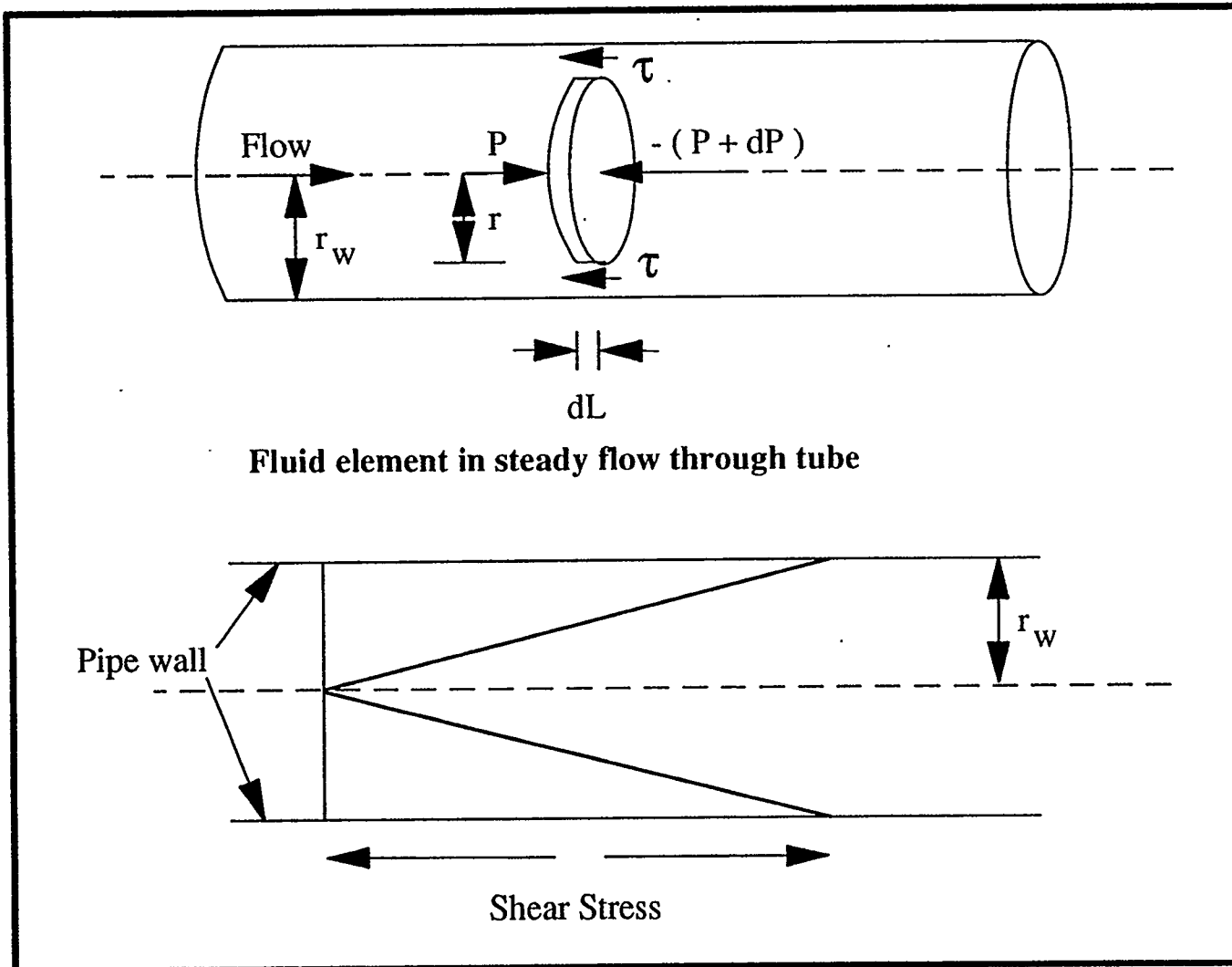
Figure A 10 : Variation of shear stress

On simplification,

$$\frac{dP}{dL} + \frac{2\tau}{r} = 0 \qquad \text{(A3)}$$

For a steady state flow, the pressure at any given cross section of a stream tube is constant. Thus equation (A3) is valid for the entire cross section of the tube if τ_w and r_w are substituted for τ and r respectively where τ_w is the shear stress at the wall and r_w is the radius of the conduit. With these substitutions, equation (A3) becomes,

$$\frac{dP}{dL} + \frac{2\tau_w}{r_w} = 0 \qquad \text{(A4)}$$

Subtracting equation (A3) from equation (A4) gives,

$$\frac{\tau_w}{r_w} = \frac{\tau}{r} \qquad \text{(A5)}$$

Bernoulli's equation is now applied to the flow under consideration. Since there is no change in either kinetic energy or potential energy and the only friction is due to the skin friction between the wall and the fluid stream, denoted by h_{fs},

$$\frac{P}{\rho} = \frac{P - \Delta P}{\rho} + h_{fs} \qquad \text{(A6)}$$

where ΔP is the pressure drop. Equation (A6) can also be written as,

$$\frac{\Delta P}{\rho} = h_{fs} \qquad \text{(A7)}$$

An expression for h_{fs} is obtained by integrating equation (A4) and combining equation (A7).

Hence,

$$h_{fs} = \frac{2\tau_w}{\rho r_w} \Delta L = \frac{4\tau_w}{\rho D} \Delta L \qquad \text{(A8)}$$

Or,

$$\tau_w = \frac{D}{4} \frac{\Delta P}{\Delta L} \qquad \text{(A9)}$$

where D is the diameter of the pipe.

APPENDIX IV

Correlations for water :

1. Friction Results :

a) Blasius Equation

$$f = \frac{0.0791}{Re^{1/4}}$$

b) Petukhov Equation

$$\frac{f}{2} = (2.236 \ln Re - 4.639)^{-2}$$

2. Heat Transfer Results :

a) Sieder-Tate Equation

$$Nu = 0.023 \, Re^{0.8} \, Pr^{1/3} \left(\frac{\mu_b}{\mu_w} \right)^{0.14}$$

for $Re > 10^4$, $0.7 < Pr < 700$

b) <u>Sleicher and Rouse Equation</u>

$$Nu = 5 + 0.015 Re^a \ Pr^b$$
$$a = 0.88 - \frac{0.24}{4 + Pr}$$
$$b = 0.333 + 0.5 \exp(-0.6 Pr)$$

for $10^4 < Re < 10^6, 0.1 < Pr < 10^4$

APPENDIX V a

Thermal Conductivity of SS 304 (ASME Handbook)

Temperature	Conductivity
°C	W/m °K
100	16.27
200	17.82
300	19.04
400	20.42
500	21.63

APPENDIX V b

Properties of water

T, °C	ρ, kg/m^3	C_p, J/kg °K	k, W/m °K
10	999.7	4192	0.5794
15	999.1	4186	0.5884
20	998.2	4182	0.5971
25	996.9	4180	0.6056
30	995.4	4178	0.6132
35	993.9	4178	0.6202
40	992.4	4179	0.6272
45	990.2	4180	0.6392